Title
The Biomechanics of Obstacle Negotiation by Hummingbirds

Author
Badger, Marc Alan

Publication Date
2016

Peer reviewed|Thesis/dissertation

The Biomechanics of Obstacle Negotiation by Hummingbirds

by

Marc Alan Badger

A dissertation submitted in partial satisfaction of the

requirements for the degree of

Doctor of Philosophy

in

Integrative Biology

in the

Graduate Division

of the

University of California, Berkeley

Committee in charge:

Professor Robert Dudley, Chair
Professor Robert J. Full
Professor Ronald S. Fearing

Fall 2016

The Biomechanics of Obstacle Negotiation by Hummingbirds

Abstract

The Biomechanics of Obstacle Negotiation by Hummingbirds

by

Marc Alan Badger

Doctor of Philosophy in Integrative Biology

University of California, Berkeley

Professor Robert Dudley, Chair

Bird flight takes various forms in nature from gliding to hovering. While flying, birds must be agile enough to maneuver around obstacles and avoid predators, yet stable enough to navigate along an controlled path. To better understand maneuvering in complex environments, I looked to an extreme—hummingbirds. Hummingbirds represent the pinnacle of avian maneuverability. In addition to being the only bird capable of continuous hovering, they also hold the fastest recorded length-specific speeds of any animal and can sustain accelerations of up to nine times the acceleration of gravity. Hummingbirds must maneuver with great accuracy to feed on the nectar of flowers, and they must navigate between trees and branches and into and out of dense vegetation as they pursue arthropods, nest, or evade predators. They also perform these tasks in changing and windy conditions, which can impose simultaneous demands on their flight system. In Chapter 1 of this thesis I investigate how hummingbirds maneuver through narrow constrictions, which represent the most difficult and constraining aspect of flight through vegetation. In Chapter 2 I report how they minimize the perturbing effects of wind gusts. Finally, in Chapter 3 I describe novel maneuvering strategies that hummingbirds display when simultaneously confronted with high winds and narrow constrictions.

Chapter 1

Many birds routinely fly fast through dense vegetation characterized by variably sized structures and voids. I show that Anna's Hummingbirds (*Calypte anna*) can negotiate structural constrictions less than one wingspan in diameter using a previously undescribed sideways maneuver coupled with bilaterally asymmetric wing motions. Crucially, this maneuver allows hummingbirds to continue flapping as they negotiate the constriction. By contrast, much smaller openings are negotiated via a faster ballistic trajectory characterized by tucked and thus non-flapping wings, which reduces force production and increases descent rate relative to the asymmetric technique. Hummingbirds progressively shift to the symmetric method as they perform hundreds of consecutive transits, suggesting increased locomotor performance

with task familiarity. Initial use of asymmetric transit may allow birds to better assess upcoming obstacles and voids, thereby reducing the likelihood of subsequent collisions. This switching strategy to aperture transit may determine the limits of flight performance within structurally complex environments and will inform design efforts for small aerial vehicles intended for flight within vegetation.

Chapter 2

Airflows near Earth's surface are highly dynamic over many spatial and temporal scales. To successfully negotiate these environments, flying organisms must mitigate aerodynamic perturbations and quickly return to their desired flight trajectories. Airborne animals maintain body orientation either by altering aerodynamic forces or shifting angular momentum from the body to appendages and other structures, such as the tail, but how these techniques enable birds to reject aerodynamic perturbations has not been well characterized. To better understand how hummingbirds modify wing and tail motions in response to individual gusts, I recorded Anna's Hummingbirds as they negotiated an upward jet of fast moving air using high-speed video. Birds exhibited large variation in wing elevation, tail pitch, and tail fan angles among trials as they repeatedly negotiated the same gust, and exhibited a dramatic decrease in body angle (27 ± 16 degrees) post-transit. Birds reached a minimum body angle and began to pitch up from this nose dive about 55 ms after leaving the gust. After extracting three-dimensional kinematic features, I identified two distinct control strategies for gust transit, one involving continuous flapping and little disruption to body angle (20 ± 13 degrees downward pitch), and the other characterized by wing holding, tail fanning and 13% faster transit, albeit with greater changes in body angle (46 ± 6 degrees downward pitch). The use of a deflectable tail on a glider model transiting the same gust resulted in enhanced stability and could easily be implemented in design of aerial robots.

Chapter 3

Hummingbirds face many environmental challenges during flight such as wind, rain, and constrictions formed by vegetation. Movement through the natural world often presents these challenges simultaneously. Whereas we know in part how hummingbirds confront individual challenges, we do not understand how they manage multiple constraints at once. In these situations, birds could use a combination of the same compensatory behaviors—such as adjustments to wing and body kinematics—that they use to overcome individual challenges. Alternatively, I hypothesized that novel behaviors would emerge when birds are confronted with simultaneous constraints for which compensatory behaviors are in conflict. To assess responses to multiple locomotor challenges, I measured behavior and kinematics of hummingbirds flying through a circular constriction in a wind tunnel with either a headwind or a tailwind. I compared these measurements with compensatory behaviors previously observed for wind or constrictions in isolation and determined that birds use a combination of pre-existing behaviors and also develop novel behaviors when faced with simultaneous

aperture and wind constraints. One novel behavior I observed in upstream transits was a precisely timed longitudinal shift in the position of the stroke plane. This shift allowed the wings to continue flapping throughout transit and to produce enough forward thrust to offset drag. If implemented in flapping wing robots, such an additional degree of freedom could improve their ability to negotiate simultaneous challenges in complex environments. These novel behaviors suggest that hummingbirds do not have a prescribed set of responses to a known list of expected environments, but instead may adapt novel wing kinematics on-the-fly when encountering to complex environments.

Dedicated to my mother, Roz Badger,
and my father, Lee Badger

Contents

List of Figures

List of Tables

Acknowledgments

I want to start by thanking my advisor, Robert Dudley, for his unbounded patience as I wound my way through various courses and almost-experiments to my eventual research topic—flight through clutter. I appreciate his guidance when I found myself considering experiments with way to many treatments, and also his advice as I became a new father. Over the last two years, I have reflected many times on the depth and truth of his simple statement, "The days are long, but the years are short."

I received help and advice from several undergraduate research students who have worked with me throughout all aspects of my experiments. I am particularly grateful to Menaka Wilhelm who helped get my research off the ground by building an initial flight chamber and brainstorming plans for our preliminary experiments. I also thank Jessica Hsueh, Emerson Sosa, Anthony Pollorneo, and Jessica Ye for being wiling to jump right into the rush of re-analysis, setup modifications, and new experiments. Finally, I cannot thank Kathryn McClain enough for her dedication to our projects through the three years we worked together at Berkeley. Without her consistent interest in research and her willingness to explore new areas and learn research techniques, I would have neither initiated nor completed many of my projects.

I also owe much of my success to Ashley Smiley, Leeann Louis, and Ignacio Escalante. These three graduate students were brave enough to collaborate with me, and they did so despite my inconceivable attention to detail and insistence on creating perfect experimental setups and procedures. Much of the experiment design, data collection, and preliminary analysis described in Chapter 3 was done in collaboration with Leeann Louis, to whom I am greatly indebted for motivating us to move the project forward.

I thank my thesis committee members Robert Dudley, Robert Full, and Ron Fearing, whose valuable feedback, insights, and advice helped improve my own understanding of my research and the presentation of my dissertation. I also thank the additional members of my qualifying exam committee, Mimi Koehl, Mark Tanouye, and Eileen Lacey, who encouraged me to think about hypotheses as explanations for why our observations come out the way they do and to always analyze data comparing multiple species in a phylogenetic context. In addition to those at Berkeley, I also want to thank my undergraduate mentors at Harvey Mudd College, Steve Adolph, Anna Ahn, and Tom Donnelly, who befriended and advised me early on and continue to inspire and motivate my research.

I am also grateful for the funding provided by an NSF Integrative Graduate Education and Research Traineeship (IGERT) from the Center for Interdisciplinary Biological Inspiration in Education and Research (CiBER), and by an NSF Graduate Research Fellowship. These fellowships allowed me to develop interests in many areas of engineering and computer science that I would not have been able to pursue otherwise. I constructed my setups with several summer research grants generously provided by the Beim, Wiley, Umbson, Suzuki, Leeper, Kirby, D&C Miller, and Resetko funds. I would also like to acknowledge several travel grants that I have received from the Center for Latin American Studies, the Graduate Division at UC Berkeley, and from the Society for Integrative and Comparative Biology.

I want to thank the members of the Dudley, Full, Koehl, and Elias labs for their valuable feedback on presentations and manuscripts. I would like to thank Erica Kim, Dennis Evangelista, Yu Zeng, Eve Robinson, Nick Burnett, Margaret Byron, Jean-Michel Mongeau, Kaushik Jayaram, Dwight Springthorpe, and Tom Libby for helping me navigate the vast expanse of research during my first few years. I also want to thank my current lab-mates Sofia Chang, Leeann Louis, Ashley Smiley, and Erik Sathe for their curiosity and questions about my research and experimental methods. Trying to explain my ideas to them helped me clarify what they were. I also I want to thank Nate Hunt for our many lunches over which we discussed the next big ideas in biomechanics and also the interesting and funny things our children were doing as they grew up over the last two years.

I also could not have completed my dissertation without the help of my parents-in-law, Nancy Crickman and John McKinstry. They have always been interested in my research and have expressed their incredible support in so many ways. Both the quality and consistency of John's culinary productions have been godsends during his many visits to Berkeley. I would particularly like to thank Nancy for taking several months off to care for Mabel so that I could focus on finishing my research and writing this dissertation. My mom, Roz Badger, also spent many weeks out in Berkeley during the final two years. I thank her for working so hard doing triple duty (caring for Mabel, editing manuscripts, and analyzing videos) during her extended visits. I also want to thank my brother-in-law, Luke McKinstry, for hours of fun together as we biked Mt. Diablo, skied in Tahoe, and backpacked in Yosemite.

My parents, Roz and Lee Badger, have both edited several drafts of each chapter and have provided insightful and detailed feedback. I thank them for greatly improving the clarity and quality of my writing. Obviously, their contribution extends throughout my whole life as they prepared and inspired me to be a scientist.

My daughter Mabel has been a source of endless joy. She encourages me to be creative and has an innate ability to find anything fascinating, including ramps, simple harmonic oscillators, and of course, hummingbirds. She played a huge role in making graduate school such a happy time in my life.

Finally, I would like to thank my wife, Katie McKinstry, who has been with me at Berkeley and loved and supported me as a scientist quite literally from day one.

Chapter 1

Adaptive shape-shifting enables narrow aperture negotiation by free-flying hummingbirds

"The bird's wings are undoubtedly very well designed indeed, but it is not any extraordinary efficiency that strikes with astonishment but rather the marvelous skill with which they are used."

— Wilbur Wright, 1903. From "Observations in soaring flight" in the *Journal of the Western Society of Engineers*. Volume 8, p. 413.

1.1 Introduction

Many birds, bats, and insects fly near and within dense vegetation when foraging, nesting, evading predators, or during aerial chases. While flying, birds presumably perceive upcoming obstacles visually, "plan a path" around or between them, and then execute the plan using wing and body motions to redirect aerodynamic thrust. This plan may be updated by incorporating sensory feedback with some delay. Animals returning to the same flower or nest many times per day may also benefit by reducing errors or improving performance through learning of obstacle positions and maneuvers.

In dense vegetation, several conflicting demands arise. Foliage can be thought of as a network of variably sized voids (i.e. small spaces empty of obstacles) which are joined by narrow openings. Flight trajectories through these connected voids are therefore punctuated by challenging constrictions. First, to maneuver along a winding path, birds must dynamically alter wing and body motions to adjust the magnitude and direction of aerodynamic thrust. Given a limited ability to generate aerodynamic forces, flight through a dense field of vertical obstacles at speeds above a critical value guarantees a collision in simulations (Karaman and Frazzoli, 2012), simply because birds cannot follow a tight enough turn radius. A conflict

arises however, when constrictions become so narrow that they inhibit normal wing kinematics. Thus clutter also introduces a geometric constraint that may at times be incompatible with aerodynamic force generation. When confronted with gaps between vertical poles less than one wingspan in diameter, both pigeons and budgerigars pause flapping altogether, with their wings either held at the top of the upstroke or folded at the wrist (Schiffner et al., 2014; Williams and Biewener, 2015) which reduces their effective size and presumably decreases the chance of wing or body impacts. For these non-hovering taxa the dual needs of maintaining forward flight speed while also assessing upcoming obstacles are also in conflict. Although faster flight may enhance escape from predators, flight at slower speeds likely improves visual assessment of upcoming obstacles and reduces the consequences of mistakes when traveling through narrow openings. For example, in experiments in which a hummingbird's visual field was suddenly rotated, hummingbirds started moving their heads to track the motion after about 50 ms (Ros and Biewener, 2016). Similarly, when hummingbirds are startled by an approaching visual stimulus, tail flaring occurs within 22–50 ms of the onset of the stimulus (Cheng et al., 2016a), which is then followed by changes in wing kinematics and body angle and velocity after an additional 20 ms delay. Given a combined 70 ms delay between visual input and effective kinematic changes, even a bird traveling at a relatively slow 1 m/s will cover a distance of about 7 cm before it can change course.

By contrast, hummingbirds have two key abilities that may allow them to sidestep these conflicting demands. In addition to their well-known ability to hover, hummingbirds are highly maneuverable along multiple axes and can fly sideways and backwards through adjustment of the wing stroke plane angle (Sapir and Dudley, 2012; Cheng et al., 2016a). Together, these abilities may enable hummingbirds to negotiate densely cluttered environments that are inaccessible to other birds. Thus choice of maneuvering technique relative to obstacle geometry dictates how birds address these conflicting demands and will have important consequences for the overall flight trajectory. The disruption of normal flight as birds negotiate tight apertures along with the resulting effects on the subsequent trajectory may determine limits of flight performance in structurally complex environments.

Here, I show that Anna's Hummingbirds (*Calypte anna*) can negotiate structural constrictions less than one wingspan in diameter, despite the inability to flex the wing about either the elbow or the wrist (Greenewalt, 1960; Hedrick et al., 2012). I found that they overcome this limitation using two well-defined strategies. In one strategy, birds perform a sideways flight maneuver that incorporates continuous, bilaterally asymmetric wing motions. Birds also perform a faster, ballistic maneuver characterized by tucked, non-flapping wings to negotiate apertures. After characterizing these strategies, I hypothesized that large variation in overall flight trajectories observed among apertures and over repeated trials is mediated in part by choice of transit strategy. To test this hypothesis, I examined the relationships among flight speed, vertical force production and transit strategy after correcting for aperture size and other experimental variables. Specifically, I investigated (i) the effect of aperture dimensions and trial number on transit technique, horizontal velocity, vertical acceleration, vertical velocity, and height lost during transit, and (ii) the effect of transit technique on horizontal velocity, vertical acceleration, vertical velocity, and height lost, after

controlling for experimental variables. Potential interactions among aperture width, aperture height, and trial number were also tested. I predicted that an increase in either height or width would have a larger effect on performance when the other dimension was smaller (a negative interaction slope), given the offsetting increase in aperture area. An interaction between width and height would be equivalent to an effect of total aperture area (the area of an ellipse is $\pi \times$ width $\times$ height). I also predicted that if birds utilized novel negotiation techniques for small apertures, performance might improve only for those apertures (i.e., a negative interaction coefficient for the width $\times$ trial number or height $\times$ trial number interactions). Alternatively, flight performance might improve with trial number only for large apertures (i.e., a positive interaction coefficient for the width $\times$ trial number or height $\times$ trial number interactions).

1.2 Materials and Methods

Animals, husbandry, and flight arena

Four adult male Anna's Hummingbirds (mean body mass $\pm$ s.d.: 4.41 $\pm$ 0.15 g; wingspans: 12.1, 12.0, 12.1, 12.0 cm) were obtained from the wild in June – August 2013 using a recessed Plexiglas window drop-trap. Hummingbirds were housed in separate $1 \times 1 \times 1$ m mesh cages, each containing four 10 mL syringes filled daily with nectar solution (Nektar-Plus, Nekton GmbH). The room containing the mesh cages was held at approximately 22 °C and was on a 12 hour light/dark cycle. After two to three days of habituation, hummingbirds were trained to fly between two feeders positioned within a flight arena (Figure 1.1 B) consisting of two $60 \times 75 \times 100$ cm volumes separated by a partition. Various apertures (Figure 1.1 C) were inserted into a 16×16 cm square cutout within the partition, and positioned such that their centers were 30 cm below the arena ceiling so as to minimize aerodynamic effects of the ceiling (Leishman, 2006). Partition walls were made of white pegboard to provide depth cues during flight. The enclosure was lit from above with two 750 W tungsten lights positioned 1 m above an acrylic ceiling, which was covered with white paper to diffuse the light. Although lighting was kept constant throughout all experiments, interior illumination of the arena ranged from 700 to 900 lux depending on location. The Animal Care and Use Committee at the University of California, Berkeley, whose activities are mandated by the US Animal Welfare Act and Public Health Service Policy, approved all experimental procedures (protocol # AUP-2014-09-6676).

Feeders and nectar access

Artificial feeders were positioned 30 cm below the ceiling at both ends of the flight arena and were aligned with the aperture so that a line of sight ran through the aperture between the two feeders. I motivated hummingbirds to transit between feeders using a custom-built nectar delivery system. Each feeder consisted of a plastic flower placed on a nectar

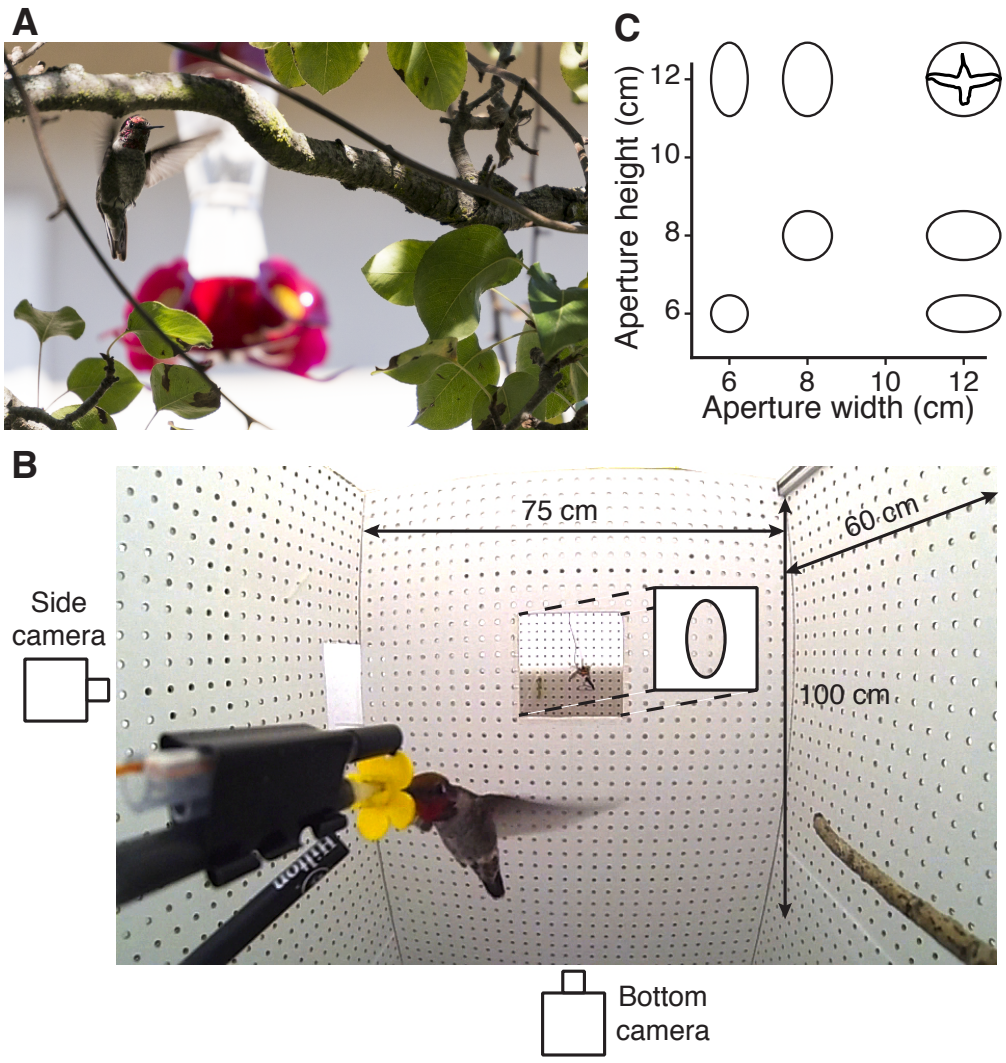

Figure 1.1: Wild Anna's Hummingbirds (*Calypte anna*) negotiate narrow apertures. (A) Hummingbird flying to a perch within vegetation (image credit: Marc Badger). (B) In the lab hummingbirds flew between two artificial feeders positioned on either side of a partition dividing an experimental flight arena. Bird transits were recorded using high-speed video from the side and from below at 500 frames per second. (C) Hummingbirds flew through apertures with dimensions ranging from one-half to one wingspan. Hummingbird inset shows relative scale.

reservoir adjacent to a photoresistor sensor, which detected presence of a bird at the feeder. Each feeder reservoir provided only a small amount of nectar (10 – 40 microliters), which I assumed hummingbirds consumed in a single visit. Feeders were automatically refilled by a servo valve, which was controlled by an Arduino Uno microcontroller (Arduino). Once a bird had visited a feeder, the nectar volume was not refreshed (via the servo valve) until the bird had been detected at the feeder on the other side of the partition. Hummingbirds thus shuttled between feeders without external motivation.

Apertures and experimental design

Circular and elliptical shapes were cut from 16 × 16 cm squares of 3/8 inch thick white foamboard and white electrical tape was used to line the cut edges. Aperture dimensions were 6, 8, and 12 cm in both height and width (i.e., about 0.5 – 1.0 wingspan). Specific apertures (listed by height/cm × width/cm) were 12 × 12, 12 × 8, 8 × 12, 8 × 8, 12 × 6, 6 × 12 and 6 × 6. A clover-shaped aperture was created from the union of the 6 × 12 and 12 × 6 apertures and was included in the aperture sequence to provide an additional comparison of the effects of aperture width to those of aperture height. Appropriate aperture sizes and training protocols were determined in a preliminary experiment using one additional hummingbird, which was not included in this study. I organized experimental trials into ten sets of consecutively presented apertures. Each aperture was presented once within each set, during which the bird completed at least two transits (i.e., back and forth through the aperture). Apertures were ordered pseudorandomly within each experimental set, but the same sequence was used for all four birds. Over the course of four to six weeks, each bird completed ten sets of eight apertures, for a total of at least 160 trials. Sets typically took between two and four hours to complete. All trials for two birds were completed with varying, but bounded intervals between sets (mean ± s.d. [range]: 3.6 ± 2.9 [0, 8] days for one bird, and 2.4 ± 3.0 [0, 7] days for the other bird). The two other birds had similar time intervals between sets (mean ± s.d. [range]: 2.4 ± 3.2 [0, 7] days for one bird, and 3.5 ± 2.7 [0, 7] days for the other), excluding two occasions in which there was a large gap between sets. Specifically, for one of these birds, the interval between sets 3 and 4 was 21 days, and for the other bird, the interval between sets 5 and 6 was 22 days. If these two gaps did affect the behavior of the birds, the generalized additive models (see the "Statistical analyses" section below) would have shown these non-linearities. The number of birds ($n = 4$) was limited by availability, and the number of trials per aperture treatment ($n = 20$ per bird) was chosen to (i) detect differences in behavior and performance among apertures, (ii) capture any learning that may occur over hundreds of trials, and (iii) sufficiently sample variation within each aperture size so that I could detect effects of behavior on performance after conditioning on aperture and experience variables.

Training and data collection

Hummingbirds were first habituated to the flight arena and feeder system for two hours, with no aperture present. I then inserted an aperture and waited for the bird to transit back and forth, before replacing the aperture with a new one. Birds typically perched and occasionally re-checked the empty feeder between transits. Waiting time between transits ranged from 3 seconds to 22 minutes between transits (exponential distribution: average waiting time was about 3.3 minutes).

Birds landed on the aperture in 12 trials early in the experiment (one bird landed 10 times and two others landed once each). Landing trials were excluded from further analyses so that results reflect only flight behaviors. Frequently (592 of 1232 total transits), a transit was not filmed because it occurred during video downloading; in these cases, the aperture was removed and the bird was permitted to fly through the 16 $\times$ 16 cm square opening to the original side of the arena, at which point the original aperture was reinserted. In statistical analyses I used the total number of aperture transits, including those not recorded on high-speed video, as a factor to model changes in performance throughout experiments. Instances of wing or body impact with the edge of the aperture were also recorded.

Video recording and analysis

Transits were filmed laterally and from below at 500 frames per second using two high-speed cameras focused on the center of the aperture (Fastec Imaging Corporation). Cameras were aligned with gravity using a spirit level, and camera mounts remained fixed throughout experiments. Cameras were positioned about 88 cm from the center of the aperture. Trials were recorded at 500 frames per second with 0.2 ms exposure per frame. Pixel coordinates from the side and bottom views were converted to absolute coordinates using a calibrated scale placed at the center and corners of the partition opening. Absolute coordinates are expected to be accurate given that bird trajectories were perpendicular to the axes of both cameras.

To quantify transit behavior, I calculated the average difference between left and right wing angles for each trial, using video sequences from the bottom view camera. Wing asymmetry was defined as the difference (in degrees) between the left and right average wing angles if one of the wings was swept forward, or as the sum of the left and right average wing angles if both wings were swept backward. Thus, wing asymmetry was greatest (about 180°) when the leading and trailing wing angles were near 90° and -90°, respectively, and wing asymmetry was least (about -180°) when both wings were folded backward at -90°. This definition allowed the wing asymmetry metric to distinguish between trials in which both wings were folded backward (wing asymmetry $\approx$ 180°) and trials in which the wings were positioned symmetrically about the sagittal plane, but not folded backward (wing asymmetry $\approx$ 0°). Wing angle was calculated from wing tip position and estimated shoulder location, which was assumed to be fixed relative to the bill tip. Wing tip and bill tip positions were automatically extracted from video data using custom code written in Mathematica

(Wolfram Inc., version 10.1, 2015). All trials were inspected visually for obvious tracking errors, which occurred in 15 out of 640 trials. These errors were fixed by hand specifying feature locations in several frames surrounding the error. Minor tracking errors (one or two isolated localization errors in a single trial) were not corrected because these errors did not noticeably affect calculated mean wing position during transit. Minor tracking errors occurred in approximately 12% of trials. Although it was not possible to blind investigators to treatments during experiments, the analysis software used to track bird kinematics was blinded to both aperture size and trial number.

Transit was defined to begin upon bill tip entry through the plane of the aperture, and to end when the tail tip exited the aperture. The trajectory of the bill tip, reflecting the stabilized head position, was tracked automatically for all trials using a set of close-up template images. A minimum-jerk trajectory (a quintic spline represented by two 5th degree polynomials; one for horizontal position vs. time and another for vertical position vs. time) was then fit to the lateral projection of the bill tip trajectory using least squares. Average velocity of the bill tip during transit was calculated as $\bar{v} = (x_{\text{exit}} - x_{\text{entry}})/(\text{transit duration})$, where x_{entry} and x_{exit} were obtained by evaluating the bill tip trajectory fit at the beginning and end of transit, respectively. The y-coordinate at these times was used to calculate the change in height of the bill tip during transit, $\delta y = y_{\text{exit}} - y_{\text{entry}}$. Average acceleration of the bill tip during transit was calculated as $\bar{a} = (v_{\text{exit}} - v_{\text{entry}})/(\text{transit duration})$, where v_{entry} and v_{exit} were obtained by first analytically differentiating the fit to obtain a velocity function and then evaluating the velocity function at the beginning and end of transit, respectively. Position error in the spline originates from both tracking error (the selected point for a given frame differs from the true position) and from fitting error (the fitted equation differs from the tracked position). Only the fitting error is quantifiable, however, because no ground truth exists for tracking error. The mean distances from tracked points to their fitted positions in the horizontal and vertical directions of the camera image were 1.5 and 0.49 pixels, respectively.

Statistical analyses

Data were analyzed using linear mixed models and the lme4 package in R (Bates et al., 2015; R Core Team, 2016). Fixed factors included aperture width and height, trial number, bird ID, and their second-order interactions as described above. To model possible correlations among trials within a particular aperture presentation sequence due to shared but unmeasured variables (such as air pressure) a unique set identifier (nested within bird ID) was included as a random factor. Bird ID was modeled as a fixed factor (except for Figure 1.5 B) because the sample size (n = 4) was less than that recommended for random factors (Fox, Negrete-Yankelevich, and Sosa, 2015). Trial number was included as a continuous variable. I included parameters for bird ID interactions with trial number, trial number by height, and trial number by width to allow the effect of trial number, trial number × height, and trial number × width to vary independently among birds. Because of potential directional asymmetries

between the two partitions of the flight arena, flight direction was included as a fixed effect in all models.

I then tested whether transit technique was correlated with horizontal velocity, vertical acceleration, vertical velocity, and height lost during transit. To control for correlation between technique and trajectory variables that could potentially arise due to their dependence on experimental variables alone, I first modeled technique, horizontal velocity, vertical acceleration, descent rate, and height loss as linear functions of bird ID, presentation set, aperture dimensions, flight direction, and trial number (i.e. the experimental variables). I then obtained bootstrapped p-values and confidence intervals for correlation coefficients between the residuals of the horizontal velocity, vertical acceleration, vertical velocity, and height lost models and the residuals of the technique model.

To assess statistical significance, 95% confidence intervals for parameter estimates and marginal (type III sums of squares) p-values were obtained from 5000 replicate bootstrap analyses using the R packages "afex" (parametric bootstrap function: mixed; Singmann, Bolker, and Westfall, 2015), "lme4" (function: lmer; Bates et al., 2015), and "boot" (nonparametric bootstrap function: boot; Canty and Ripley, 2015; Davison and Hinkley, 1997). Normality of residuals was checked qualitatively for all models and homogeneity of variance was checked for all variables in all models. As expected, variance in wing asymmetry was slightly lower for the smallest aperture than for the others because birds only used the symmetric technique to transit the smallest aperture. Incorporating unequal variance across apertures into the wing asymmetry model (to account for this mild heteroscedasticity) changed neither the direction nor magnitude of the parameter estimates, so I present results based on the model with a single variance parameter for simplicity.

I also conducted analyses with aperture shape parameterized as a categorical variable (rather than using values for aperture width and height) followed by post-hoc comparisons among apertures, but doing so did not change the significance or interpretation of the main results. In addition, I evaluated the effect of cumulative trial number on transit technique and performance variables using generalized additive models but the observed relationships did not appear nonlinear and the subsequent analyses of the associations between residual performance variables and residual wing asymmetry did not differ in magnitude or significance between the additive and linear models. I therefore chose to use linear mixed models because these models allowed estimation of a slope parameter for cumulative trial number.

1.3 Results

Wing Angles Define Two Postures for Narrow Aperture Negotiation

Two well-defined methods were used to negotiate narrow apertures, one of which was a distinctive sideways maneuver characterized by asymmetric wing motions (Figure 1.2 A–C). Here, birds shifted the mean position of the leading wing forward and that of the trailing

wing backward, but continued to flap throughout transit. Thus, the leading wing, body, and then trailing wing sequentially entered and exited the aperture. A second transit strategy involved bilaterally symmetric positioning of the wings, whereby birds paused flapping and held both wings approximately 90° backwards from the shoulder (Figure 1.2 D–F). For this case, birds varied the extent to which the wings were posteriorly positioned, but did so symmetrically about the sagittal plane.

The Asymmetric Technique Enables Cautious Flight

I found that transit strategy significantly influenced flight performance and the overall trajectory (Figure 1.3). Mean horizontal velocity for the first set of transits (the first 16 transits for n = 4 birds) was 1.18 ± 0.16 m $^{-1}$, which increased to 1.62 ± 0.28 m $^{-1}$ for the last set. Mean vertical acceleration, on the other hand, decreased from -5.0 ± 1.0 m $^{-2}$ to -8.2 ± 1.1 m $^{-2}$ between the first and last sets. These changes in trajectory were partially due to a simultaneous change in transit technique (as measured by wing asymmetry). After controlling for individual bird identity (fixed effect), aperture dimensions (continuous variables), cumulative trial number (continuous variable), flight direction, and aperture presentation set (random effect), hummingbirds flew more slowly and produced more upward aerodynamic force (as indicated by vertical acceleration of the bill tip) when using the asymmetric technique. Greater bilateral wing asymmetry was inversely correlated with flight velocity ($r = -0.37$, $p < 0.001$; Figure 1.3 C), but yielded an increased vertical acceleration ($r = 0.61$, $p < 0.001$; Figure 1.3 B), a slightly but significantly slower descent rate ($r = -0.16$, $p < 0.001$), and a somewhat smaller height loss during transit ($r = -0.10$, $p < 0.001$) (Table 1.1).

Association between wing asymmetry and:	Correlation coefficient (r)	P-value	95% CI for r
Flight velocity	-0.37	< 0.001	[-0.44, -0.29]
Vertical acceleration	0.61	< 0.001	[0.56, 0.67]
Descent rate	-0.16	< 0.001	[-0.26, -0.083]
Height loss	-0.10	< 0.001	[-0.21, -0.033]

Table 1.1: Correlation coefficients and statistics for the associations between wing asymmetry and flight velocity, vertical acceleration, descent rate, and height loss. Correlations calculated among residuals after conditioning on aperture dimensions, cumulative trial number, flight direction, bird ID, aperture presentation set. Type 3 sums of squares p-values and confidence intervals are based on a 5000 replicate nonparametric bootstrap.

All four hummingbirds used both symmetric and asymmetric transit strategies to negotiate each of the tested apertures except for the smallest (6 × 6 cm), for which they used only the symmetric technique (Figure 1.4). Wing motions were significantly more asymmetric for larger apertures (aperture height: $\beta = 7.07$ degrees/cm, $p < 0.001$; aperture width: *beta* = 14.5 degrees/cm, $p < 0.001$; Figs. 3, 4B; Table 1.2), but there was no significant

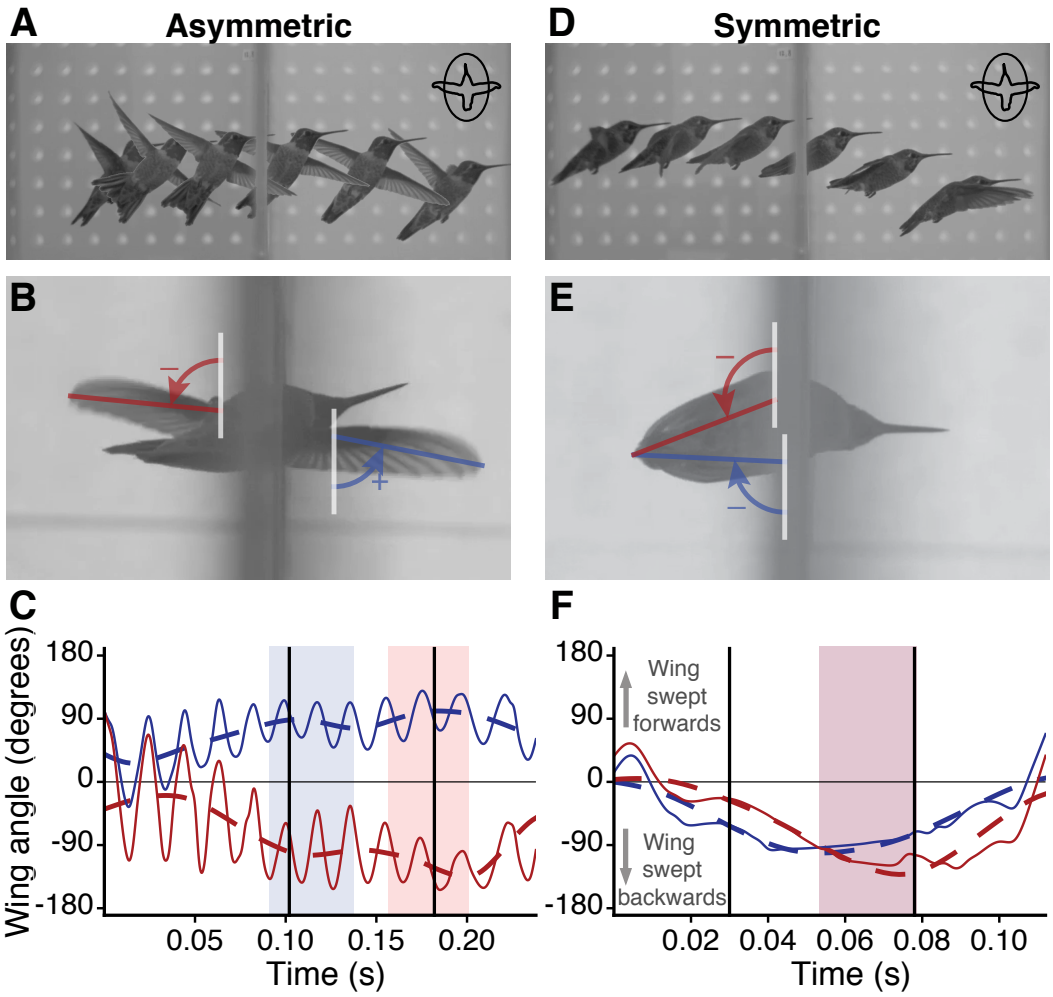

Figure 1.2: Two well-defined transit techniques used to negotiate small apertures. (A–C) The asymmetric technique was characterized by sideways flight (A), bilaterally asymmetric wing motions (B), and continuous flapping (C). (D–F) In the symmetric technique, birds fold both wings posteriorly at the shoulder (D and E) and pause flapping (F). (A, D) Overlain images show wing and body position from the side every 46 ms (A) and 26 ms (D). Inset shows aperture size relative to wingspan. (B, E) View from below showing difference in wing positioning. (C, F) Wing angles (thin sold lines) and mean wing offset angles (thick dashed lines) through time. Sinusoidal oscillation is due to wings beating at $\sim$ 50 Hz. Video frame rate is 500 fps, giving $\sim$ 10 samples per wing stroke. Vertical black lines indicate bill tip entry and tail exit from the aperture. Shaded regions indicate periods when the left wing (blue), right wing (red), or both wings (purple) are within the aperture.

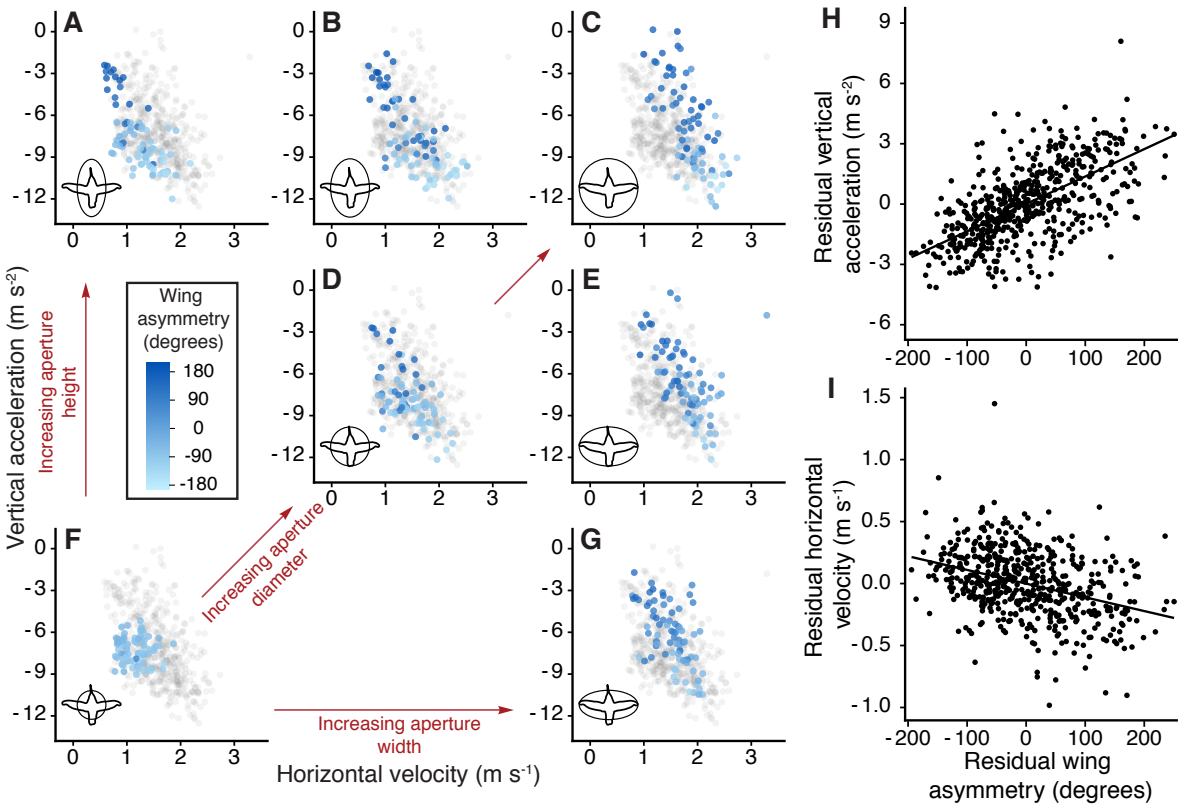

Figure 1.3: Effect of aperture dimensions and transit technique on horizontal flight speed and vertical force production. (A–G) Vertical acceleration versus horizontal velocity as functions of aperture width (6, 8, and 12 cm) and aperture height (6, 8, and 12 cm), pooling data from all four birds. Disk color represents wing asymmetry, ranging from -180° (symmetric, light blue) to 180° (asymmetric, dark blue). In each panel, trials from all other apertures are shown in light grey to aid comparison. Inset shape and bird outline indicate relative size of the aperture with respect to mean wingspan (12.0 cm). For each aperture, vertical acceleration and horizontal velocity were negatively correlated, except for the smallest aperture (F). Birds also almost exclusively used the symmetric technique for the smallest aperture (F). Asymmetric trials (dark blue dots) had higher (less negative) vertical acceleration and faster horizontal velocity than did symmetric trials (lighter blue dots). Velocity and acceleration both increase with aperture radius (diagonal from F to D to C). Aperture width (A–C) had a much larger effect on transit velocity than did aperture height (G, E, C; see text for statistical analysis). (H) Residual wing asymmetry was positively correlated with residual vertical acceleration ($n = 548$, $p < 0.001$), after controlling for individual bird identity, aperture dimensions, cumulative trial number (continuous variable), flight direction, and aperture presentation set (random effect). (I) Residual wing asymmetry was inversely correlated with residual horizontal velocity ($n = 548$, $p < 0.001$).

interaction effect between aperture width and height on wing asymmetry ($p = 0.20$). Because all birds successfully negotiated the smallest aperture using the symmetric technique, the minimum aperture diameter that hummingbirds could negotiate using only flight was not identified. In preliminary experiments, however, birds were also able to transit smaller apertures (5 cm diameter circle), tall and narrow slits (12 × 3 cm), and short and wide slits (3 × 12 cm), but always used their feet to temporarily grasp the edge of the aperture.

Regression parameter	Regression slope (β)	Unit	P-value	95% CI for β
H	7.07	deg. cm^{-1}	< 0.001	[4.15, 9.85]
W	14.5	deg. cm^{-1}	< 0.001	[11.7, 17.3]
E	-0.405	deg. $trial^{-1}$	< 0.001	[-0.492, -0.327]
H × W	-0.698	deg. cm^{-2}	0.20	[-1.77, 0.321]
H × E	-0.0387	deg. cm^{-1} $trial^{-1}$	0.02	[-0.0704, -0.0038]
W × E	0.0239	deg. cm^{-1} $trial^{-1}$	0.16	[-0.0083, 0.0563]

Table 1.2: Coefficients and statistics for the effect of aperture width (W) , aperture height (H), and experience (E) on wing asymmetry. The model WingAsymmetry ∼ H + W + E + H:W + H:E + W:E + BirdID + E:BirdID + H:E:BirdID + W:E:BirdID + FlightWest + (1|SetUnique) was fit to the data in R using the package lme4. Type 3 sums of squares p-values and confidence intervals are based on a 5000 replicate nonparametric bootstrap.

Experienced Birds Switch Strategies from Asymmetric to Symmetric

Hummingbirds tended to switch from the asymmetric to the symmetric technique with increased number of transits ($\beta = -0.405$ degrees/trial, $p < 0.001$, Table 1.2). Mean wing asymmetry for the first set (the first 16 transits for n = 4 birds) was 74 ± 35 degrees. Mean wing asymmetry for the last set was -65 ± 43. Thus experience affected transit technique to roughly the same degree as did the combined effects of aperture width and height (Figure 1.5). Furthermore, experienced birds flew just as quickly through the smallest aperture as did inexperienced birds through apertures either twice as wide ($p = 0.31$) or tall ($p = 0.18$).

Although all birds used similar transit techniques, with comparable switching from asymmetric to symmetric technique (Figure 1.6), one bird flew consistently more slowly than the other birds (decrease of 0.43 m/s, Tukey's post-hoc test, all $p < 0.001$), and also exhibited significantly higher vertical acceleration (increase of 1.3 m/s^2, Tukey's post-hoc test, all $p < 0.005$). Interestingly, this bird also used the asymmetric technique more often than other birds (with a greater wing asymmetry of 25°; Tukey's post-hoc test, all $p < 0.032$), indicating that the relationships between flight technique, horizontal flight speed, and vertical force production observed among trials for each individual may also occur among birds.

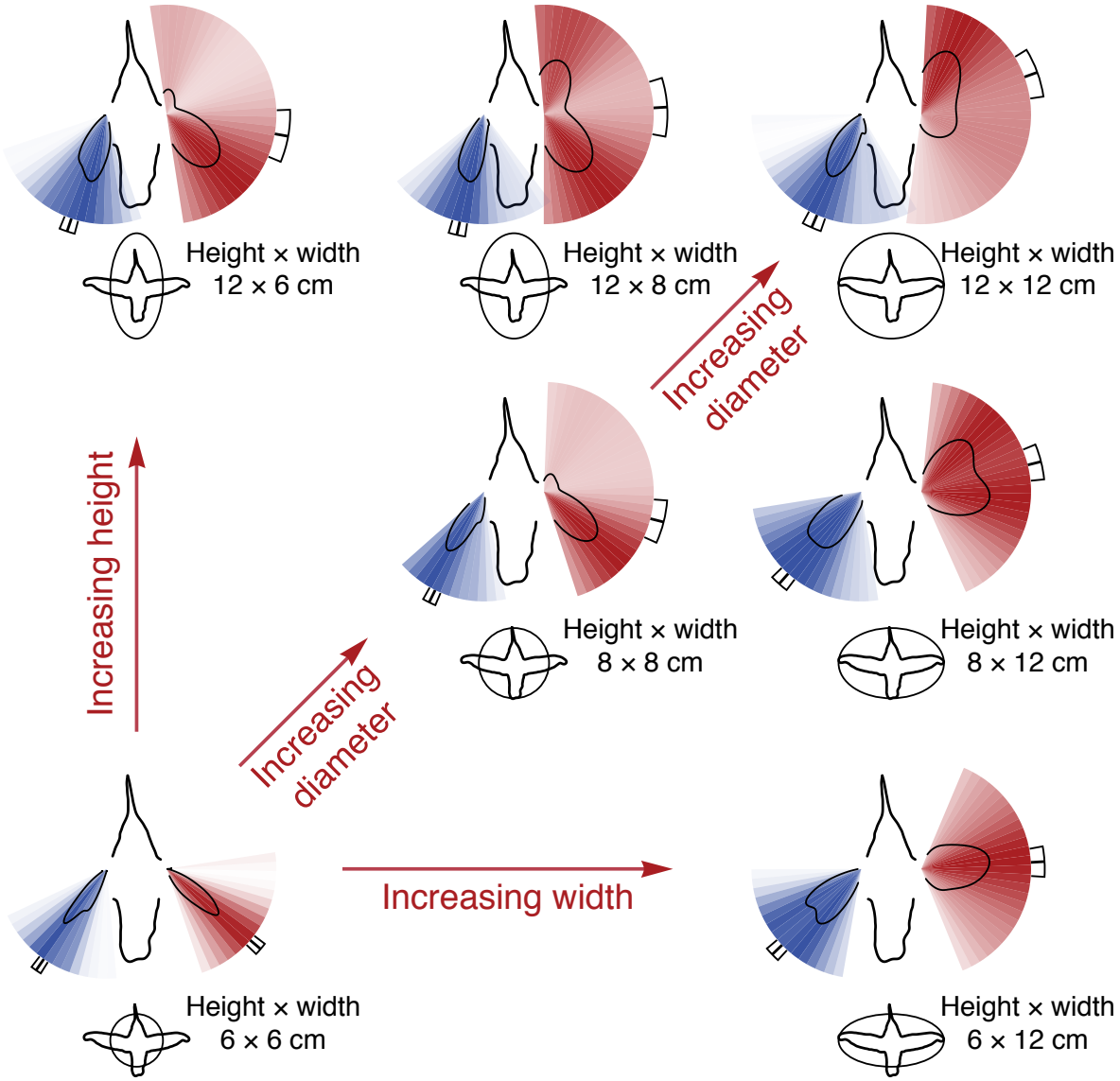

Figure 1.4: Hummingbirds switch from symmetric to asymmetric transit techniques in response to increased aperture size. Density plots of time-averaged leading and trailing wing angles (red and blue, respectively) during transit as functions of aperture width and height. Tab extending beyond the density plot shows mean wing angle (center line) and 95% confidence interval (edges).

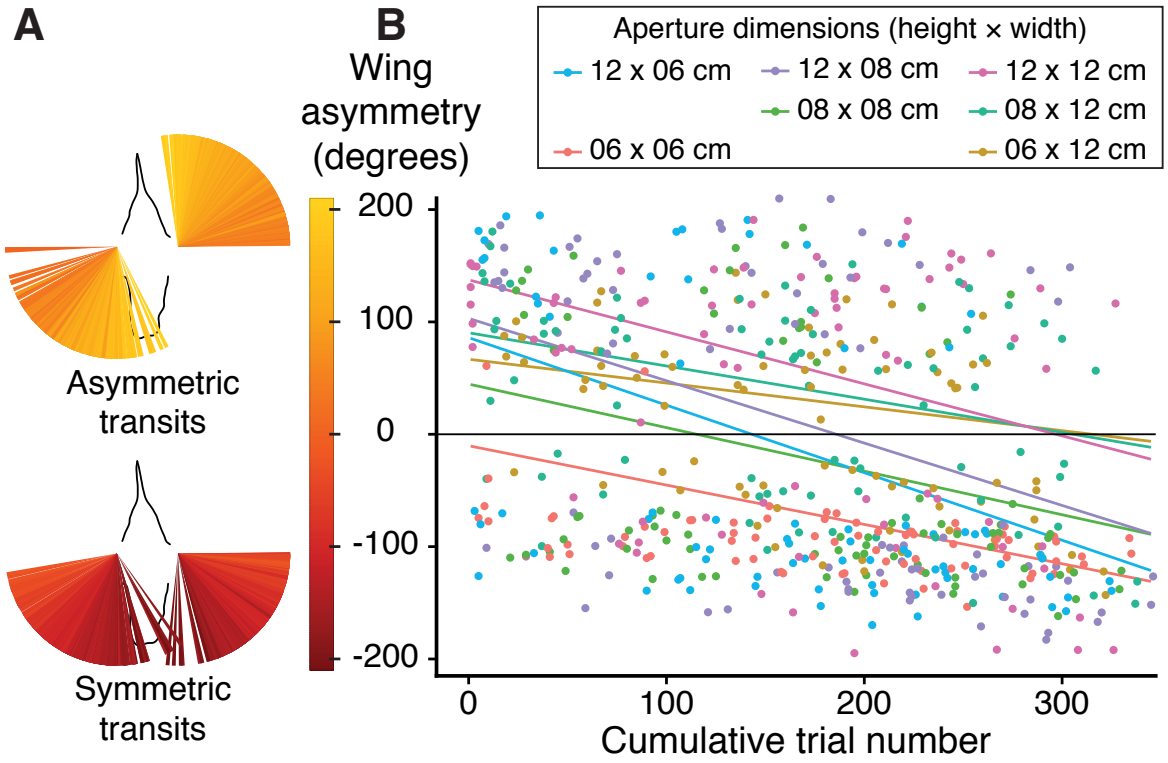

Figure 1.5: Hummingbirds switch from asymmetric to symmetric transit techniques over repeated transits. (A) Leading and trailing wing angles for all trials. Top and bottom show asymmetric and symmetric transits, respectively. Ray color shows corresponding wing asymmetry. Trials with very similar wing angles may have overlapping rays. (B) Transit technique shifted from asymmetric to symmetric over repeated transits for all apertures. Lines show predicted wing asymmetry from a linear mixed model with bird ID ($n = 4$) as a random factor. There was a small but significant individual effect (see Figure 1.6), but the overall shift from asymmetric to symmetric transit technique occurred in all birds. Experience (cumulative trial number) affected transit technique to roughly the same degree as did the combined effects of aperture width and height.

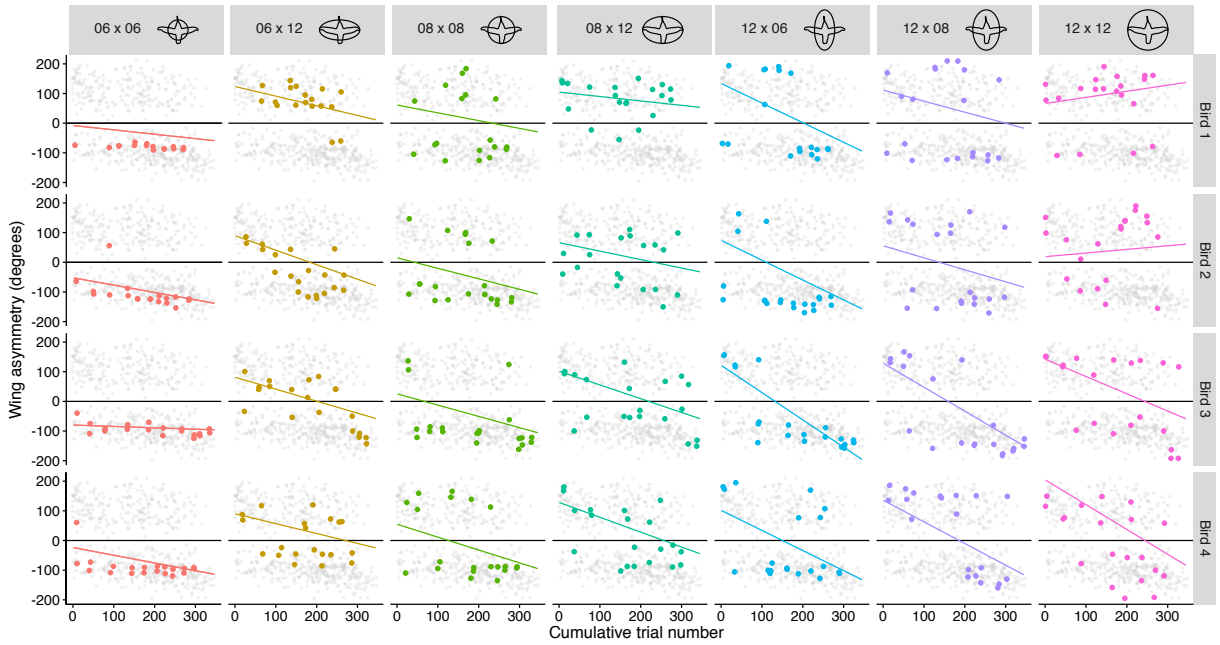

Figure 1.6: Transit technique shifted from asymmetric to symmetric over repeated transits for all but two aperture–bird combinations. Lines show predicted wing asymmetry from a linear mixed model with bird ID as a fixed factor, including interactions of bird ID with aperture height, aperture width, aperture height × aperture width, and cumulative trial number. There were small but significant interaction effects for bird ID with aperture height × width (likelihood ratio test, df = 3, $p = 0.017$), and cumulative trial number (likelihood ratio test, df = 3, $p = 0.035$).

I did not observe lateralization across birds, and lateralization did not change significantly throughout repeated trials (likelihood ratio tests on generalized linear models, $p = 0.35$ and $p = 0.22$, respectively). Two individual birds exhibited significant handedness in leading versus trailing wing when using the asymmetric technique, although the preference was for different wings (bird with preference for right wing: Chi-squared test: $\chi^2 = 12.8$, $p < 0.001$, likelihood ratio test: $p < 0.001$; bird with preference for left wing: Chi-squared test: $\chi^2 = 4.73$, $p = 0.03$, likelihood ratio test: $p = 0.03$).

I also included a clover-shaped aperture in this study as another way to test the effect of increasing aperture width and height. The clover shape was created by taking the union of the 6 × 12 cm and 12 × 6 cm aperture openings. Changing from the 6 cm high × 12 cm wide aperture to the clover increased horizontal velocity and decreased vertical acceleration (Tukey's post-hoc test, both $p < 0.001$) but changing from the 12 cm high × 6 cm wide aperture to the clover increased both wing asymmetry and horizontal velocity (Tukey's post-hoc test, both $p < 0.001$). Similarly, purely changing aperture orientation from the 12 cm high × 06 cm wide to 06 cm high × 12 cm wide increased wing asymmetry, horizontal

velocity, and vertical acceleration (Tukey's post-hoc test, all $p < 0.001$). These comparisons agree with the findings using ellipse-shaped apertures—changing aperture width has a greater effect on technique and trajectory parameters than changing aperture height.

1.4 Discussion

Flight within dense vegetation requires animals to repeatedly negotiate openings that connect obstacle-free regions. Here, hummingbirds negotiating single apertures less than one wingspan in diameter demonstrate multiple strategies, which have significant affects on their overall trajectory. Initially, hummingbirds used a cautious technique characterized by continuous flapping, which enabled slower flight and provided greater aerodynamic forces. Over time, however, hummingbirds gradually shifted to a faster technique in which flapping was paused.

Initial use of the asymmetric technique may indicate cautiousness in novel environments—slow flight allows greater time to observe and react to upcoming obstacles. Between the first and last sets, transit speed increased by 27% (ranged from 18–60%, depending on aperture size) and vertical acceleration decreased by 63% (ranged from 2–269%, depending on aperture size). Meanwhile, mean wing asymmetry decreased by 188% between the first 16 transits and the last 16 transits. A significant portion of each change (35% and 57% for velocity and acceleration, respectively) was associated with the simultaneous change in transit behavior (Figure 1.3 H and I). These effects increase post-transit recovery distance, but may allow birds to better negotiate known obstacles. Specifically, the use of the non-flapping symmetric technique may reduce the intensity of wing impacts with the aperture. Whereas I did not detect any association between the likelihood of a wing impact and transit technique (likelihood ratio test, $\chi^2_{(1)} = 0.16$, $p = 0.69$), a much greater wing speed during flapping will intensify wing impacts and increase damage relative to birds using the static-wing, symmetric technique. In only one of 640 trials was body collision with the aperture observed (i.e., contact of head or torso, excluding tail feathers), following which the bird recovered in eight wing strokes (about 96 ms after start of collision) and proceeded through the smallest aperture only 0.5 seconds post-recovery.

These transit techniques used by hummingbirds highlight the potential benefits of shape-shifting when negotiating cluttered environments. Because there is no substantial flexion of the wing about either the elbow or the wrist (Greenewalt, 1960; Hedrick et al., 2012), hummingbirds must use distinctive strategies to transit narrow apertures. For insect-scale flying robots, independent bilateral control of wingstroke amplitude (Figure 1.2 C) is used to produce roll torque (Ma et al., 2013; Zhang, Cheng, and Deng, 2016), but asymmetric shifts in amplitude or mean stroke angle may also aid negotiation of cluttered environments by allowing robots to partially maintain weight support during aperture transits (Figure 1.3 H). Symmetric forward and backward shifts in the mean stroke angle affect pitch in flapping robots (Ma et al., 2013; Zhang, Cheng, and Deng, 2016), but because hummingbirds performing the asymmetric maneuver always shift one wing forward and one wing backward, no

appreciable shift in the center of aerodynamic force occurs and no net pitching torque is generated. These insect-scale physical and mathematical models provide valuable platforms on which to investigate the power, control effort, and wingstroke timing needed to execute novel maneuvers in tuned resonant systems (Fearing et al., 2000). When negotiating constrictions less than one body width in diameter, quadrotors (i.e. flying robots with four propellors) must transit ballistically and then recover following a period of reduced aerodynamic support during transit (Mellinger, Michael, and Kumar, 2012). Because propellors have a fixed diameter and modulate thrust either through angle of attack or rotation frequency, rotating propellors cannot produce downward thrust if the diameter of the constriction is less than that of the propeller. The ability to produce partial, but significant downward thrust by reducing wingstroke amplitude when flying through constrictions may be an important advantage of flapping wing robots over to those that produce thrust using propellors.

A decrease in aperture width reduced hummingbird flight speed twice as much as did a similar decrease in aperture height (Figure 1.3 A). Therefore, foliage geometry may also play an important role in determining movement strategies. Hummingbirds can hover, and also force-vector with respect to initial body orientation (Altshuler et al., 2012; Cheng et al., 2016a). Thus the limits to clutter negotiation at the low speeds considered here ($\sim$1–3 m/s) likely derive from environmental geometry or dynamic stability during maneuvers (Cheng et al., 2016b), rather than from constraints on visual processing as they do for non-hovering birds (Lin, Ros, and Biewener, 2014). Unlike in the case of pigeons (Williams and Biewener, 2015), the difference in energetic cost between gap traversal techniques is likely to be very small compared to the energetic cost of sustained flight, which comprises about 34% of a hummingbird's daily energy budget (Wolf and Hainsworth, 1971). Energetic efficiency is therefore unlikely to be a driver of technique choice in these experiments. In addition to feeding from flowers, hummingbirds routinely fly near and within vegetation while foraging for arthropods (Stiles, 1995). Both tasks may require the ability to adaptively switch between transit strategies in the course of complex aerial maneuvers. Such experiential learning of a complex locomotor task may be particularly advantageous when flying through diverse types of vegetation and other obstacles that present unpredictable spatial challenges.

Chapter 2

Avoiding topsy-turvy: how Anna's Hummingbirds (*Calypte anna*) fly through upward gusts

2.1 Introduction

Natural aerial environments are dynamic. Variable airflows can be generated by weather systems, wind shear, or interactions of wind with vegetation, and occur on time-scales ranging from fractions to many multiples of a characteristic wingbeat period. Gusts, turbulence, and variable winds challenge both animals and small flying vehicles (Hoblit, 1988; Suomi et al., 2013). Turbulence can limit maximum forward flight speed in orchid bees (Combes and Dudley, 2009), and other insects flying within turbulent flows exhibit increased variance in body translation and rotation (Ravi et al., 2013; Ortega-Jimenez et al., 2013). Hummingbirds flying either in von Kármán vortex streets (Ortega-Jimenez et al., 2014) or in homogeneous free-stream turbulence (Ravi et al., 2015) compensate by rapidly adjusting wing and body kinematics, and intermittently fan the tail to effect stability. Flying in sustained turbulence is also known to increase the energetic costs of flight, especially at higher flight speeds (Bowlin and Wikelski, 2008).

Flight responses to wind transients, by contrast, are much less studied, although ventral wing tucks have been identified for a large eagle flying through headwind gusts (Gillies, Thomas, and Taylor, 2011; Reynolds, Thomas, and Taylor, 2014). Perturbation studies of insects have also demonstrated rapid kinematic responses to air puffs, typically using asymmetric responses in stroke amplitude (Vance, Faruque, and Humbert, 2013). Volant taxa must fly under a diversity of atmospheric conditions, and the range of transient responses is likely to be similarly variable and taxon-dependent. One of the problems of studying such rapid and unsteady aerial tasks is that of standardization; the temporal and spatial structure of the physical challenge as well as patterns of animal behavior can be difficult to repeat systematically within an experimental context. In this regard, the flight of hummingbirds

presents a unique opportunity, given that their obligate nectar-feeding habits enable a high level of repeatability for spatially constrained flight trajectories if they are given suitable reward. Multiple perturbation trials per individual can thus be obtained using similar initial dynamic conditions.

Here, I challenged Anna's Hummingbirds (*Calypte anna*) to fly through an artificial vertical gust of air, and measured both wing and body kinematics as they transited this disturbed region. I identified a spectrum of behavioral responses, with one extreme dominated by wing flapping (which I refer to as wing-dominated) and the other by tail fanning with stationary wings (which I refer to as tail-dominated). Because the wing-dominated technique incorporates continuous wing motion, birds may be able to retain flight control when using this technique. I therefore hypothesized that use of the wing-dominated technique would reduce the pitch perturbation imparted by the air knife compared to the tail-dominated technique in which the wings were tucked above the body. Because the tail is also angled upward and fanned in the tail-dominated technique, the upward gust on the tail likely produces an upward and forward force on the tail. Thus, I also hypothesized that the tail-dominated technique would enable faster transits than the wing-dominated technique, albeit with a greater pitch perturbation. Finally, because the tail was always deflected upward during gust traversal in hummingbirds, I tested the hypothesis that a bio-inspired and passively deflectable tail would enable a model glider to successfully negotiate the same gust.

2.2 Materials and Methods

Filming and kinematic analysis

Individual birds were placed inside a mesh flight arena (30 × 40 × 130 cm) with an artificial flower at one end and a perch (30 cm from the mesh of the arena floor) at the other (Figure 2.1 B). A vertically oriented airknife (6" Super Air Knife, model #110003, Exair Corp., Cincinnati, OH, USA) was positioned in the center of the flight arena; when activated by a constant air pressure (18 psi), this device produced a wedge of fast-moving air (Figure 2.1 A, C) that was nominally uniform along the crosswise axis of the arena. Birds within the flight arena volitionally flew from the perch to feed at the flower, and then returned to the perch. Following a 2 min period of habituation, the airknife was turned on while the bird was on the perch. Following a minimum of five consecutive transits, a series of flights through the gust in both directions was recorded using two orthogonally positioned high-speed video cameras (HiSpec1 2G Mono, Fastec Imaging Corporation). Synchronized videos were recorded at 500 Hz, and with a shutter speed of 200 μs. Videos were saved and evaluated in an uncompressed AVI format. Flights were recorded from a total of four adult male Anna's Hummingbirds (mean body mass of 4.46 g), and for a total of 38 trials (range of 8–10 per bird).

Landmarks on birds (Figure 2.2) were digitized in each frame for three-dimensional reconstruction of wing and body kinematics using DLTdv5 (Hedrick, 2008) and custom MATLAB (Mathworks) scripts. The base of the beak and the tail base were used to define the body lon-

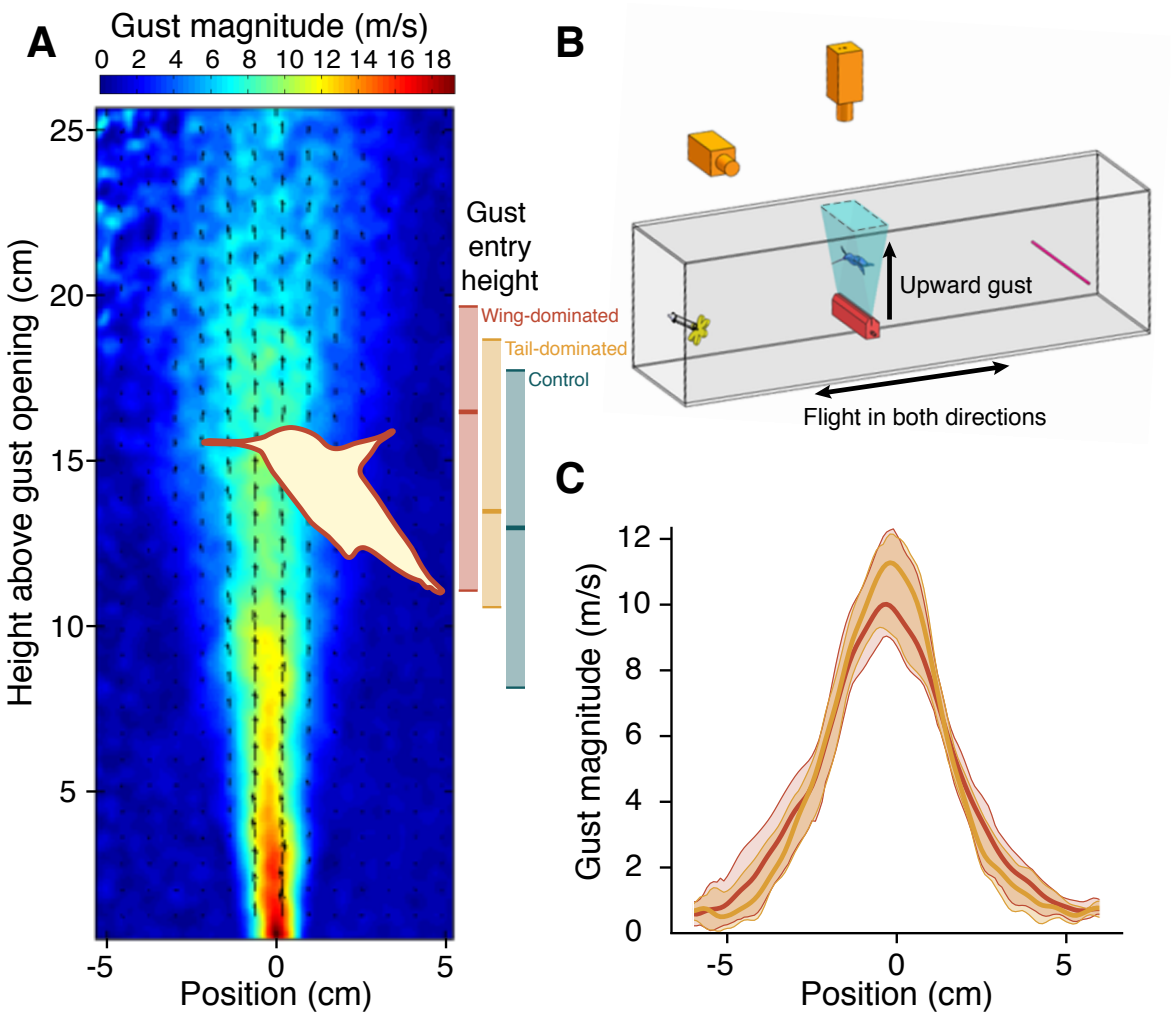

Figure 2.1: Experimental setup and characterization of the upward gust. (A) Averaged velocity vector field of the air jet, with a hummingbird outline at typical entry height overlain for scale. Red, yellow, and green bars to the right show mean and 5th and 95th percentile entry heights for wing-dominated, tail-dominated, and control trials, respectively. (B) Diagram of the flight arena. The gust generator (in red) was located at bottom center of a 130 $\times$ 30 $\times$ 40 cm mesh arena. Two high-speed cameras were mounted orthogonally at 80 cm above and lateral to the gust disturbance. Hummingbirds were trained to fly through the inactive disturbance zone (in blue) between the perch and nectar source before beginning experimental trials. (C) Mean airspeed profile along the horizontal axis at the corresponding entry height for all wing- and tail-dominated trials (shown by thick red and yellow lines, respectively). Shading indicates the 5^{th} to 95^{th} percentile of gust magnitude experienced by birds along each profile.

gitudinal axis (i.e., the x-axis), with the former point treated as the origin of the body-fixed coordinate system. The z-axis of the body was aligned in the sagittal plane perpendicular to the x-axis, and the y-axis was then determined using the right-hand rule. Flapping motion of the wings were characterized using three angles: the elevation angle (θ), sweep angle (ϕ), and rotation angle (α) about an axis connecting the wing base and wing tip (see Figure 2.2). The elevation angle is positive when the wing span axis lies dorsally, whereas the sweep angle is positive when the wing span is positioned anteriorly. Pitch of the body relative to the global horizontal (χ; 2.2 A) is positive when the body pitches up, according to the right-hand rule. Deflection of the tail relative to the longitudinal body axis (α_{tail}) was determined from the orientation of tail tip and base (Figure 2.2 A) relative to the longitudinal body axis, and was assumed to be positive when the tail was deflected upwards. The tail extension fan angle was estimated from the landmarks of the tail base and the lateral tip of the tail (Figure 2.2 B). The wing rotation angle was defined to be positive when the leading edge of the wing surface plane (defined by three landmarks: the wing base, wing tip and the tip of primary feather #4; see Figure 2.2 B) was rotated upwards relative to the horizontal.

High-speed videos of gust transits from the four birds yielded trajectory data for 11–22 gust transits and for 2–6 control trials per bird (87 transits in all). For each trial, the minimum body angle attained following gust transit (χ_{min}) was used to quantify the overall effects of perturbation. For synchronization, time zero of each trial was defined as the moment when the beak base crossed the virtual geometric centerline of the gust (see Figure 2.3), and gust transit was assumed to be complete when the trailing tip of the tail subsequently crossed this virtual line. I then compared mean values of wing elevation angle and sweep angle within a normalized time bin in the middle range of the gust transit (i.e., $t = 0.5$ to 0.7) for the two strategies. For each transit, a wing holding time (t_{hold}) was also defined as the ratio of the duration that wings were elevated and held posteriorly (i.e., elevation angle $< 0^\circ$ and sweep angle $> 0^\circ$; see Fig. 3) relative to the entire duration of each transit, and was compared for the two strategies.

Statistics

I first clustered gust entry height, wing holding, tail fan angle, and tail pitch angle data into discrete strategies using Gaussian mixture models in the "mclust" package in R (*mclust Version 4 for R: Normal Mixture Modeling for Model-Based Clustering, Classification, and Density Estimation, 2012*; Fraley and Raftery, 2002). The number of mixture components, as well as the size, axes, and shape of the distributions, were selected by choosing the model with the maximum Bayesian Information Criterion value. To test whether various performance metrics were different among the three strategies (two associated with the gust trials, and one with control trials), I used two-way ANOVAs with individual as a factor, and implemented Tukey pairwise comparisons. I use linear models to assess differences in technique variables between gust-on and gust-off treatments. Reported P values are for tests of the corresponding effect after all other main effects have been included (i.e., they are Type II sums of squares). I also make the a priori assumption that there is no interaction between

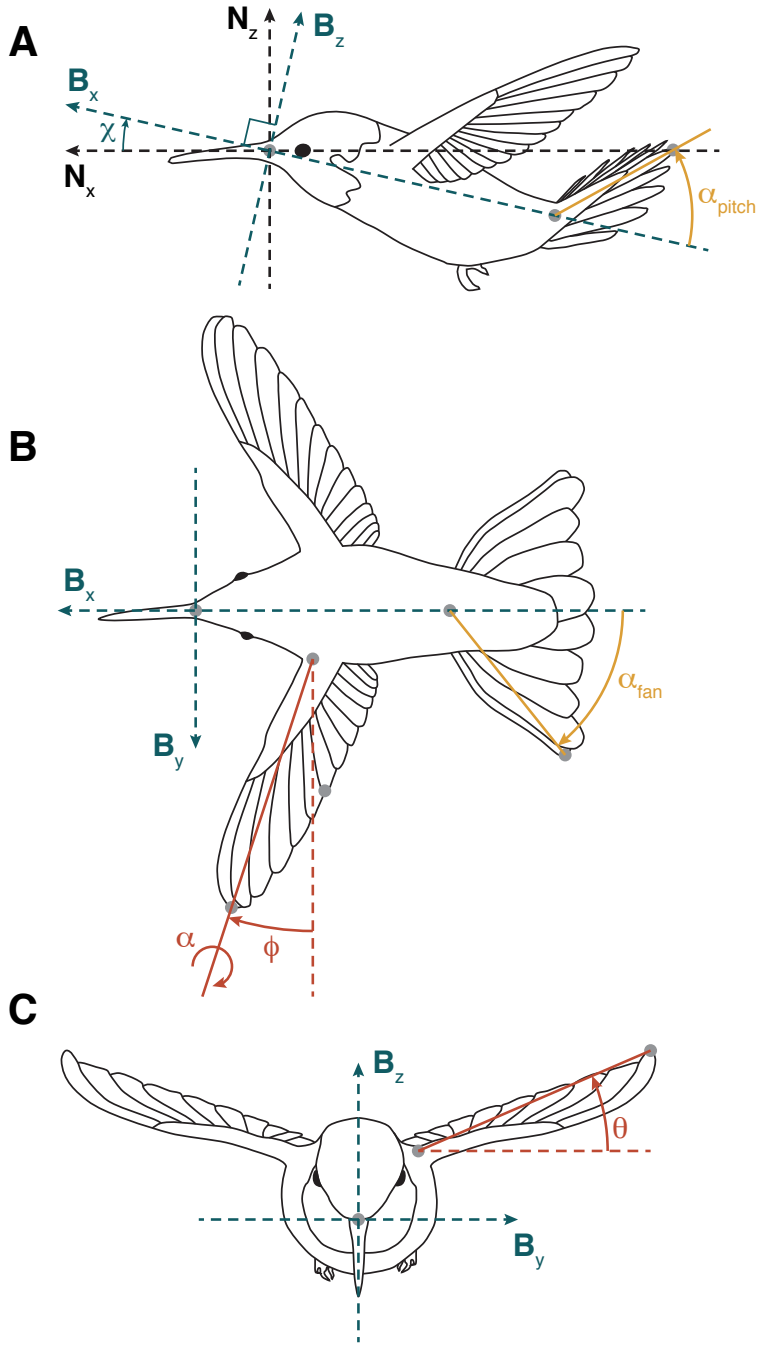

Figure 2.2: Kinematic parameters and body and wing landmarks (gray points) used in digitization. (A) Lateral view of a hummingbird showing the vertical ($\mathbf{N}_z$, $\mathbf{B}_z$) and forward ($\mathbf{N}_x$, $\mathbf{B}_x$) axes in the global and body-fixed coordinate systems, respectively, along with the body angle (χ, in green) and tail deflection angle (α_{pitch}, in yellow). Note that positive $\mathbf{N}_z$ is downward following aeronautical convention. (B) Dorsal view of a hummingbird showing angles of wing sweep (ϕ, in red), wing span rotation (α, in red), and the tail extension angle (α_{fan}, in yellow). (C) Frontal view of a hummingbird in the body coordinate system showing wing elevation angle (θ, in red).

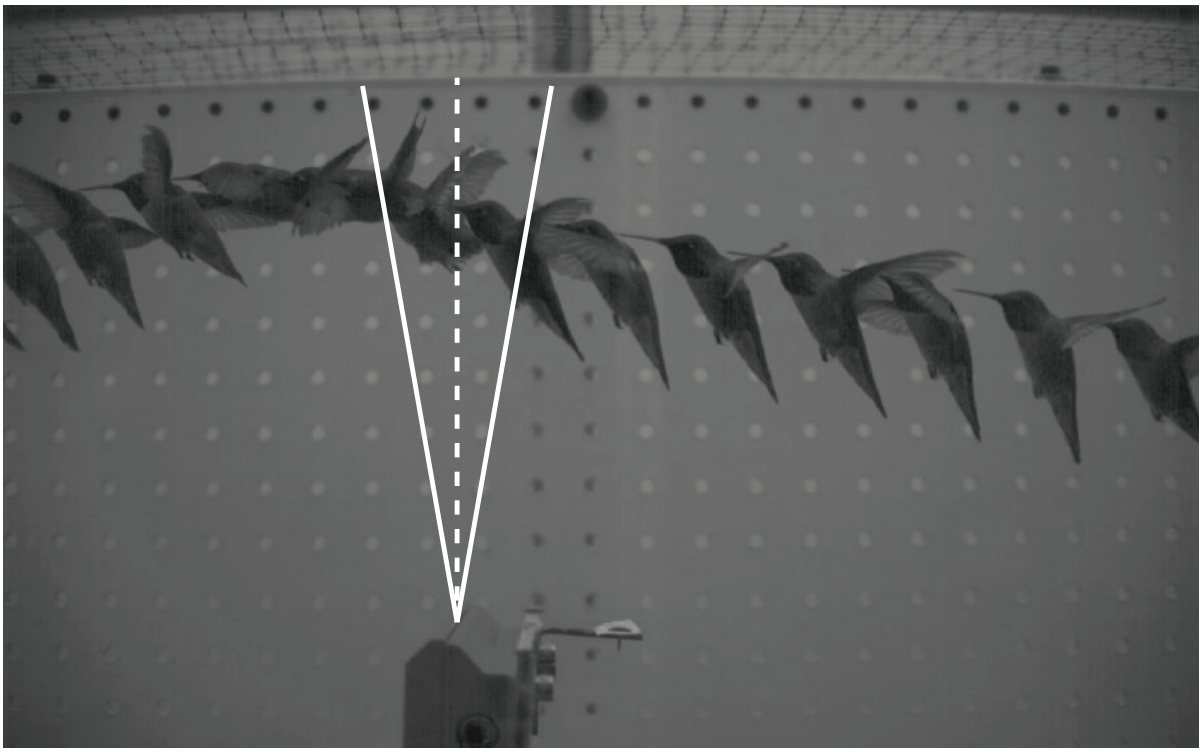

Figure 2.3: A photomontage using one representative recording of gust transit (interval between frames is 40 ms). The white dotted line indicates the central plane of the gust, and the solid white lines indicate the approximate gust margins. Gust entry (i.e., $t = 0$) is defined as the moment when the beak base of the bird passed through the central plane.

strategy and Bird ID because other physical and morphological factors not captured by wing and body kinematics (e.g., sex and size) were very similar among birds.

Because gust entry conditions could potentially confound any observed relationship between technique and trajectory, I analyzed response as a continuous variable. To control for experimental variables (trial number, flight direction, bird identity, and presence of the air gust) and gust entry conditions (gust entry height, bird velocity, and initial body angle) I first used these variables as predictors in linear models, using technique variables (tail fan and pitch angles, wing elevation and sweep angles, and percent wing holding) and trajectory variables (transit duration and minimum body angle) as response variables. I then conducted Pearson's product-moment correlation tests between residuals of these models by selecting sets of residuals from one of the technique models (i.e., percent wing holding, tail fan angle, or tail pitch angle; wing elevation and sweep angles were both highly correlated with percent wing holding, so percent wing holding was selected as a proxy for this dimension of technique) and from one of the trajectory models (i.e., transit duration or minimum body angle). All P values were corrected for false discovery rate (Benjamini and Yekutieli, 2001). Residuals of all models except for those corresponding to wing sweep angle satisfied

normality assumptions.

Glider model

A mechanical glider (Figure 2.4) was built as a physical model from balsa wood with a total mass of 2.6 g. In some trials, weight was added (Figure 2.5 A) so that the total mass was 4.3 g, which is comparable to those of male Anna's hummingbirds (4–6 g). The tail area (430 mm^2) was intermediate to a typical hummingbird's folded ($\sim$ 200 mm^2) and fully fanned tail ($\sim$ 500 mm^2). A counterweight near the front of the glider was used to adjust the center of mass and to effect stable gliding.

The tail was mounted onto the body with a small hinge that enabled passive upwards deflection. A small magnet (11 mg) was embedded in the fuselage of the glider directly below the center of the tail. An identical magnet was glued to the bottom of the tail in line with the embedded magnet. The relative force required to deflect the tail was modulated by inserting either a third magnet or a balsa wood shim of the same thickness into the gap between the fuselage and tail magnets. The third magnet provided a strong enough attachment force that the tail did not deflect when hit by the gust. The balsa wood shim provided enough force to keep the tail fixed during normal flight, but it was easily deflected when the glider encountered the upward gust. The wings of the glider were rigidly mounted using stronger magnets. The glider was launched from a wooden platform with rubber band stretched between two posts (Figure 2.5 B). The wooden platform was leveled with a calibrated iPhone inclinometer. The glider was drawn back to and released from the same location every trial, which ensured equivalent launch position and launch angle for all trials. A total of eight glides was recorded for each of four trial types: control (i.e., the wind gust was turned off) with both fixed and deflectable tail configurations, fixed tail, and deflectable tail. Trials were filmed at 500 fps using three high speed cameras. Two cameras had wide angle (25 mm) lenses while the third had a zoomed (50 mm) lens, which provided a close-up of the tail motion during transit. Cameras were calibrated using functions provided with MATLAB's Computer Vision System Toolbox (The MathWorks, Inc., 2016). Trajectories of the front and rear markers were reconstructed in three dimensions, and the tail pitch angle was obtained from the close-up camera.

Glider entrance velocity into the gust averaged 3.01 ± 0.11 m/s (mean $\pm$ SD for this and following results) at an angle of $8.5 \pm 1.9^\circ$ below the horizontal. Mean body angle upon entrance averaged $-0.2 \pm 2.9^\circ$. These values did not differ significantly between the two control conditions (t-tests: entrance speed, $P = 0.76$; entrance angle, $P = 0.69$; entrance body angle $P = 0.37$); control trials were thus pooled for subsequent trajectory analyses. Furthermore, entry trajectory metrics did not differ significantly between the fixed and deflectable tail treatments (t-tests: entrance speed, $P = 0.40$; entrance angle, $P = 0.93$; entrance body angle $P = 0.39$), nor did they differ significantly among the four experimental and control conditions (ANOVAs: entrance speed, $P = 0.094$; entrance angle, $P = 0.422$; entrance body angle, $P = 0.19$).

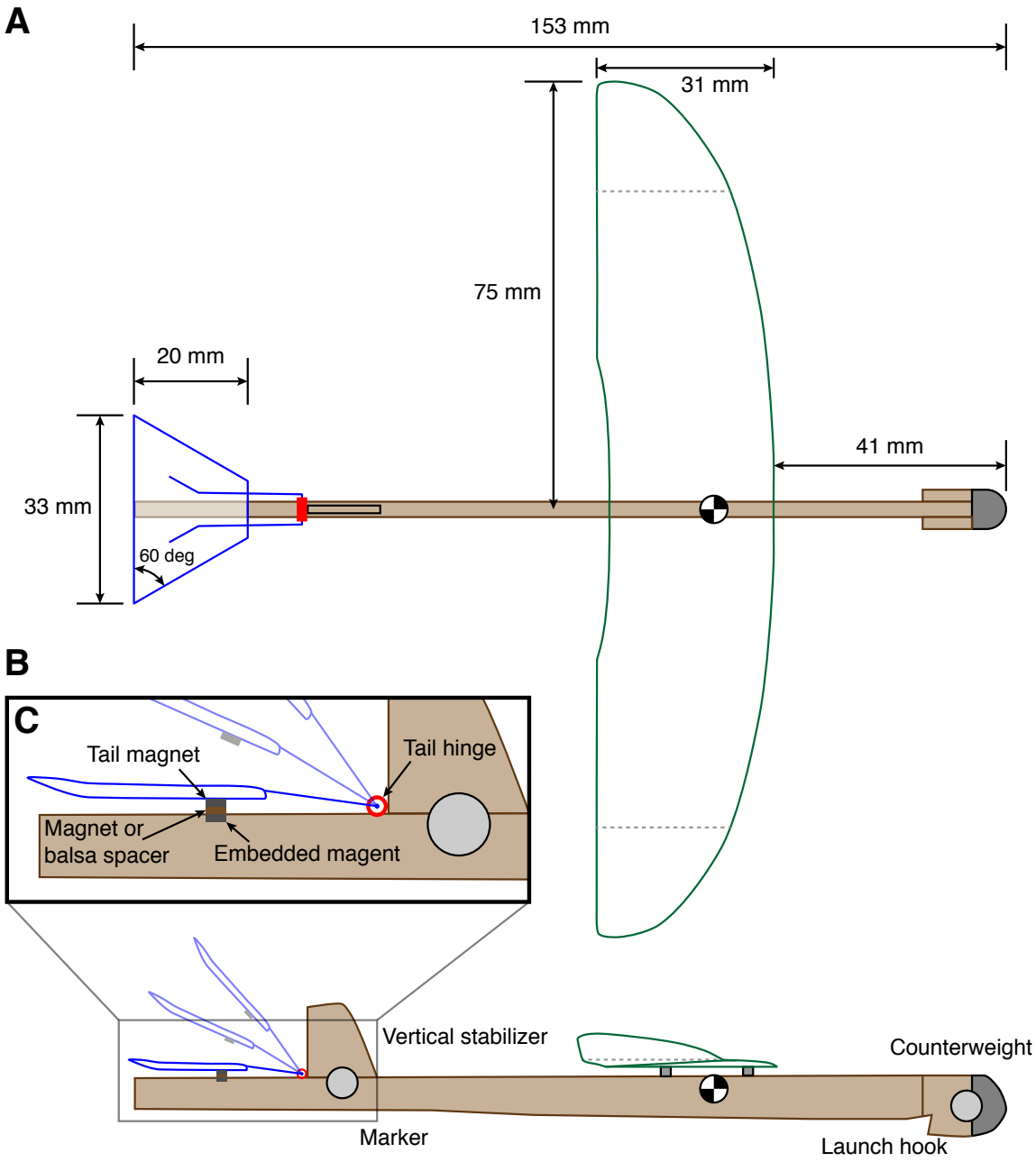

Figure 2.4: Top (A) and lateral view (B) of the model glider. The tail (in blue) can rotate passively around the hinge (in red) under aerodynamic forces imposed by the upward gust. Absent the gust and after gust transit, the tail was held fixed by the attracting force between the tail and embedded magnets (C). This attraction force was modulated by either inserting another magnet or a balsa spacer, which prevented or allowed the gust to deflect the tail, respectively. A counterweight near the front of the glider was used to adjust the center of the gravity so as to effect stable flight.

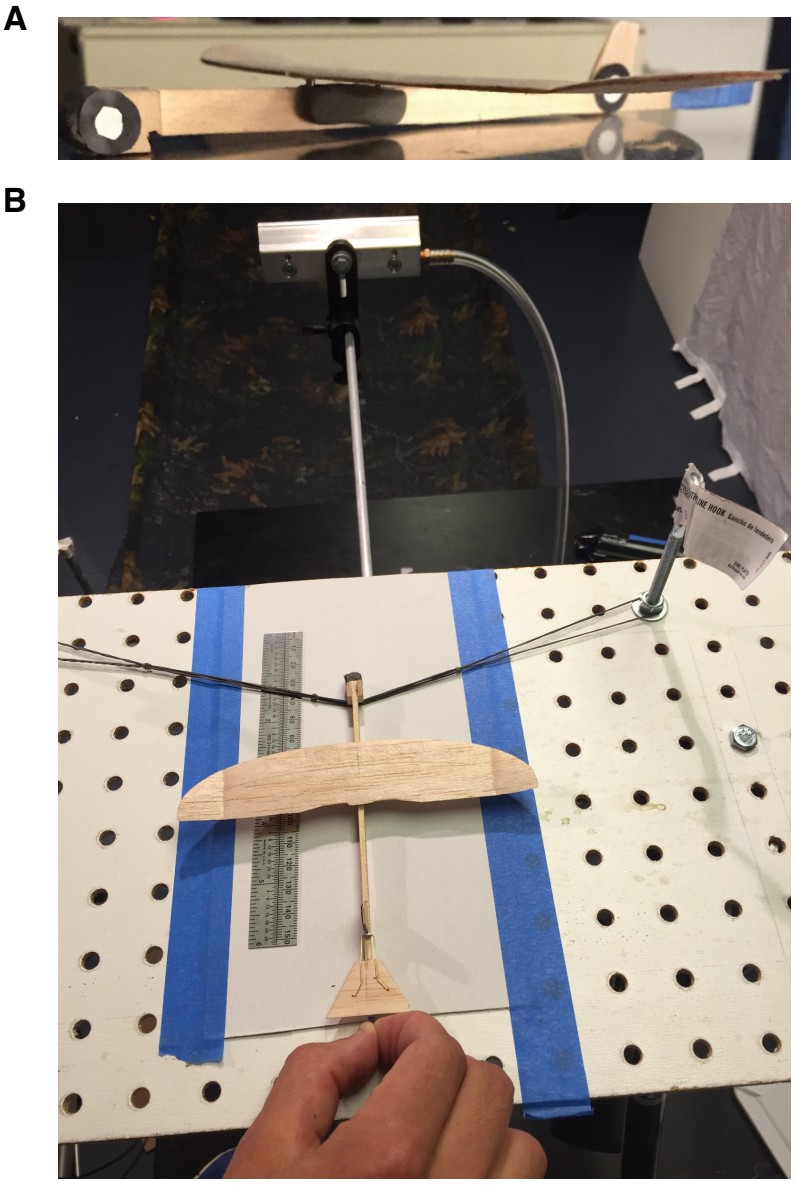

Figure 2.5: In some trials, weight was added (A) so that the total mass was 4.3 g, comparable to those of male Anna's hummingbirds (4–6 g). Gliders were launched from a platform using a band stretched between two pegs (B). Gliders were released from the same position for trials within each glider configuration.

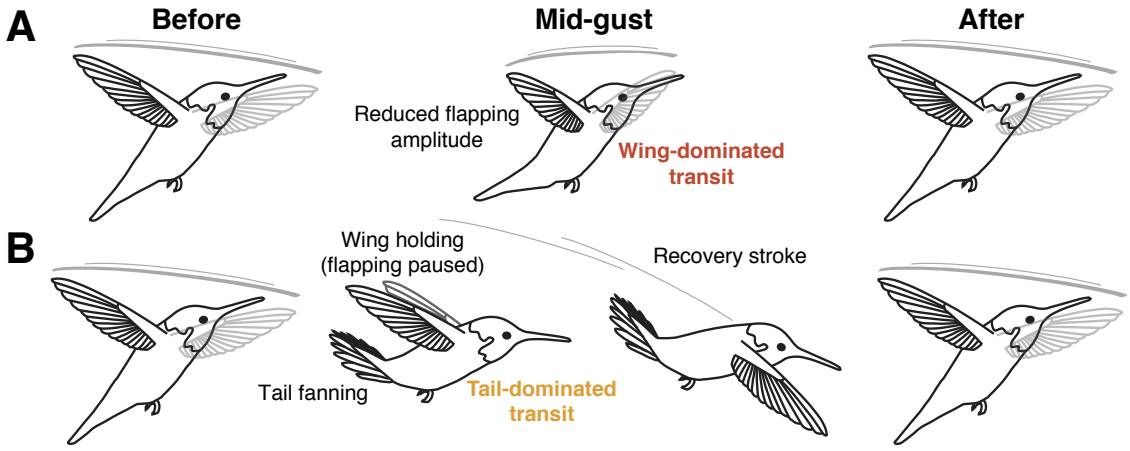

Figure 2.6: Two general methods are used in gust traversal: (A) the wings-dominated case during which the wings are continuously flapped and tail fanning is limited, and (B) the tail-dominated case in which the wings are held stationary at the top of upstroke with variable tail fanning, and with wing flapping resuming post-traversal. In most wings-dominated trials, the minimum body angle occurred during gust traversal; for most of the tail-dominated cases, minimum body angle occurred post-traversal ($P < 0.001$).

2.3 Results

Wing- and tail-dominated responses to perturbation

Two general control strategies were used by hummingbirds when transiting the vertical gust (Figure 2.6). I first performed a clustering analysis to assess the relationships between initial conditions and trajectory variables. A maximum Bayesian Information Criterion (BIC) Gaussian mixture model incorporating gust entry height, wing holding (defined as the fraction of time in the gust that the wings were both elevated and swept posteriorly), tail fan angle, and tail pitch angle data partitioned control kinematics and gust maneuvers into three clusters (Figure 2.7 A). In wing-dominated responses (first technique cluster), wings were flapped mostly anterior to the wing base with low-amplitude strokes, and the tail was elevated, but remained un-fanned or minimally fanned (Figures 2.6 A, 2.7 A). Alternatively, in tail-dominated responses (second technique cluster), wings were retracted posteriorly and held still above the body while the tail was simultaneously elevated and fanned (Figures 2.6 B, 2.7 A). The wingbeat flapping cycle was then resumed following transit of the gust.

Dorsoventral deflection of the tail was observed in all gust transits (average upward deflection angle of 26° compared to unperturbed flight; range 6.7°–41.5°). Relative to control trials, which formed the majority of the third technique cluster, birds transiting the gust (with either technique) had significantly higher tail pitch angles ($\beta = 29.2°$, $P < 0.0001$) and tail fan angles ($\beta = 13.0°$, $P < 0.0001$) after controlling for individual, flight direction, and

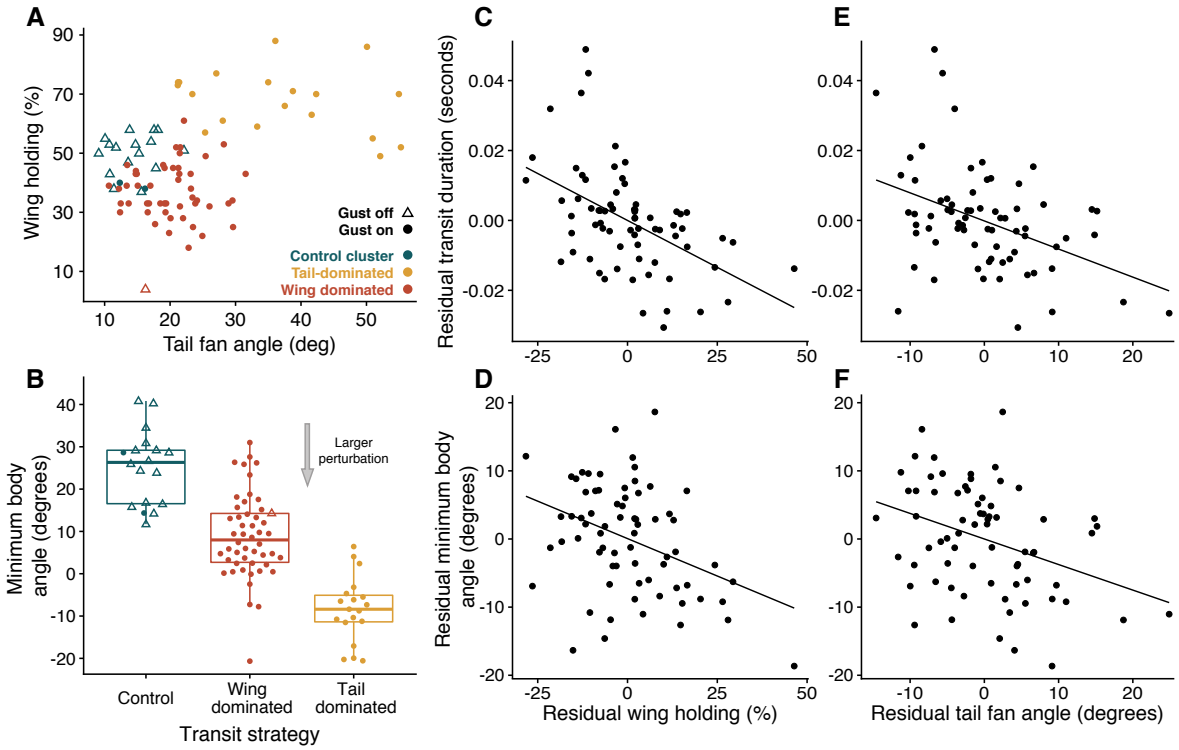

Figure 2.7: Effects of control strategy on transit duration and minimum body angle before recovery. (A) Wing and tail kinematics data were classified into control strategy clusters using Gaussian mixture models (see text), with the number of clusters selected using the Bayesian Information Criterion. Wing holding is defined as the percentage of transit time that the wings were both elevated and swept backward relative to the total time the bird was within the gust (i.e., the transit duration). The "control" cluster (green) is largely composed of control trials for which the gust was turned off (open triangles, 16 out of 18 trials in the cluster). Note that clusters appear to overlap because data points and clusters are projected from four dimensions onto two. (B) Relative to control trials (open triangles), gust transits (filled circles) resulted in intense downward perturbations to body angle ($P < 0.001$). Gust-associated pitching (i.e., a lower minimum body angle) was significantly more pronounced for the tail-dominated response than for the wing-dominated response (yellow vs. red; $P < 0.001$). After controlling for gust entry height and velocity, bird identity and other experimental variables (see text for details), greater wing holding and tail fan angle (i.e. a shift towards a tail-dominated strategy) significantly decreased transit duration (C and E, respectively) and resulted in a much larger pitch perturbation (D and F, respectively).

trial number. Wing holding and wing elevation and sweep angles exhibited a larger range among perturbation trials (holding: 70%, elevation: 45°, sweep: 71°) than among control trials (holding: 54%, elevation: 29°, sweep: 22°), but their means were not significantly different from controls ($P > 0.5$ in all cases). Note that I do not compute between-cluster statistics for entry height and technique variables because these variables were used to form clusters, and performing such comparisons after clustering would inflate the false-positive rate. Although mean wing elevation and sweep angles were independent of the presence of the gust, wing elevation angles differed significantly between wing- and tail-dominated responses (mean 5.7° and 18.0°, respectively; two-way ANOVA with Tukey's post-hoc test, wing vs. tail: $P < 0.001$, individual effect: $P = 0.24$). Wing elevation angles under unperturbed flight (mean 4.5°) were not significantly different from those under wing-dominated responses ($P = 0.08$), but were different from those under tail-dominated responses ($P = 0.017$). Wing sweep angles (ϕ) were similarly different between wing- and tail-dominated responses (4.07 and $-20.1°$, respectively; wing vs. tail: $P < 0.001$, individual effect: $P = 0.96$). Wing sweep angles under unperturbed flight ($-0.71°$) were not significantly different from those under wing-dominated responses ($P = 0.14$), but were different from those under tail-dominated responses ($P < 0.001$). Thus the wings were generally positioned anteriorly for wing-dominated responses but posteriorly for tail-dominated responses. The presence of the air gust significantly increased entry height (linear model; $\beta = 8.60$ mm, $P < 0.001$), vertical entry speed ($\beta = 0.02$ m s^{-1}, $P = 0.015$), and initial body angle ($\beta = 0.048°$, $P < 0.001$), but horizontal speed was not significantly affected ($\beta = 0.105$ m s^{-1}, $P = 0.06$), after controlling for bird identity, flight direction and trial number.

Upward gusts cause intense pitch perturbations

Gust-associated pitching was significantly more intense for hummingbirds using the tail-dominated response (mean minimum body angle = -8.4°) than for those using the wing-dominated response (mean minimum body angle = 9.3°; tail vs. wing: $P < 0.001$, individual effect: $P = 0.012$; Figure 2.7 B). In fact, when using the wings-dominated response, the minimum body angle ($\chi_{\min}$) was usually attained within the gust (20 out of 21 trials), whereas $\chi_{\min}$ for the tail-dominated response was typically reached after passing through the gust (14 out of 17 trials; Chi-square test, $\chi = 20.5$, $P < 0.001$). Regardless of technique, transits through the gust resulted in intense pitch perturbations relative to control trials (mean minimum body angle for control trials = 24.9; $\beta = -23.4°$, $P < 0.001$). As expected, birds also exhibited a larger pitch perturbation (i.e lower minimum body angle) when they entry height was closer to the gust opening ($\beta = 0.276°$ mm^{-1}, $P = 0.004$).

Transit duration increased when the air gust was on ($\beta = 0.0684$ s, $P = 0.012$), and was also higher when horizontal entry speed was lower, as expected ($\beta = -0.0603$ s^2 m^{-1}, $P < 0.001$). Transit duration was not significantly different between wing- and tail-dominated strategies ($P = 0.23$), but did vary among individuals ($P < 0.001$). There were no significant differences between the two gust-associated strategies in initial horizontal velocity ($P = 0.31$, individual effect: $P < 0.001$). The initial flight path, however, was inclined upward for the

tail-dominated technique relative to the other two techniques (tail vs. control: $P < 0.001$, tail vs. wing: $P = 0.008$, individual effect: $P = 0.15$). Furthermore, entrance height above the aperture of the gust generator was slightly greater for the wing-dominated strategy compared to the tail-dominated strategy (mean±s.d. [range], 164.5±26.3 [95, 208] mm vs. 135.3±26.1 [101, 191] mm; Figure 2.1 A), and also varied significantly among birds ($P < 0.001$). Mean jet speed evaluated at the entry height of all tail-dominated trials averaged 5.62 m/s (maximum 10.01 m/s), whereas that for entry heights of all tail-dominated responses averaged 5.69 m/s (maximum of 11.28 m/s). The greater entrance heights for the wing-dominated strategy thus corresponded to a mean gust speed increase of only 0.07 m/s, or about 1% of the overall flow experienced by transiting birds (for peak gust magnitude, the equivalent numbers were 1.27 m/s and 12.7%, respectively).

Wing-holding and tail fanning enable faster transits, but at the cost of greater perturbations in pitch

Because the highest BIC clusters were not completely isolated (Figure 2.7 A), and because gust entry conditions could potentially confound any observed relationship between technique and trajectory variables, I also assessed response as a continuous variable on the subset of trials for which the gust was present. I included initial entry height above the gust opening, entry velocity (V_x, V_z), and initial body angle, along with individual bird identity, flight direction, and trial number as predictors in linear models, with transit duration, minimum body angle, percent wing holding, tail fan angle, or tail pitch angle as the response variable. The ensuing residuals from these models were then used to assess associations between technique and performance variables. Note that percent wing holding, wing elevation angle, and wing sweep angle were all highly correlated ($r > 0.6$ and $P < 0.001$ in all cases). Percent wing holding was therefore selected as a proxy for this dimension of technique. Tail fanning and wing holding were significantly correlated ($r = 0.34$, $P = 0.021$) as were tail fanning and tail angle ($r = 0.33$, $P = 0.021$). Thus, as I found with the clustering analysis, the tail was often fanned and angled upward when the wings were held in an elevated and swept position (i.e. when percent wing holding is high). Wing holding was associated with faster transits ($r = -0.49$, $t = -4.7$, d.f. $= 85$, $P < 0.001$; Figure 2.7 C) and greater perturbations in pitch (i.e., lower minimum body angle; $r = -0.38$, $t = -3.4$, d.f. $= 85$, $P = 0.011$; Figure 2.7 D), indicating that greater wing holding may result in a more intense pitch perturbation. Tail fan angle was similarly associated with faster transits ($r = -0.41$, $t = -3.7$, d.f. $= 85$, $P = 0.005$; Figure 2.7 E) and greater perturbations in pitch ($r = -0.36$, $t = -3.2$, d.f. $= 85$, $P = 0.014$; Figure 2.7 F), indicating the greater tail fanning may also result in a faster transit, albeit with a more intense perturbation in pitch. Although tail angle was significantly correlated with tail fanning, it was not significantly correlated with either trajectory variable ($P > 0.5$ in both cases). These results agree with those reported above for the clustered strategies while simultaneously controlling for multiple possible confounding variables. The tail-dominated strategy, which was typified by greater wing holding and tail fanning relative

to the wing-dominated strategy, was thus reliably associated with faster transits and with more intense perturbation in pitch.

A deflectable tail improves upward gust rejection in a model glider

The effectiveness of tail deflection in response to upward gusts was demonstrated empirically through the use of a dorsally deflectable tail on a glider model (Figures 2.8, 2.4). Mean post-gust body angles of the glider in the deflectable tail condition were not significantly different from those of observed with the gust turned off and with the glider in either the deflectable ($P = 0.094$) or fixed tail condition ($P = 0.79$). Body angle decreased significantly (i.e., the body rotated nose downward) when the tail was held fixed ($P < 0.001$; Figure 2.8). These results were qualitatively similar for a glider carrying additional mass, so that its total mass was comparable to that of a hummingbird (Figure 2.9), and for a glider launched downward at -15° rather than horizontally (Figure 2.10).

2.4 Discussion

Gust rejection and recovery from gust-induced perturbations

Mid-air disturbance is commonplace for animals flying within the atmosphere, and requires compensatory kinematics. Here, hummingbirds traversing a fast vertical gust used two general control strategies. Although the wing-dominated response was 14 ms (15%) slower on average than the tail-dominated response (Figure 2.7 C, E), the minimum body angle was 17 degrees higher (9 degrees vs. -8 degrees). Thus, the tail-dominated response, in which wings were held stationary behind the body and the tail was fanned, was associated with faster transits, but also resulted in more intense downwards pitching of the body (Figure 2.7 B). Dorsal elevation of the transiently static wings in this condition decreased the projected wing span relative to the oncoming flow, and likely also improved stability in roll and yaw (Hedrick, Cheng, and Deng, 2009). Following gust passage, body pitch was recovered via aerodynamic torques generated by the subsequent one to three wingbeats. Similar to escape maneuvers, the majority of the pitching torque is likely produced during these recovery downstrokes (Cheng et al., 2016a; Cheng et al., 2016b). As in pigeons, exchange of angular momentum between the wings and body (i.e. inertial effects) is unlikely to explain body reorientation during recovery because of the relatively low moment of inertia of the hummingbird wings about the center of mass compared to that of the body (Ros et al., 2015). Body motions could also control body pitch. By exchanging angular momentum between the abdomen and thorax, hawkmoths are able to tilt their stroke plane and redirect aerodynamic forces without first generating aerodynamic torques (Dyhr et al., 2013; Penskiy et al., 2012). The internal anatomy and mass distribution of a hummingbird body are very different from that of a hawkmoth, however and more experimentation is needed to determine the extent to which hummingbirds use body motions for flight control.

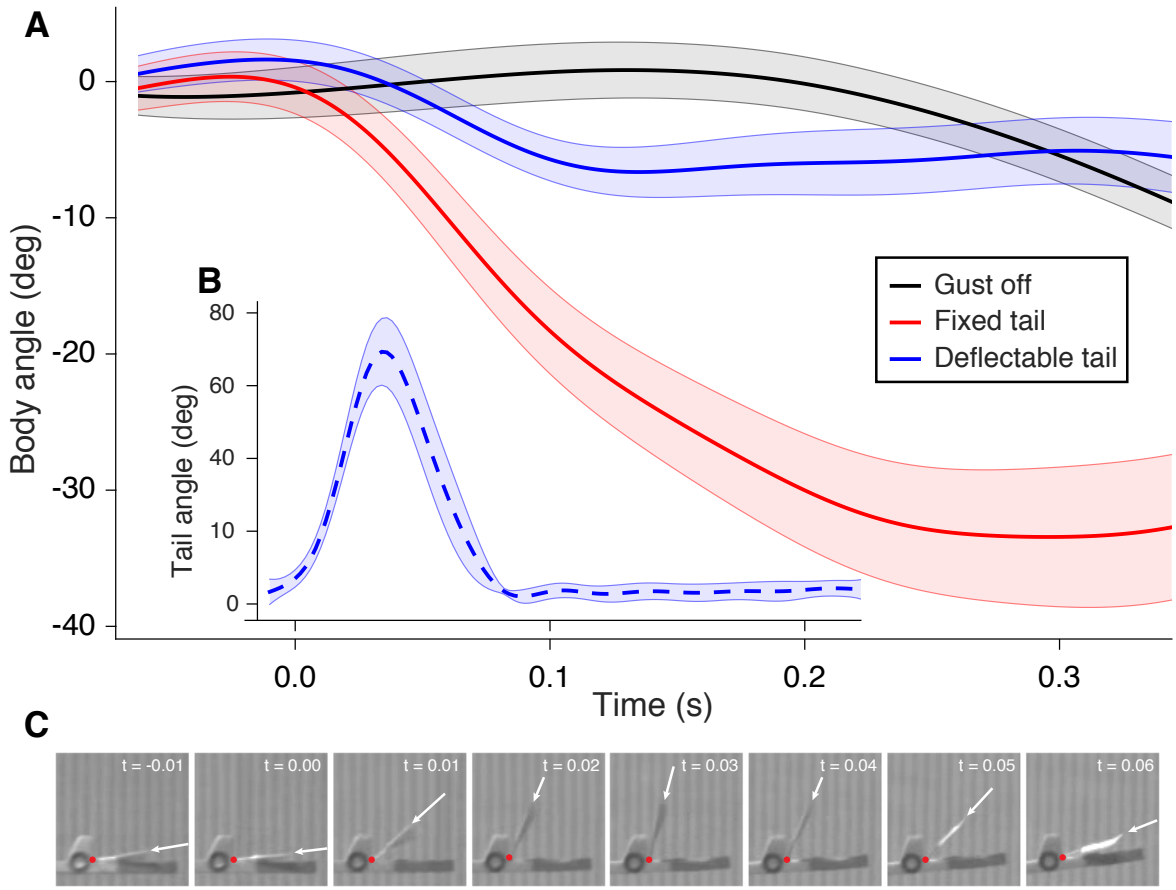

Figure 2.8: A deflectable tail improves pitch stability of a glider in gust traversal. The glider is launched horizontally with a body angle near 0°. (A) Absent a vertical gust (in black), the glider exhibits only slight upwards and downwards changes in pitch. In a vertical gust, the glider with a fixed tail (in red) pitches up when its wings encounter the airflow (at about -0.03 s), but then dives when the tail encounters the gust ($\sim$ 0.00 s). The glider with a deflectable tail (in blue) avoids this downward pitching torque because the tail deflects upward with the gust (B, C). (C) Close-up view of the rear portion of the glider as the tail deflects upward after encountering the upward gust. In each frame, the axis of rotation and tail angle are shown by the red dot and white arrow, respectively. Initial glider angle did not differ among treatments ($P = 0.19$), but the mean glider angle (i.e. body angle between $t = 0.002$ and $t = 0.344$ averaged within each trial) following gust traversal was significantly lower for the fixed tail condition compared to either of the control conditions with no gust ($P < 0.001$ in both cases) or with the deflectable tail ($P < 0.001$). There was also no significant difference between the deflectable tail and either control treatment ($P = 0.094$, $P = 0.79$). Lines and colored bands indicate mean values and 95% confidence intervals (n = 8 each for fixed and deflectable treatments, n = 16 for control), respectively. All statistical tests are one-way ANOVAs with Tukey pairwise comparisons.

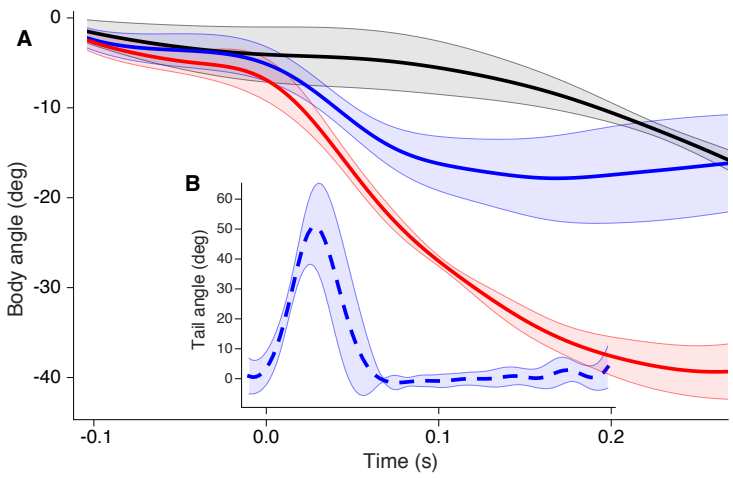

Figure 2.9: A deflectable tail also improves pitch stability of a heavier glider in gust traversal. Glider mass was increased from 2.6 g to 4.3 g by adding a small ball of clay beneath the estimated center of aerodynamic pressure of the wing. Panels and colors are described in Figure 2.8, except that here, n = 3 each for fixed and deflectable treatments and n = 6 for control.

Advantages of wing holding vs. flapping

Although transit strategy varied with gust entry height, the distributions overlap considerably (Figure 2.1 A) indicating that gust intensity is not the only factor driving transit behavior. If birds can choose their transit strategy, the correlation of transit strategy with both transit speed and pitch perturbation (Figure 2.7 C–F) may allow them to adjust their trajectory according to the relative costs of transit speed, body angle disruption, and stress on the wings. One potential advantage of wing holding (Figure 2.6 B) performed in the tail-dominated transit strategy is that it may reduce the high torque on otherwise extended wings; in aircraft, gust load may yield wing-root bending moments that may lead to wing failure (e.g., Hoblit, 1988, Moulin and Karpel, 2007). On the other hand, flapping wings may themselves mitigate the aerodynamic effects of unexpected gusts because lift fluctuations decrease as flapping frequency is increased (Fisher et al., 2016). These effects, along with the ability of hummingbirds to alter wing kinematics on a stroke-by-stroke basis (Cheng et al., 2016a), may explain why the wing-dominated technique is associated with a less intense pitch perturbation.

The role of deflectable tails in gust rejection

Some dorsoventral deflection of the tail was observed in all gust transits and likely contributed to pitch control, as passive tail deflection on the mechanical glider (Figure 2.4) yielded much higher stability (Figure 2.8). Similarly, computational modeling of steady-state forward flight for an ornithopter shows that periodic dorsoventral motions of the tail can reduce

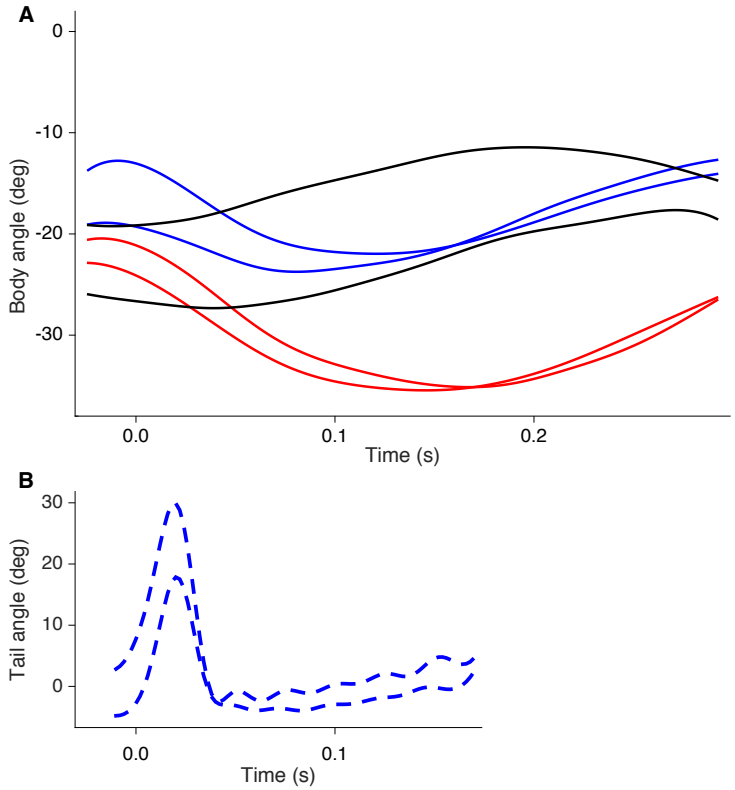

Figure 2.10: A deflectable tail also improves pitch stability for gliders launched downward at a $-15°$ angle from the horizontal. Panels and colors are described in Figure 2.8, except that here, n = 2 each for fixed, deflectable, and control treatments.

oscillations in body pitch (Lee et al., 2012). Because tail motions may involve lateral fanning as well as dorsoventral motion at variable amplitudes, a wide range of control strategies can potentially derive from a mobile tail, and deserve further investigation in both biological and technological contexts. Tails of birds are highly variable in size and shape, and likely serve a variety of mechanical functions, including stabilization, in both steady flight and in maneuvers, including gust rejection. Caudal filaments characteristic of many insect taxa may serve a similar role in stabilizing flight when transiently perturbed.

Conclusion

This study confronted hummingbirds flying horizontally with a sudden vertical gust, but animals can potentially experience aerial perturbations at any orientation, and for variable durations (Ortega-Jimenez et al., 2016). Although it is unknown whether such isolated upward gusts are common in natural aerial environments, animals flying on windy days almost certainly cross similarly sharp boundaries between high- and low-speed flows, such as when passing through eddies behind stationary objects. Given the wide range of potential aerial

disturbances found in natural environments, together with the high level of morphological diversity seen among volant taxa (and particularly insects), many different control strategies using flexible wings and tails are possible. To date, only three such studies address gust responses in volant taxa. Rapid headwind gusts induce ventral and bilaterally symmetric curling of the wings in a raptor (Reynolds, Thomas, and Taylor, 2014), whereas flying insects exposed to rapid puffs of air respond with asymmetric responses in wing motions (Vance, Faruque, and Humbert, 2013) by combining both visual and mechanosensory information (Fuller et al., 2014). As demonstrated here, even simple implementation of a rigid deflectable tail in a fixed-wing glider improves gust response. Flexible wings and tails, combined with variable kinematics, should thus yield a large and as yet undescribed set of control responses that could also be implemented in small flying machines.

Chapter 3

Aperture negotiation by hummingbirds flying with and against the wind

3.1 Introduction

Compared to manufactured robotic systems, animals display incredible robustness to environmental perturbations and can negotiate complex obstacles that have not been previously encountered. For difficult obstacles that involve the animal performing two or more simultaneous tasks, animals may develop maneuvers they have never performed before. For easier obstacles, on the other hand, a linear combination of compensatory behaviors for each individual task (i.e. doing both compensatory behaviors at the same time) may succeed. For many task combinations, however, no linear combination of maneuvers will succeed. It is in these situations that animals may develop novel locomotor strategies. Given the importance of planning and executing potentially novel locomotor behaviors, it is surprising that most studies have only addressed this question for cognitive tasks (see Reader, Morand-Ferron, and Flynn, 2016, for a recent review). Hummingbirds are well known for both their aerial agility (Altshuler and Dudley, 2002) and their ability to learn and remember the locations of rewarding flowers (Healy and Hurly, 1998; Hurly, 1996). The unique combination of cognitive and aerial abilities of hummingbirds makes them an ideal system for studying how animals develop novel locomotor behaviors.

To study whether hummingbirds would display novel maneuvers when presented with a challenge that incorporated two simultaneous tasks, I investigated how Anna's Hummingbirds (*Calypte anna*) (i) negotiate a 7 cm diameter circular aperture while (ii) flying within the test section of a wind tunnel. Individually, the compensatory behaviors hummingbirds use in (i) aperture negotiation and (ii) forward and backward flight are unlikely to produce successful transits. When negotiating apertures in still air, hummingbirds typically use one of two strategies. In the first strategy, birds stop flapping, tuck their wings toward the tail,

Table 3.1: Table of hypotheses describing how hummingbirds may compensate for the dual challenge of aperture negotiation while flying upstream in the wind tunnel.

Nominal technique	Use forward momentum	Descending trajectory	Shift stroke plane	Adjust body angle	Novel trajectory	Novel wing motions
H1: Symmetric	Yes	Yes	Neutral → tail	No	No	No
H2: Asymmetric	Yes	No	No	Upwards	No	No
H3: Asymmetric	No	Yes	No	No	Yes	No
H4: Asymmetric	No	No	Head → tail	No	No	Yes

and coast through the aperture. In the other strategy, the mean wing angle shifts forward for one wing and backward for the other wing, which is accomplished to some degree by rolling the body (Figure 3.1 B). The anatomical stroke plane remains relatively constant throughout transit, with wing trajectories following predominantly elevation and depression motions. For narrow apertures, I also observed a temporary reduction in wingstroke amplitude, which prevented wings from contacting the sides of the aperture. In both of these transit strategies, birds rely on initial horizontal momentum to carry them through the aperture because the net force production remains approximately vertical. If a bird attempted to transit using either of these techniques while flying upstream, horizontal deceleration from aerodynamic drag on the wings and body (Figure 3.1 B) could halt and reverse forward motion before transit is completed (this is not the case for downstream flights). One hypothesis is that birds will build up enough forward momentum in the unconstrained space downstream of the aperture to carry them through the aperture before the decelerating effects of drag reverse the flight trajectory (See H1 and H2 in Table 3.1). If the symmetric technique is used, no vertical forces are produced either (with the possible exception of lift produced by the body itself) and the bird will likely descend throughout transit. Note that the first two hypotheses require neither novel trajectories nor novel wing motions.

If birds cannot build up enough forward momentum to complete transit, they must produce forward thrust—as they do in forward flight—to offset drag while negotiating the aperture. In steady forward flight, hummingbirds rotate their stroke plane into the wind (Figure 3.1 C). Tilting the stroke plane directs thrust upward and forward to balance the simultaneous needs to offset gravity and drag, respectively. For forward flight at 3 m/s, the angle between vertical and the normal to the stroke plane is about 21 degrees (i.e. the stroke plane is tilted 21 degrees into the wind). For hovering, this angle is lower (about 10 degrees), and for backward flight at 3 m/s, the stroke plane is nearly level (about 0.1 degree into the wind). Unlike most other birds, however, hummingbirds have a large and highly rigid handwing (Greenewalt, 1960; Hedrick et al., 2012), which cannot bend at either the

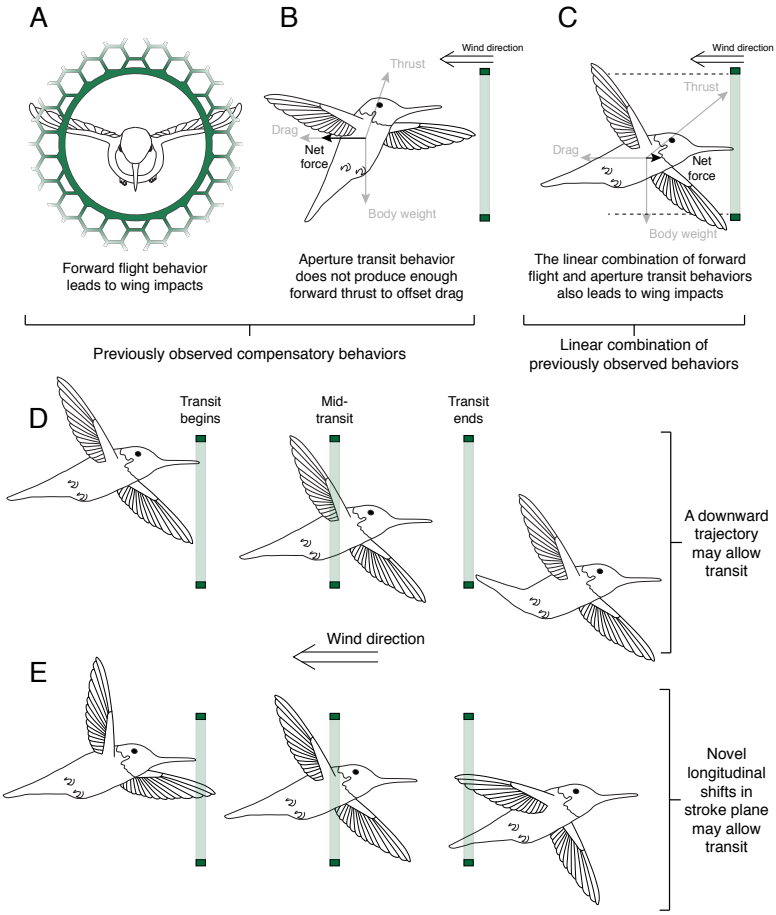

Figure 3.1: Geometric constraints and hypothesized solutions for aperture negotiation while flying upstream in the wind tunnel. (A) Frontal sketch of a bird approaching the aperture. If the stroke plane were simply inclined into the oncoming wind, as it is during normal forward flight, transit would not be possible because the wingspan ($\sim$ 12 cm) is greater than the diameter of the aperture (7 cm). (B) Side view of a bird in the rolled asymmetric posture used to negotiate apertures in still air (from this view wings flap in and out of the page, as they also do for C–E). In the unmodified asymmetric posture, the forward component of thrust is not enough to offset drag. (C) Side view of the linear combination of compensatory behaviors; the stroke plane is tilted into the wind and the body is in the rolled asymmetric posture used in still air. Even with wing forward and lower and the other behind and above, the vertical distance between the two wingtips may be greater than the height of the aperture, which would preclude a level flight path. (D) One hypothesized solution (H3, Table 3.1) is that birds may descend as they transit the aperture, allowing each wing to flap continuously while it is within the aperture. (E) Another hypothesized solution (H4, Table 3.1) is that birds may be able to shift the longitudinal position of their stroke plane first toward the head and then toward the tail, which would also enable continuous flapping during transit.

wrist or the elbow. If a bird attempted to transit while flapping with the stroke plane tilted into the wind as in normal forward flight, the wings would impact the aperture because the wingspan is greater than the diameter of the aperture (Figure 3.1 A). Thus, with the exception of maneuvering hypotheses H1 and H2 in Table 3.1, no individual compensatory strategy is likely to be successful.

Birds could also incorporate aspects of both compensatory behaviors in a linear combination. For some strategies, compensatory behaviors may be incompatible, as is the case for symmetric transits and tilting of the stroke plane into the wind (because the wings have stopped flapping, there is no stroke plane to tilt). The asymmetric strategy, however, can be combined with a tilted stroke plane. To do so, a bird could first pitch downward so that the stroke plane is pointed into the wind, and then roll, so that one wing points downward and upwind and the other points upward and downwind (Figure 3.1 B). Note, however, that if drag is large enough (as it is in the diagram) that the stroke plane must be tilted more than $\sin^{-1}(7\,\text{cm}/12\,\text{cm}) \approx 36$ degrees into the wind, then the difference in height between the upstream and downstream wingtips will be greater than the height of the aperture and will prevent a level flight path through the aperture (see dashed lines in Figure 3.1 B). The stroke amplitude of each wing is also limited by the horizontal diameter of the aperture when it is within the aperture. A wing near the vertical center of the aperture can flap across the whole diameter, whereas a wing near the bottom of the aperture will have almost no room to flap.

I hypothesize that birds will develop additional strategies that both tilt the stroke plane into the wind, and also allow continuous flapping throughout transit. Specifically, hypothesis H3 in Table 3.1 describes a maneuver in which a bird first rolls about the longitudinal axis while maintaining an upwind stroke plane angle (i.e. a linear combination of the separate compensatory strategies for forward flight and aperture transit), and then progressively descends throughout transit (Figure 3.1 C). Initially, the upstream wing—which is flapping forward and below the bird's body—is inserted near the center of the aperture, allowing for maximal wingstroke amplitude. As the bird moves through the aperture, it also descends so that by the time the downstream wing—which is behind and above the bird's body—enters the aperture, it can also flap within full width of the aperture. This hypothesis can be seen as a linear combination of the separate compensatory behaviors for forward flight and aperture transits (i.e. stroke plane tilt and an asymmetric maneuver), albeit with a intentionally descending trajectory. A final hypothesis, H4, describes a maneuver in which a bird again rolls about the longitudinal axis while maintaining an upwind stroke plane angle, but then instead of descending, shifts its stroke plane longitudinally forward during the beginning of transit, and then toward the tail during the end of transit (Figure 3.1 D). This maneuver accomplishes similar wingtip trajectories relative to the aperture as in the third hypothesis, without also forcing the body to descend. Such a shift in the longitudinal position of the stroke plane would represent a novel maneuver different from those seen for aperture transits in still air alone.

In summary, based on the above hypotheses, I predicted that for a simultaneous task in which the linear combination of behaviors will likely succeed (e.g., downstream transits) I

should simply observe a linear combination of the two independent compensatory behaviors, whereas for a simultaneous task in which the independent compensatory strategies are in conflict (e.g., transits into the wind) I should either observe novel behaviors or see no transits at all.

3.2 Materials and Methods

Wind tunnel and aperture

Two male Anna's Hummingbirds (*Calypte anna*) were captured from the wild using a drop-net trap in October and November 2014. Birds were housed individually in the same room and cages described in previous chapters. Birds were allowed to habituate at least 24 hours after capture before participating in experimental trials. Flight trials were conducted in an open-circuit wind tunnel (Model 404, Engineering Laboratory Design, Lake City, MN, USA) with a working section measuring $45.5 \times 45.4 \times 91.5$ cm over the course of four days (two days of habituation to the wind tunnel, two days of experiments) for each bird. The working section was partitioned into two regions using an wire mesh screen with 1.25 cm $\times$ 1.25 cm openings (Figure 3.2). The partition could not be placed in the middle of the working section because it prevented access to the tunnel through the access port on the side of the working section. For this reason, it was positioned to one side of the port. For downstream flights, the mesh was positioned 25 cm from the upstream end of the working section so that birds had adequate space to recover downstream of the aperture after transit. For upstream flights, the mesh was positioned 25 cm from the downstream end of the working section. Thus the volumes available for preparation and recovery were the same for upstream and downstream flights, which prevented available starting and recovery distance from confounding any differences I observed between upstream and downstream flights. When conducting experiments, hummingbirds could transit the aperture in all wind conditions for both locations of the screen, but only transits in the configurations above were recorded. Trials were recorded by two high-speed cameras, both positioned within the plane of the aperture. One was placed laterally, giving a side view, and the other was placed above the aperture, giving a top view of transits. Cameras recorded video at 500 frames per second with a 600 μs exposure for each frame. Cameras were calibrated using a calibration shape and custom software in MATLAB (Hedrick, 2008).

An aperture insert was laser cut from a piece of thin acrylic and was held onto the screen using paired magnets embedded within the insert and screen. In addition to the main opening, a hexagonal pattern of holes was cut out of the acrylic to allow airflow, thus preventing large eddies or other non-uniform flow from forming to the side of the aperture (Figure 3.3). The edge of the aperture was also lined with foam to prevent physical damage from wing impacts and remove any sharp edges from the aperture, resulting in a final aperture diameter of 7.0 cm during experiments. Once completed, the initially transparent aperture insert was painted green. The flow field through and around the aperture was qualitatively

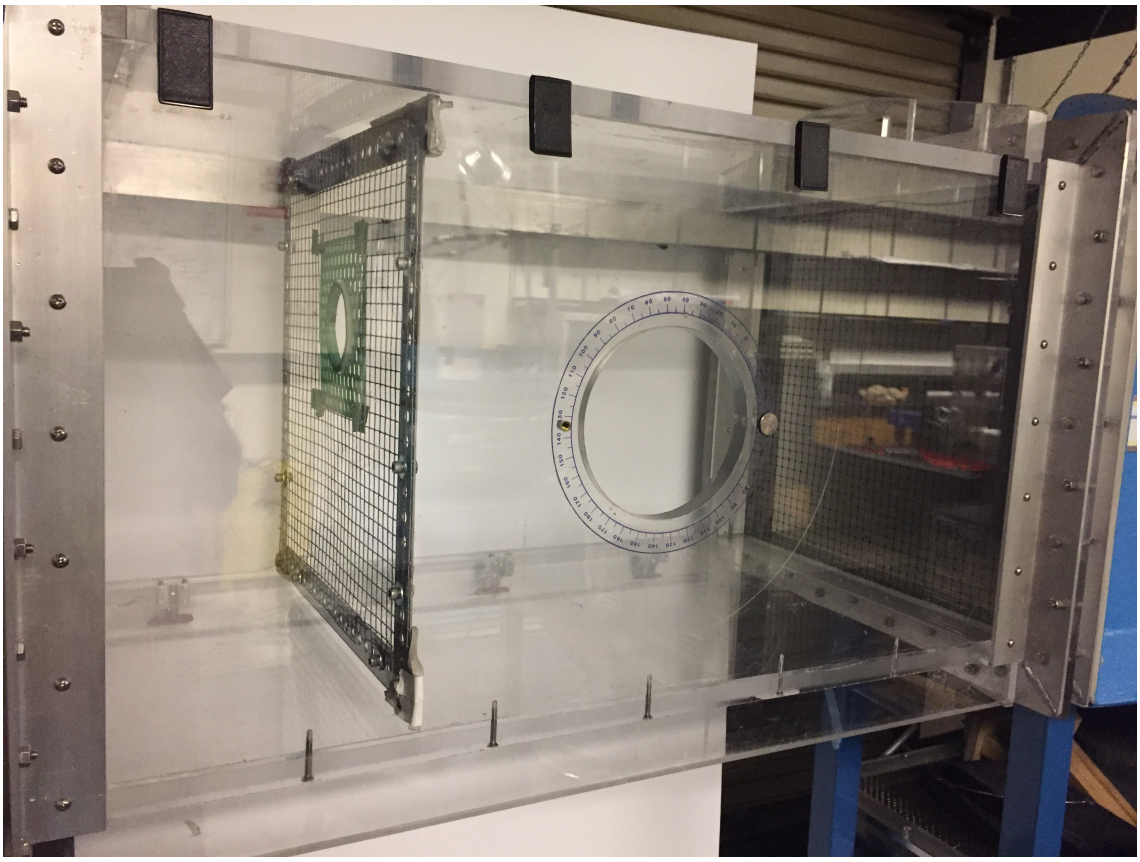

Figure 3.2: The wind tunnel working section is divided into two regions by a wire mesh partition and aperture. Mesh wire spacing is 1.25 cm × 1.25 cm. Wind flow is from the right to the left and the partition is positioned to record upstream transits in this configuration.

assessed using a smoke wire (Figure 3.4). The lower edge of the aperture sheds some vortices (Figure 3.4 C, D), but at 4 m/s, these structures are only expected to require very minimal compensatory changes in wing kinematics (Ortega-Jimenez et al., 2014).

Experimental protocol

On the first day of experiments, hummingbirds were habituated to the wind tunnel for two hours with the wind tunnel off. During this time, hummingbirds were trained to fly between two artificial feeders positioned on either end of the working section using the method described in Chapter 1. Each feeder contained only a small amount of nectar ($\sim 25\ \mu$L), which was presumably consumed in a single visit. Each feeder was manually refilled only when the bird fed from the opposite feeder. This refilling condition ensured that hummingbirds frequently flew through the aperture between feeders. After habituation and feeder training, hummingbirds were returned to their housing cages for the day.

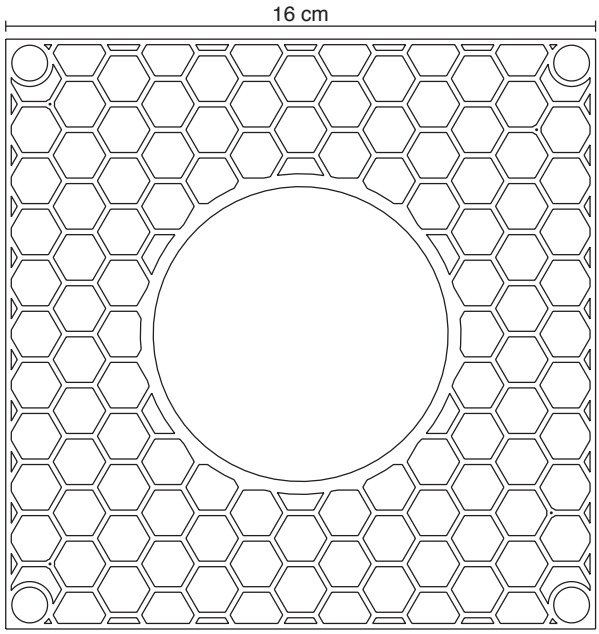

Figure 3.3: Schematic of the aperture insert. A honeycomb pattern of holes was cut out of a piece of thin acrylic using a laser cutter to allow air to flow through the structure, and to prevent the formation of large vortices to the side of the aperture. The largest diameter of the hexagonal openings is 14.3 mm, leaving thin structural segments 1.5 mm thick. This pattern had an void fraction (ratio of open area to closed area) of ~ 0.80, excluding the completely open region created by the aperture. A thin protective foam strip was applied to the inner edge of the aperture during experiments, which reduced the diameter of the aperture to 7.0 cm.

At the beginning of the second, third, and fourth days of experiments, hummingbirds were again allowed to habituate to the wind tunnel for 30 minutes or 10 back-and-forth flights (whichever came second) prior to turning the on the wind. I then set wind speed at either 2 m/s or 4 m/s. I chose 2 m/s and 4 m/s because this range of speed is known to require changes in wing and body kinematics relative to those of hovering (Sapir and Dudley, 2012). Thus birds transited apertures at the following flow velocities: -4, -2, 2, and 4 m/s, where positive and negative indicate flight into and with the wind, respectively. On the second day, birds were exposed to one full set of experimental treatments, but no videos were recorded for that day. Finally, experimental treatments were presented over the final two days in a balanced design to minimize the influence of long-term learning as a factor (see Days 3 and 4 in Table 3.2). During the final two days, to minimize the effects of short-term learning and in an attempt to capture established and consistent behaviors, I also allowed birds to traverse the aperture each direction 10 times (a total of 20 traversals) prior to recording high-speed video. Each day of experiments at least five transits in the desired direction for each condition were recorded on video, after which birds were returned

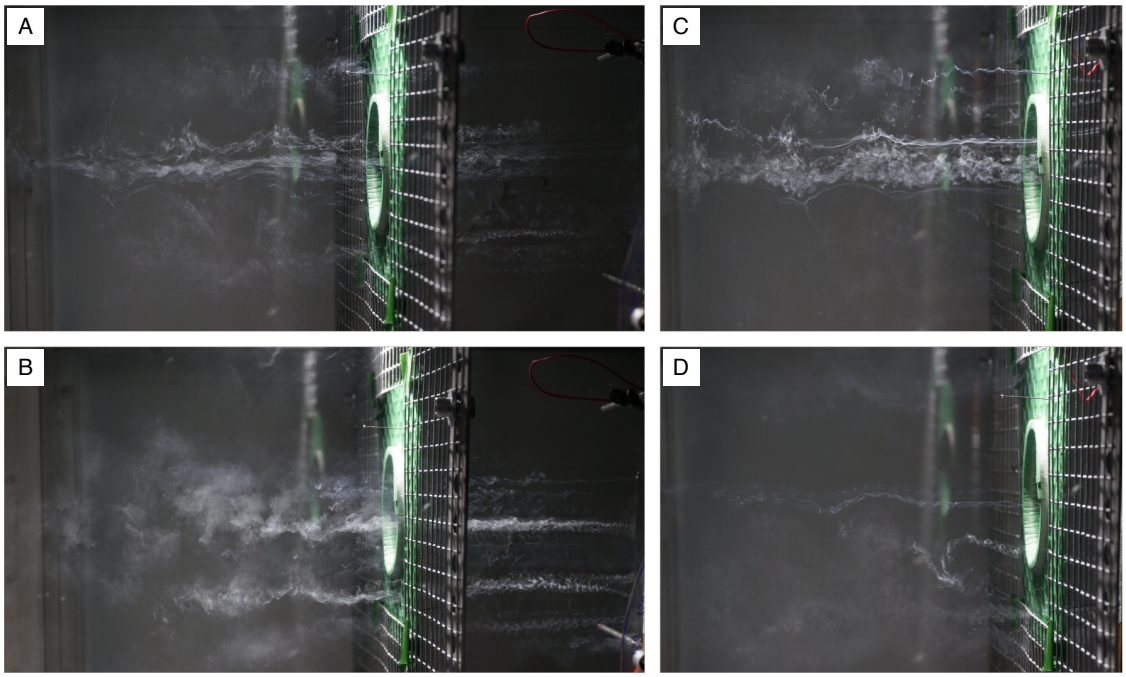

Figure 3.4: Smoke visualizations of air flowing at 4 m/s through the aperture insert. Flow direction is from right to left. Smoke is generated upstream by a vertically aligned, heated wire, which has been covered in mineral oil. (A) Smoke wire aligned with the midline of the insert, such that smoke is flowing above, through, and below the aperture. Smoke flows freely through the aperture and remains relatively unperturbed compared to smoke flowing through the honeycomb grid of the aperture insert (B). (B) Smoke wire aligned off to one side of the aperture cutout, such that smoke flows only through the honeycomb grid of the aperture insert. Smoke is disrupted by the grid, but no large-scale structure develops. (C, D) Closeups of flow structure generated by the insert. The lower edge of the aperture sheds some vortices, which can be seen in the repeated arches just below the main section of smoke in (C) and by the curling structure in (D).

to their housing cages. Styrofoam markers (half spheres 2 mm in diameter) were also placed on the back and head to aid in tracking. Only transits for which these markers were visible from both views were saved on video.

Table 3.2: Sequence of wind speed and directions over three days of experimental treatments. Days 1 and 2 were designed to be habituation days during which no videos were recorded.

	Condition 1	Condition 2	Condition 3	Condition 4
Day 1:	Into wind 0 m/s	Into wind 0 m/s	With wind 0 m/s	With wind 0 m/s
Day 2:	Into wind 2 m/s	Into wind 4 m/s	With wind 2 m/s	With wind 4 m/s
Day 3:	Into wind 2 m/s	Into wind 4 m/s	With wind 2 m/s	With wind 4 m/s
Day 4:	With wind 4 m/s	With wind 2 m/s	Into wind 4 m/s	Into wind 2 m/s

Qualitative analysis of videos and statistics

Transit behavior was assessed qualitatively using the presence or absence of several behaviors identified in preliminary trials (see Table 3.3). Transit duration (the time from bill entry to tail exit from the aperture) as well as the number of wingbeats during transit were also quantified for each trial. Trials were assessed in pseudo-random order. Statistical tests were performed in R (R Core Team, 2016).

Quantitative analysis of shifts in the stroke plane

Shifts in the stroke plane along the longitudinal axis were very challenging to assess visually, even when looking at motion from multiple views. To determine whether visual shifts I observed actually occurred, I hand tracked one trial that exhibited a *head-to-tail* stroke plane shift during transit, and another trial that exhibited a *tail-to-tail* shift (See Results). From digitized positions of the base of the bill, base of the tail, right shoulder, left shoulder, right wingtip, and left wingtip, I extracted the orientation and position of the body frame relative to the lab frame and used these data to calculate wing elevation and sweep angles over time. I also calculated the wingtip-to-wingtip height difference over the course of the trial. Finally, I extracted the time-varying stroke plane by fitting a plane to 3D wingtip positions sampled over a sliding window of 11 consecutive frames, which captured approximately one wingstroke cycle. From the stroke plane, I extracted the degree to which it was tilted into the wind (i.e., the angle between the stroke plane normal and vertical), as well as the position of its intersection with the longitudinal axis over time.

Table 3.3: Variables used to qualitatively analyze videos of aperture transits in head- and tailwinds. See Table 3.4 for decision boundaries used in qualitative analysis.

Variable	Levels	Explanation
Approach to aperture:	front, side, perch	The overall approach to the aperture. Whether bird first hovered in front, to the side, or flew directly from the perch.
Body roll/yaw:	CW, CCW, none	Body motions performed between aperture approach and during aperture transit. CW is clockwise, CCW is counterclockwise.
Body elevation angle:	higher, lower, normal	Angle between the body longitudinal axis and the horizontal plane. Higher, lower, or normal relative to the elevation angle while hovering in still air.
Stroke plane shift during bill tip entry:	head, tail, none	Shifts of the stroke plane along the longitudinal axis of the bird accomplished via abduction or adduction of both wings. Whether the shift was toward the head, toward the tail, or did not shift relative to normal flight.
Stroke plane shift during tail exit:	head, tail, none	See above.
Downstream wing in body wake:	yes, no	If the bird flew through the aperture sideways, whether the downstream wing was flapping through the presumed downstream wake generated by the body.
Pivot around aperture side:	left, right, no pivot	Birds occasionally yawed during and after transit so that their body axis remained facing toward one side of the aperture for most of the transit. This pivoting motion could be around the left or right edge of the aperture.
Reduced wingstroke amplitude:	yes, no	Whether wingstroke amplitude was reduced during transit, relative to flight before and after transit.
Overall trajectory:	up, down, flat	Whether the height change during the overall trajectory from pre- to post-transit was upward, downward, or flat.
Wing/tail contact:	yes, no	Whether there was any wing or tail contact with the aperture.

Table 3.4: Decision boundaries used in qualitative analysis of aperture transits.

Variable	Levels	Boundary
Approach to aperture:	front	hover $<$ 1 body width away from aperture centerline.
	side	hover $>$ 1 body width away from aperture centerline.
	perch	Flew directly from the perch.
Body roll/yaw:	present	rotations $>$ 15 deg.
	none	rotations $<$ 15 deg.
Body elevation angle:	higher	$>$ 10 deg. above value for normal hovering.
	lower	$<$ 10 deg. below value for normal hovering.
	normal	Within 10 deg. of value for normal hovering.
Stroke plane shift:	head	$>$ 70% toward head.
	tail	$<$ 30% toward head.
	none	$>$ 30% but less than 70% toward head.
Pivoting motion:	present	Body yaw continues after transit ending in longitudinal body axis pointed $>$ 45 deg. upstream.
	none	Longitudinal body axis pointed $<$ 45 deg. upstream after transit.
Reduced wingstroke amplitude:	yes	flapping stops, or amplitude $<$ aperture width during transit.
	no	amplitude $>$ aperture width during transit.
Overall trajectory:	up	$>$ 1 cm height gain during aperture transit.
	down	$>$ 1 cm height loss during aperture transit.
	flat	$<$ 1 cm height change during aperture transit.

3.3 Results

Qualitative behavioral variables

The two birds analyzed in this study took different approaches to the aperture. For transits into the wind, one bird (Bird 2) usually hovered directly in front of the aperture (14 of 16 transits), whereas the other bird (Bird 1) usually hovered just to the side (17 of 23 transits; see red lines in Figure 3.5). When flying with the wind, in about half of the transits (8 of 15 for the first bird and 10 of 26 for the second) the birds flew directly from the perch through the aperture without pausing to hover in front or to the side.

Two general techniques were used by both birds to negotiate apertures in the wind tunnel. In the first technique—which is qualitatively indistinguishable from the symmetric technique described in Chapter 1—both wings are rotated backward at the shoulder shortly after the bill enters the aperture, flapping is halted, and the wings are held fixed until the tail exits the aperture (Figure 1.2 D). Upon exit, birds perform a large recovery stroke. In the second technique—which is also qualitatively similar to the asymmetric technique described in Chapter 1—one wing is shifted forward and the other is shifted backward such that the leading wing, body, and trailing wing enter and exit the aperture sequentially (Figure 1.2 A). Again, flapping continues throughout transit, albeit always with a reduced wingstroke amplitude relative to unconstrained flight ($p < 0.0001$). Bird 1 almost exclusively used the asymmetric technique, except for one symmetric transit at 4 m/s into the wind. Bird 2 also used the asymmetric technique more often than the symmetric technique (23 asymmetric trials out of 31 total trials; binomial test, $p = 0.011$), but exhibited both techniques at all wind speed and direction combinations except at 4 m/s with the wind, for which it only used the asymmetric technique.

Relative to hovering flight in still air, birds flying into the wind almost always maintained lower body elevation angle (the angle between the body longitudinal axis and the horizontal plane) before, during, and after transit (Table 3.5). Birds transiting apertures while flying with the wind displayed increased body elevation angle relative to normal hovering in about half of all trials. In the other half of the trials, body elevation angle during transit was either the same, or in a few cases at 2 m/s, lower than that of normal hovering.

In addition to adjusting body elevation angle in response to wind direction, birds using the asymmetric technique also rolled about the longitudinal axis just before they transited the aperture (Table 3.6; note that direction of roll motion is not reported because the distribution is likely affected by the video selection and procedure, which ensured I only saved videos in which the back of the bird was not facing away from the side camera). When flying into the wind, whenever either bird used the asymmetric technique, it always included some body roll ($p < 0.0001$). On the other hand, when flying with the wind, birds using the asymmetric technique only rolled about the body axis approximately half the time (range 0.25 to 0.78), but the fraction of trials in which birds rolled was not significantly dependent on bird identity or wind speed (Generalized Linear Model, $p = 0.051$ for interaction term).

Birds differed in the frequency with which they yawed about the dorsoventral axis, but

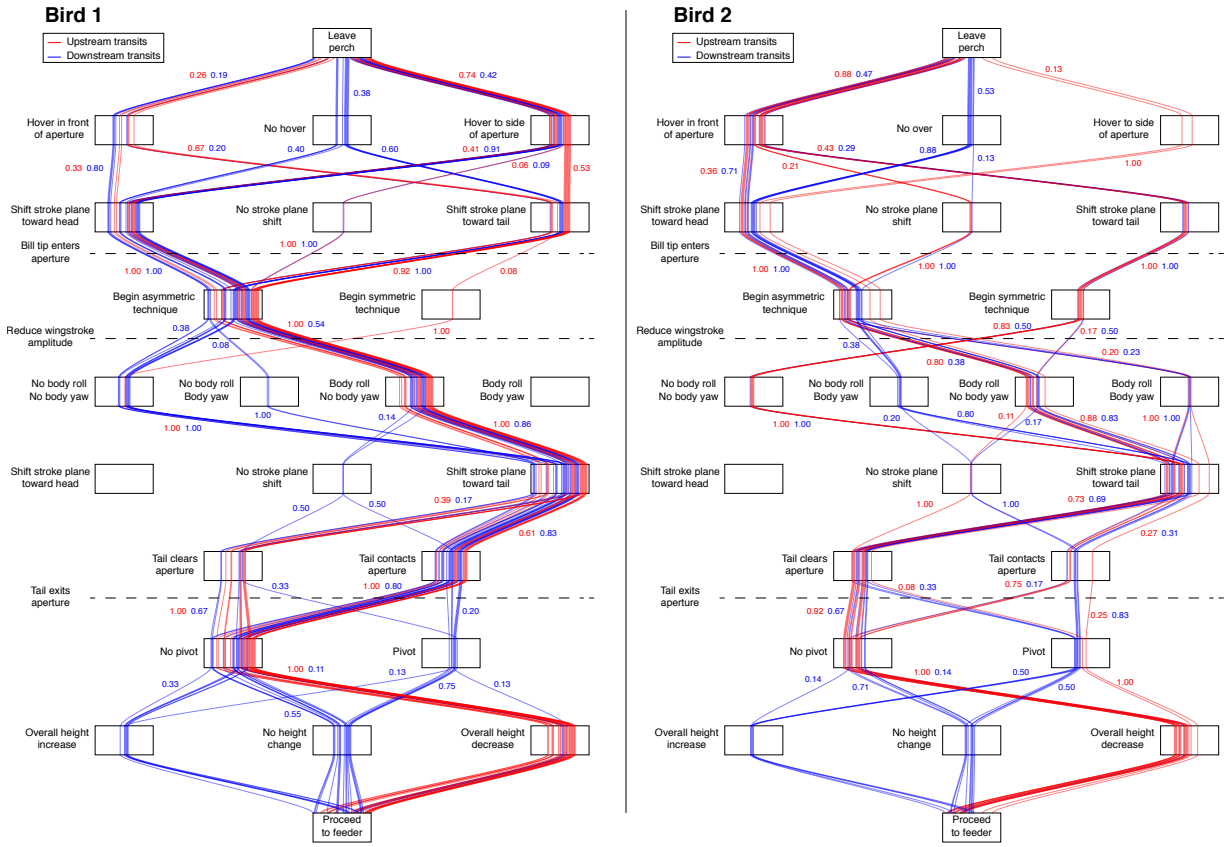

Figure 3.5: Hummingbirds negotiated apertures in the wind tunnel using a variety of movements. In each ethogram (Bird 1 is on the left and Bird 2 is on the right), each colored line corresponds to a single trial. Upstream trials are colored red and downstream trials are colored blue (trials are pooled by wind direction and include transits at both 2 and 4 m/s. Qualitatively assessed behaviors are shown by black labeled rectangles and are arranged in approximate temporal sequence from top to bottom. The sequence of behaviors demonstrated in a particular trial is indicated by the sequence of blocks encountered by its colored line. Colored numbers next to bundles of lines indicate the probability of transitioning to each of the next behaviors, given its current behavioral state. For example, after leaving the perch, Bird 1 hovered to the side of the aperture in 74% percent of upstream (red) trials. For this subset of transits, it then shifted the stroke plane toward the head or tail in 41% and 53% of these transits, respectively. Covariance patterns (which would normally be lost if only single connecting arrows and probabilities were shown), are also apparent. For example, in downstream (blue) trials in which Bird 1 hovered in front of the aperture (left-most blue lines), the bird always used the asymmetric technique and did not exhibit any body roll. On the other hand, Bird 1 only exhibited body roll when it had either (i) flown directly from the perch and shifted the stroke plane toward the tail, or (ii) hovered to the side of the aperture and shifted the stroke plane toward the head. Paths are best viewed when zoomed in.

Table 3.5: Distribution of qualitative body elevation angle assessments as a function of wind speed and flight direction. Body elevation angle assessed relative to normal hovering. Lower corresponds to a more horizontal posture and higher corresponds to a more upright posture.

			Body elevation angle		
	Direction & wind speed	n	Fraction lower	Fraction same	Fraction higher
Bird 1	Into wind 4 m/s	12	1.00	0.00	0.00
	Into wind 2 m/s	11	0.82	0.18	0.00
	With wind 2 m/s	13	0.23	0.38	0.38
	With wind 4 m/s	13	0.00	0.23	0.77
Bird 2	Into wind 4 m/s	9	1.00	0.00	0.00
	Into wind 2 m/s	7	1.00	0.00	0.00
	With wind 2 m/s	11	0.18	0.45	0.36
	With wind 4 m/s	4	0.00	0.50	0.50

Table 3.6: Fraction of asymmetric trials in which qualitative body motions along the roll axis were observed as a function of wind speed and flight direction.

			Body motion along the roll axis	
	Direction & wind speed	n	Fraction present	Fraction absent
Bird 1	Into wind 4 m/s	11	1.00	0.00
	Into wind 2 m/s	11	1.00	0.00
	With wind 2 m/s	13	0.46	0.54
	With wind 4 m/s	13	0.62	0.38
Bird 2	Into wind 4 m/s	6	1.00	0.00
	Into wind 2 m/s	4	1.00	0.00
	With wind 2 m/s	9	0.78	0.22
	With wind 4 m/s	4	0.25	0.75

both birds primarily used yaw only for aperture transits with the wind (10 out of 12 trials in which yaw was present were with the wind). One bird yawed in only 2 out of 49 trials, whereas the other yawed in 10 out of 31 trials. This yawing behavior was tightly associated with a pivoting motion birds occasionally used to negotiate apertures when flying with the wind (Fisher's exact test, $p = 0.0039$; pivoting motion described below).

Trajectory outcome variables

Transit duration varied significantly among the wind speeds and transit directions tested in experiments (Likelihood ratio test on linear models, $p < 0.0001$ for both birds). Models with a categorical factor for the combination of wind speed and transit direction (i.e. a variable with levels: -4, -2, 2, and 4 m/s) fit the data better than those incorporating treatment as a continuous variable between -4 and 4 m/s. Transit duration increased significantly between each treatment as wind velocity changed from -4 m/s for transits with the wind to 4 m/s for transits into the wind (Tukey's post-hoc test, $p < 0.02$ for all comparisons, averaged over the levels of bird identity and transit technique; Figure 3.6). Bird 1 only used the symmetric technique once so the association between technique on transit duration could not be determined for that bird. For Bird 2, use of the symmetric technique vs. the asymmetric technique was associated with a 0.018 ± 0.008 second decrease in transit duration, which corresponds to an 11% and 23% reduction for transits at 4 and -4 m/s, respectively (Likelihood ratio test on linear models, $p = 0.027$).

Both transit technique and wind velocity significantly affected the number of wingbeats during transit, which increased significantly from downstream to upstream transits at 2 m/s, and again from upstream transits at 2 to 4 m/s (Tukey's post-hoc test, $p < 0.043$ for all comparisons except between downstream transits at 2 and 4 m/s). The number of wingbeats was almost completely explained by transit duration, and residuals of this linear model were not significantly associated with wind velocity ($p = 0.97$), indicating that this rough estimate of wingbeat frequency did not change among treatments.

Both birds always lost significant height during transits into the wind, whereas trajectories for downstream transits were mostly flat and in some cases increased in height (Figure 3.7; Table 3.7).

Wing contact with the aperture occurred in eight of the 72 trials recorded on video (three for one bird and five for the other). The probability of wing contact was not significantly affected by bird identity (likelihood ratio tests, $p = 0.15$), wind speed and transit direction ($p = 0.48$), or transit technique ($p = 0.25$), but these tests have very low power because of the extremely small sample size (n = 8). Tail contact on the other hand, occurred in 45 out of 72 trials (35 trials for one bird and 10 for the other). The probability of tail contact was not significantly different between birds (likelihood ratio test, $p = 0.79$), but did depend on both wind velocity ($p = 0.026$) and bird identity ($p = 0.0013$). Tail contact with the aperture was most likely for downstream transits at 4 m/s and was least likely for upstream transits at 2 m/s (Tukey's post-hoc test, p = 0.040), but no other treatment pairs were significantly

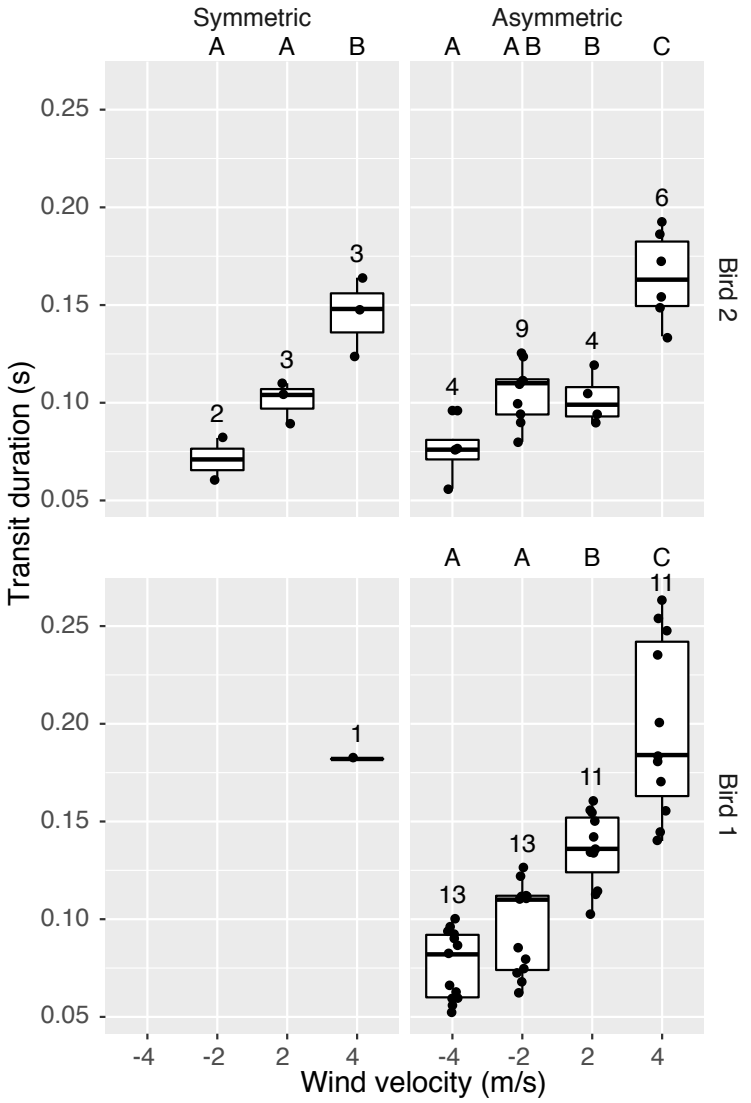

Figure 3.6: Transit duration as a function of wind velocity and bird identity. Sample size for each treatment is given by the number positioned above each box. Negative velocity corresponds to transits with the wind, whereas positive velocity corresponds to transits into the wind. Between two treatments, matching letters above each treatment indicate transit duration is not significantly different at the 5% confidence level. For example, for the asymmetric technique and Bird 2, transit duration is significantly different between -4 m/s and 2 m/s, but not between -4 m/s and -2 m/s.

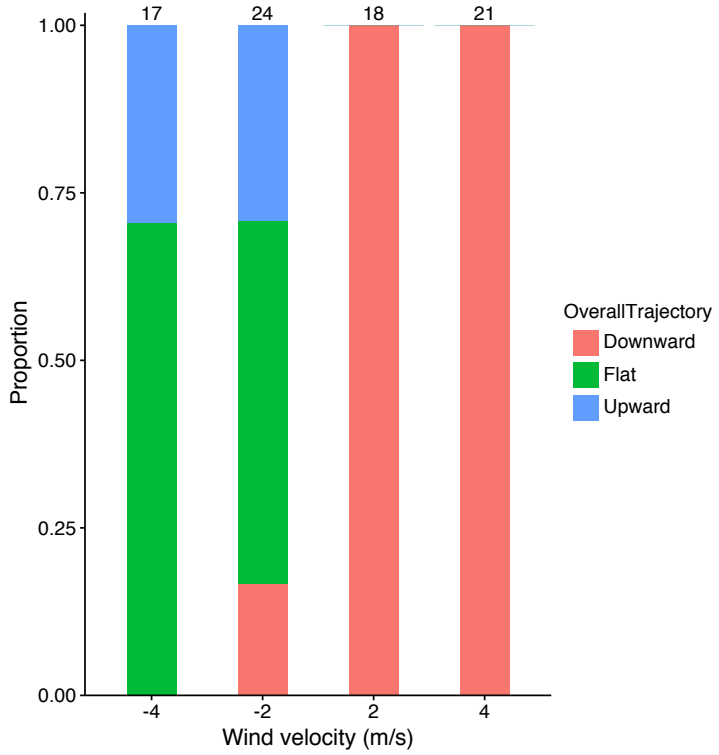

Figure 3.7: Proportion of trials in which height decreased, was flat, or increased as a function of wind velocity. Sample size for each treatment is given by the number positioned above each bar.

Table 3.7: Distribution of overall trajectory height change as a function of wind speed and flight direction.

			Overall trajectory height change		
	Direction & wind speed	n	Fraction down	Fraction flat	Fraction up
Bird 1	Into wind 4 m/s	12	1.00	0.00	0.00
	Into wind 2 m/s	11	1.00	0.00	0.00
	With wind 2 m/s	13	0.23	0.46	0.31
	With wind 4 m/s	13	0.00	0.77	0.23
Bird 2	Into wind 4 m/s	9	1.00	0.00	0.00
	Into wind 2 m/s	7	1.00	0.00	0.00
	With wind 2 m/s	11	0.09	0.64	0.27
	With wind 4 m/s	4	0.00	0.50	0.50

different from each other. Furthermore, the probability of a tail impact showed no consistent pattern across direction or wind speed.

Description of notable behaviors

The results described above seem to indicate that birds may simply be using a linear combination of the two behaviors they use to negotiate these situations in isolation. For upstream flight, body elevation angle is typically lowered relative to hovering flight, whereas for downstream flight, the body elevation angle is raised. Birds also display qualitatively similar symmetric and asymmetric aperture negotiation techniques. However, as I described in the introduction, geometric constraints predict that the linear combination of reduced body elevation angle and wing kinematics associated with the asymmetric technique still lead to wing impacts given a level flight trajectory. Specifically, if body elevation angle is adjusted downward, body roll no longer brings the wings into alignment with the aperture by pointing one wing forward and the other backward, and instead points one wing downward and the other upward. Thus, additional alterations to wing and body kinematics or overall flight trajectories, such as those described in Table 3.1, should still be apparent.

One such behavior was a time-varying shift in the position (rather than tilt) of the stroke plane along the longitudinal axis. Birds shifted the position of the stroke plane toward the head as the bill and head approached the aperture (this motion is the same as increasing the mean value of sweep of both wings, while still flapping primarily along the elevation-depression axis). Birds then shifted the stroke plane towards the tail as the tail entered and exited the aperture (this motion is equivalent to decreasing the mean value of sweep of both wings). The net result was that the vertical position of the forward, lower wing was higher, and much closer to the hummingbird's head and bill tip when it was going through the aperture, and the position of the trailing, higher wing was lower and closer to the tail tip, satisfying the spatial constraint imposed by the aperture for both vertical height as well as maximizing the horizontal extent birds could flap their wings (i.e wings could flap back and forth across the center of the aperture, rather than close to the bottom or top). These kinematics were observed for transits both into and with the wind.

I assessed stroke plane shifts visually according to its longitudinal position while (i) the bill and head entered the aperture and (ii) the tail entered and exited the aperture. The position during each of these times was categorized as towards the head, neutral, or towards the tail. Thus a trial in which the stroke plane did not shift would be described as *neutral-to-neutral* or *tail-to-tail*, whereas one exhibiting the shift described above would be *head-to-tail*.

The most common shifts were *head-to-tail* and *tail-to-tail*. All symmetric transits were characterized by *tail-to-tail* shifts (9 out of 9), which accounted for nine of the 28 *tail-to-tail* observations. Within the remaining asymmetric transits, both birds exhibited *head-to-tail* stroke plane shifts more often than *tail-to-tail* shifts at all wind velocities (Table 3.8), except for Bird 1 flying upstream into a 2 m/s headwind. Bird 2 never used the *tail-to-tail* stroke plane shift in an asymmetric transit. I observed some form of head-to-tail motion in the stroke plane (i.e., pooling all trials labeled *head-to-tail*, *head-to-neutral*, and *neutral-to-tail*)

in 28 of 48 asymmetric trials for Bird 1, and in 22 of 23 asymmetric trials for Bird 2. The presence of stroke plane shifts (versus *neutral-to-neutral* or *tail-to-tail* categories) did not depend significantly on wind speed (general linear models, $p = 0.089$ and $p = 0.29$ for the first and second birds, respectively).

Table 3.8: Distribution of longitudinal stroke plane shifts for asymmetric transits as a function of wind speed and flight direction. Note that overall shifts in the direction of the head during transit (i.e., *tail-to-neutral*, *neutral-to-head*, and *tail-to-head*), were never used by either bird and are not shown. Letters *H*, *N*, and *T* correspond to *head*, *neutral*, and *tail*, respectively. Dashes indicate shift combinations that did not occur in these experiments.

			Shift in stroke plane				
	Direction & wind speed	n	$H \to T$	$H \to N$	$N \to T$	$N \to N$	$T \to T$
Bird 1	Into wind 4 m/s	11	0.55	–	0.09	–	0.36
	Into wind 2 m/s	11	0.27	–	–	–	0.73
	With wind 2 m/s	13	0.62	–	–	–	0.38
	With wind 4 m/s	13	0.69	0.08	–	0.08	0.15
Bird 2	Into wind 4 m/s	6	0.67	–	0.33	–	–
	Into wind 2 m/s	4	0.50	0.25	0.25	–	–
	With wind 2 m/s	9	1.00	–	–	–	–
	With wind 4 m/s	4	0.50	0.25	–	0.25	–

Shifts in the longitudinal position of the stroke plane were difficult to assess visually, so I also quantitatively analyzed the three-dimensional wing and body angles of two sample transits, which I had previously categorized as having *head-to-tail* and *tail-to-tail* shifts in the stroke plane. Many of the kinematics were very similar between these two trials, so I present figures only for the *head-to-tail* trial, except when directly comparing the shifts in longitudinal position of the stroke plane (Figure 3.15). As is apparent from a sequence of video frames (Figure 3.8), the bird began to roll just before bill tip entry (Figure 3.9), which rotated the dorsoventral axis of the bird toward the camera and the $\mathbf{N}_y$ axis (Figure 3.10).

While the body rolled, changes in wing kinematics also occurred. Mean wing elevation angle for both wings decreased during transit, as did the amplitude of flapping along this dimension (Figure 3.11). Wing sweep for the two wings, on the other hand, was highly asymmetric (Figure 3.12). As the bill tip approached the aperture (left most black line in Figure 3.12), the mean sweep angle of both wings shifted slightly toward the head. Then just before the base of the bill entered the aperture, the mean sweep angle of the left wing shifted back toward the tail while the mean sweep angle of the right wing was kept shifted toward the head. Finally, as the body and tail proceeded through the aperture (time between the 2nd and 4th black lines from the left in Figure 3.12), the mean sweep angle of both

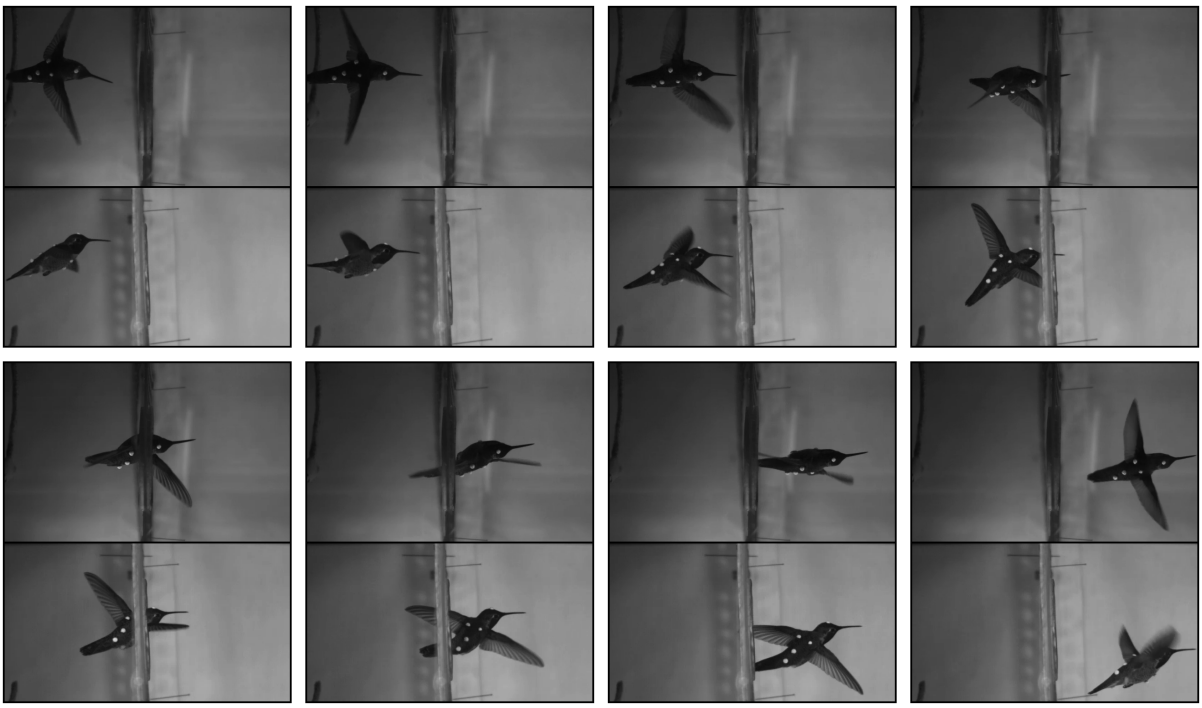

Figure 3.8: Image sequence showing a trial in which the bird shifted its stroke plane from head to tail during transit. Time increases across the first row from left to right, then across the second row. Panels are 25 frames (50 ms) apart. Top and bottom portions of each panel show top-down and side views, respectively.

wings decreased simultaneously, indicating a shift in the stroke plane (see also Figure 3.15). Flapping amplitude along the sweep dimension is also reduced during transit.

These changes in mean sweep and elevation angle allowed the right and left wings to flap continuously as they passed through the open portion of the aperture (Figure 3.13). The stroke plane was first inclined about 45 degrees into the wind, but became less inclined during the latter half of transit (Figure 3.14). Anatomical stroke plane angle varied between 56 and 87 degrees as the bird negotiated the aperture, which is comparable with the range exhibited during sustained forwards and backwards flight (Sapir and Dudley, 2012).

In addition to tilting, the stroke plane also shifted position along the longitudinal axis of the bird. Before transit, the point at which the stroke plane intersects the longitudinal axis of the bird was about 60% along the line from the base of the tail to the base of the beak (Figure 3.15). In a trial which was qualitatively labeled *head-to-tail* (Figure 3.15 A), as the bill tip approached the aperture, the stroke plane shifted toward the bill, so that it almost intersected the base of the bill (96 % towards the bill at its closest). In contrast, in a trial which was qualitatively labeled *tail-to-tail* (Figure 3.15 B), the longitudinal position of stroke plane did not increase as the bird approached the aperture and was not shifted as far towards the head (79 % towards the bill at its closest). In both transits, as the body passed

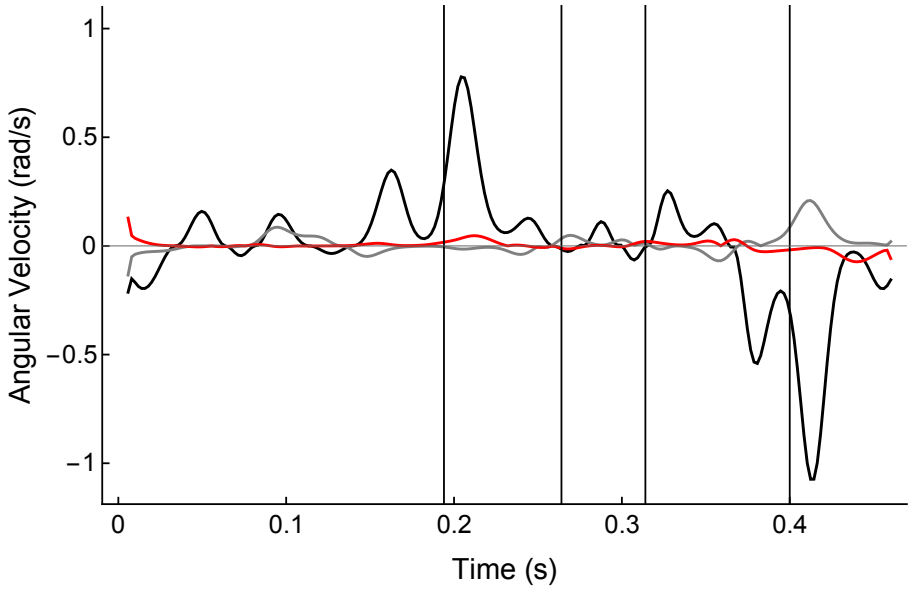

Figure 3.9: Instantaneous roll (black), pitch (gray), and yaw (red) motions over time for a selected trial for a single bird (wind speed 4 m/s, transit upstream into the wind; see Figure 3.8). The four black vertical lines from left to right indicate bill tip entry, bill base entry, tail base entry, and tail tip entry to the aperture. As the bill and head approached the aperture, there was a large roll to the right (around 0.2 s). Once the bird was clear of the aperture, it rolled back the other way (at around 0.4 s) to regain normal flight posture.

through the aperture the stroke plane was quickly shifted toward the tail, where it remained until transit was nearly complete.

Finally, in downstream trials, hummingbirds sometimes displayed a pivoting behavior as they transited the aperture (Figure 3.16). In this behavior, birds started facing the aperture with the midline of the body just inside one edge of the aperture. Then as the body yawed and rolled almost 180 degrees, the leading wing, body, and trailing wing went through the aperture sequentially.

3.4 Discussion

In this study, birds negotiated a narrow aperture while flying in a wind tunnel. Birds successfully transited apertures while flying upstream and downstream at wind speeds up to 4 m/s. I tested four plausible maneuvering hypotheses (Table 3.1) that included either combinations of previously observed wing motions (hypotheses H1–H3) or hypothesized longitudinal shifts in the stroke plane (i.e., novel wing motions; hypothesis H4). Novel wing motions were defined as motions of the wing relative to the body that were not previously observed in either unconstrained horizontal flight in the wind tunnel, or in aperture transits in still air. Birds used aspects of all four hypothesized techniques in these experiments. Only for

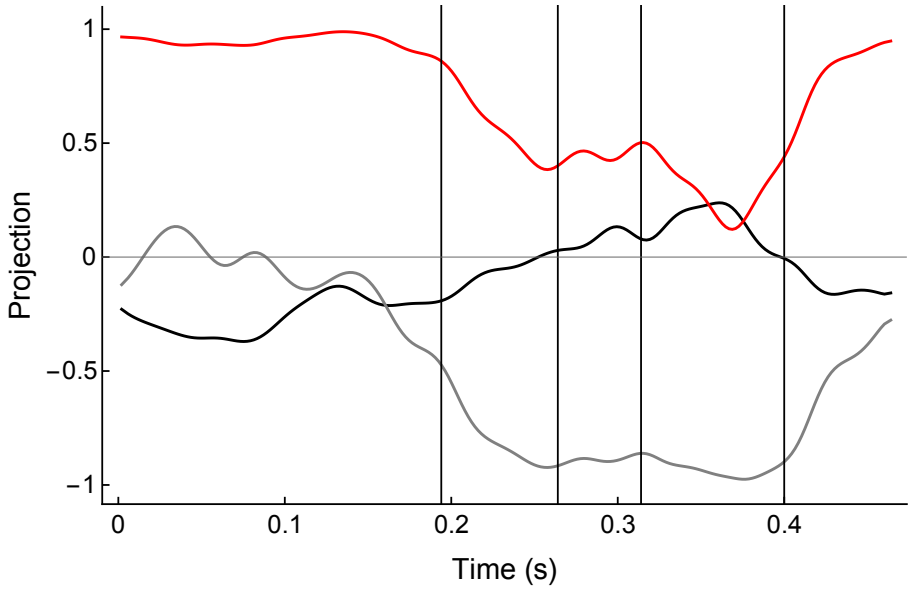

Figure 3.10: Components of $\mathbf{B}_z$, the bird's dorsoventral axis, projected onto $\mathbf{N}_x$ (black), $\mathbf{N}_y$ (gray), and $\mathbf{N}_z$ (red), where $\mathbf{N}$ is the lab frame. Data are from the same transit shown in Figures 3.8 and 3.9. $\mathbf{N}_z$ points upward and is aligned with gravity and $\mathbf{N}_x$ points upstream. The four black vertical lines from left to right indicate bill tip entry, bill base entry, tail base entry, and tail tip entry to the aperture. The dorsal axis first pointed along the lab vertical axis, but then as the bird rolled to the right it became more aligned with the lateral axis.

the first hypothesis, however, did birds use the exact combination of all trajectory attributes listed in Table 3.1 (7 out of 39 trials). Surprisingly, even with a 4 m/s headwind and a short distance (25 cm) downstream of the aperture in which to accelerate, birds were able to build up enough momentum to coast through the aperture using the symmetric technique. I also observed some degree of coasting when birds used the asymmetric maneuver (similar to hypothesis H2), but unlike the flat trajectory predicted by hypothesis H2, birds always followed a descending trajectory for upstream transits. When birds coasted using the asymmetric maneuver, they often decelerated rapidly as their stroke plane became less tilted into the wind (Figures 3.14 and 3.13). Thus birds frequently relied on forward momentum to transit the aperture, as described in the first two hypothesis. These observations demonstrate that birds could transit the aperture in this experiment using only wing and body motions previously observed in horizontal flight and aperture transits in still air.

Birds also incorporated aspects of the third and fourth maneuvering hypotheses. The third hypothesis combined the asymmetric maneuver and tilted stroke plane observed in previous experiments with a descending overall trajectory. Counter to the third hypothesis, birds never completed upstream transits without shifting their stroke plane toward the tail at the end of transit. In the 3D reconstruction of the sample transit, the stroke plane angle just before transit ranged between 40 and 60 degrees (Figure 3.14). Based on the 3D

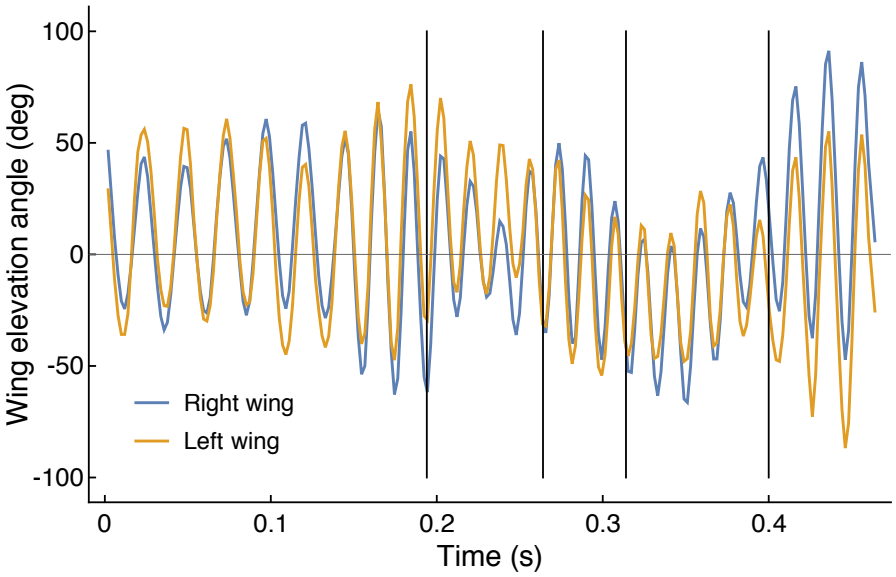

Figure 3.11: Left and right wing elevation angles over time for the same transit shown in Figures 3.8–3.10. Angles are measured relative to the mid-frontal plane defined by the $\mathbf{B}_x$ and $\mathbf{B}_y$ axes (see Figure 2.2). The four black vertical lines from left to right indicate bill tip entry, bill base entry, tail base entry, and tail tip entry to the aperture.

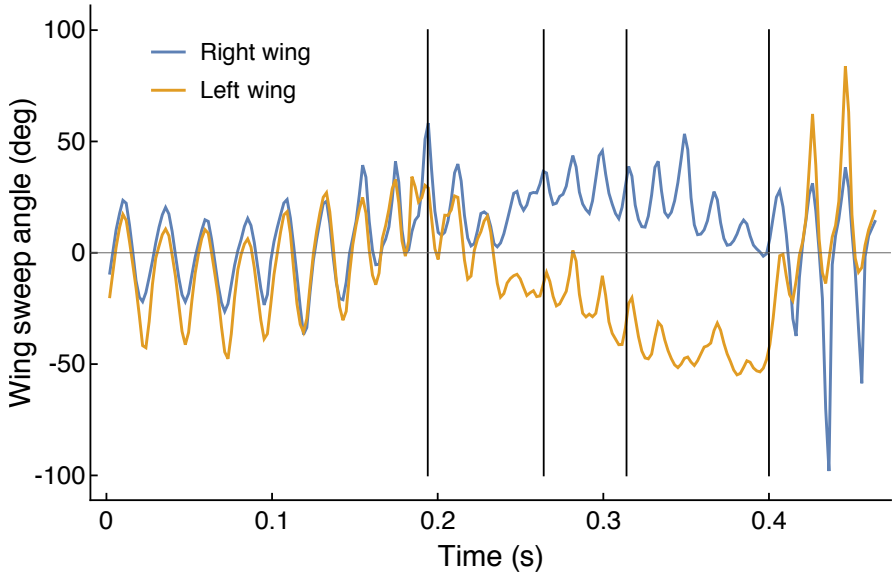

Figure 3.12: Left and right wing sweep angles over time for the same transit shown in Figures 3.8–3.11. Angles are measured relative to the plane defined by the $\mathbf{B}_z$ and $\mathbf{B}_y$ axes (see Figure 2.2). The four black vertical lines from left to right indicate bill tip entry, bill base entry, tail base entry, and tail tip entry to the aperture.

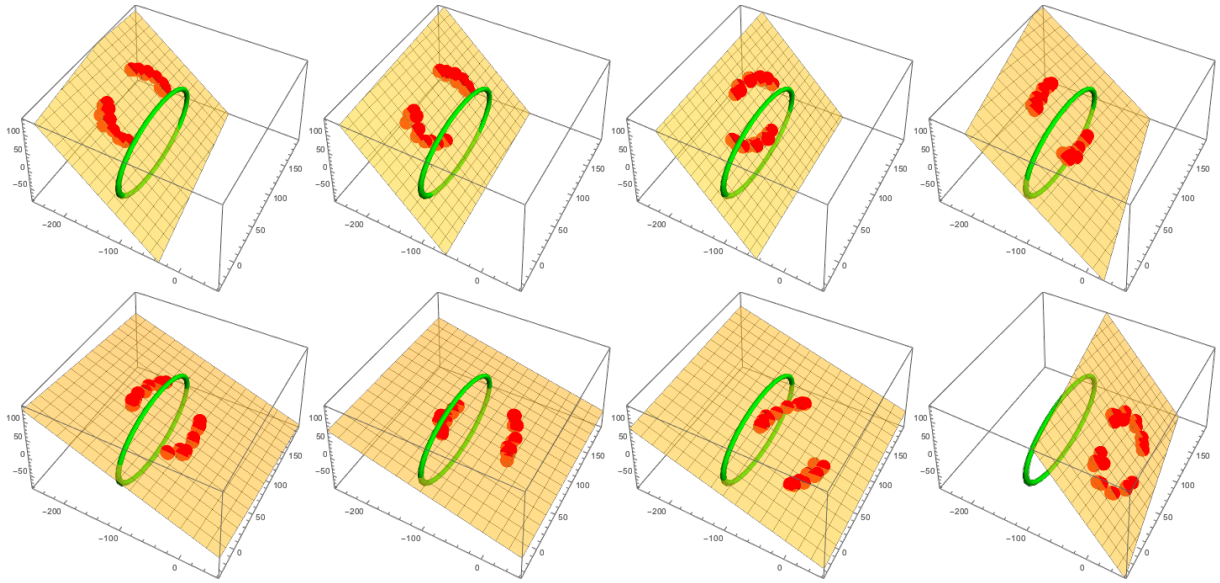

Figure 3.13: Three dimensional reconstruction of wingtip locations and fitted stroke plane during upstream aperture negotiation (data are from a selected transit; see Figure 3.8). The sequence begins with the bird to the left (downstream) of the aperture (shown as a green annulus) and proceeds across the first row from left to right, then across the second row. The right wingtip was inserted first into the aperture (upper row) and was then followed by the left wingtip (lower row). The stroke plane was initially inclined about 45 degrees into the wind, but became less inclined during the latter half of transit (see also Figure 3.14). Panels are 25 frames (50 ms) apart, and are the same times as the images shown in Figure 3.8).

reconstruction, the vertical distance between the left and right wingtips was between 7 and 8 cm while the bill was within the aperture, offering a possible explanation for why birds did not transit the aperture without either descending or shifting their stroke plane angle longitudinally. The fourth hypothesis, predicted longitudinal shifts in the stroke plane–which represent novel wing motions that had not been previously observed—with a level overall flight path. Counter to the fourth hypothesis, birds always lost elevation when completing upstream transits. In these experiments, however, birds demonstrated clear and extreme shifts in the longitudinal position of the stroke plane as they negotiated the aperture while flying upwind (Figure 3.15). Thus the fourth hypothesized technique is clearly used to some extent, except for the fact that hummingbirds always descended during upstream transits. It is possible that measuring height change during transit for a full set of trials would be able to distinguish between trials in which birds use the third and fourth hypothesized strategies. In fact, aspects of all three hypothesized asymmetric maneuvers in Table 3.1 were combined in many trials (20 out of 39 trials), where hummingbirds relied on forward momentum, followed a descending trajectory, and shifted the longitudinal position of the stroke plane.

For downstream flights, I predicted that a linear combination of behaviors would be used

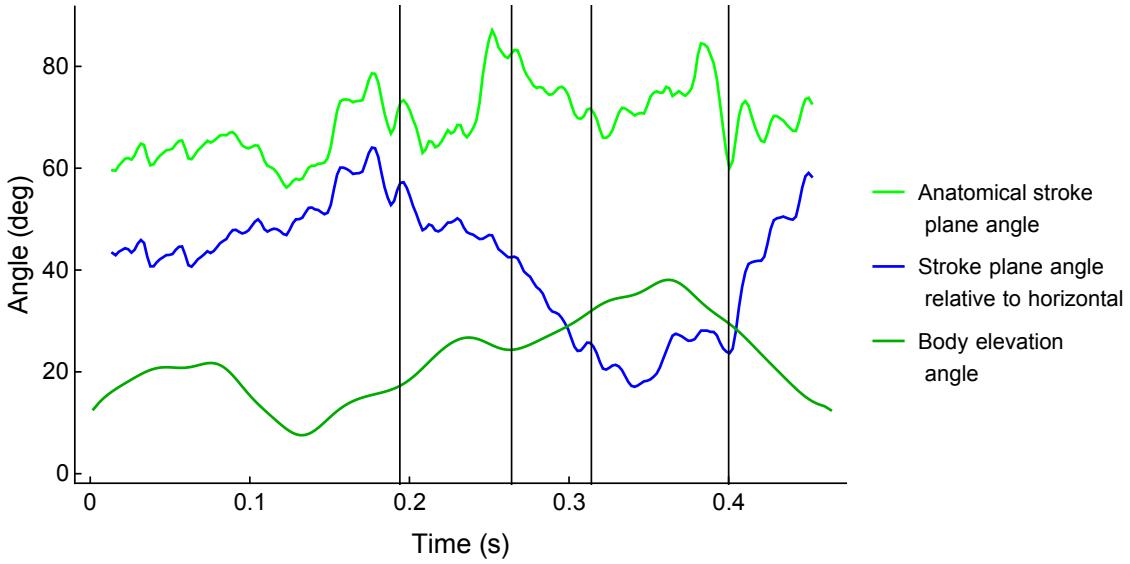

Figure 3.14: Stroke plane and body angles over time for a sample transit. Anatomical stroke plane angle and stroke plane relative to the horizontal are the angles between the normal to the fitted stroke plane and $\mathbf{B}_z$ and $\mathbf{N}_z$, respectively. The four black vertical lines from left to right indicate bill tip entry, bill base entry, tail base entry, and tail tip entry to the aperture.

because the need to produce horizontal aerodynamic thrust during transit was eliminated or greatly reduced (because parasite drag is in the direction of desired motion, rather than against it). In many cases, however, I observed similar head-to-tail longitudinal shifts in the stroke plane. Furthermore, birds often gained height during downward transits, which may be a response similar to the maneuver described in the third hypothesis, but where birds follow an ascending trajectory because their stroke plane is angled pointing away from the aperture instead of towards it. A more detailed kinematic analysis of the maneuvers described in Chapter 1 is needed to determine the extent that the stroke plane shifting behavior is used or not used during aperture negotiation in still air.

Aperture transits in wind showed several similarities to those performed in still air. In still air, the symmetric technique was associated with faster transits than the asymmetric technique and I observed the same trend between symmetric and asymmetric techniques used to negotiate apertures in the wind. Also similar to the experiments described in Chapter 1, it is interesting that even after several hours of aperture transits there still exists significant variation in technique from trial to trial. The factors or initial conditions determining which technique birds choose for any given trial would be interesting to investigate further.

Another interesting observation that is common to both experiments is that birds almost always avoided wing impacts with the aperture by modulating their wingstroke amplitude on a wingstroke-to-wingstroke basis, a feat that is both visually and physically challenging. The bill is usually kept oriented in the direction of travel during transit, which orients the eyes laterally. Therefore, when the trailing wing is within the aperture, the relevant visual

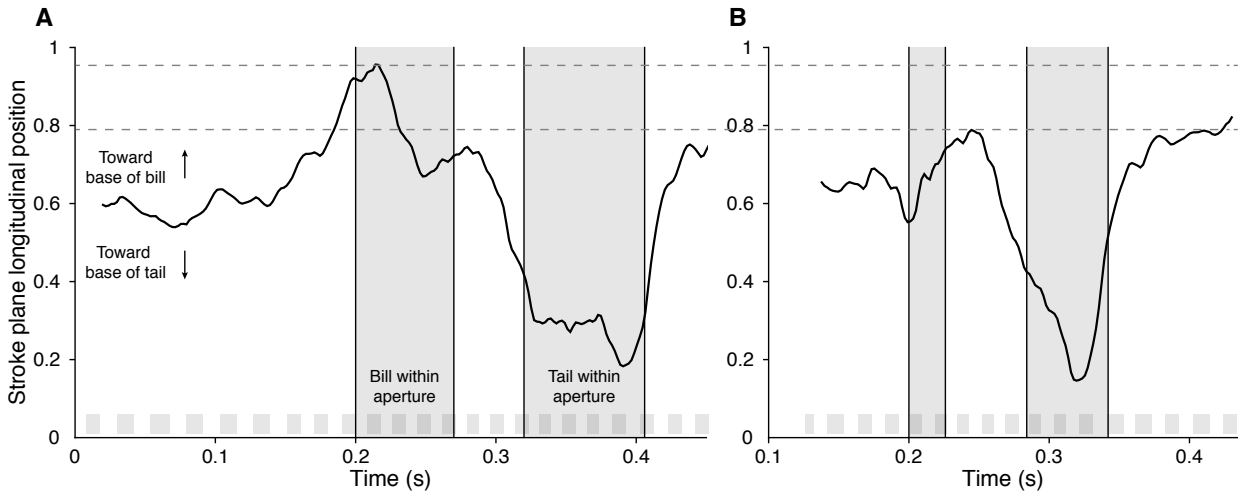

Figure 3.15: Position of the stroke plane along the longitudinal body axis over time for two sample transits. Transits are sampled from trials labeled *head-to-tail* (A) and *tail-to-tail* (B). The vertical axis describes the relative position along the line from the base of the tail to the base of the bill of the intersection of the stroke plane and the longitudinal body axis. At 0, the stroke plane intersects the body axis at the base of the tail and at 1, the stroke plane intersects the body axis at the base of the beak. Shaded bands indicate the times from bill tip to bill base entry and from tail base entry to tail tip entry to the aperture. Small shaded rectangles just above the x axis indicate downstrokes. The *tail-to-tail* transit in (B) was much faster than the *head-to-tail* transit in (A), but the stroke plane did not shift nearly as far towards the head (see dashed horizontal lines for comparison). Whereas the stroke plane position in (A) increased to a peak while the bill approached and was within the aperture, the position in (B) shifted much less during the approach, and only peaked after the base of the bill was through the aperture. Both transits show large shifts of the stroke plane towards the tail when the tail was within the aperture.

features are at the very back of the visual field, where optical quality is low (Martin, 2007). In birds, the region of highest visual acuity is along the optical axis of the eyes, but many birds may have other high-acuity regions, such as the region of binocular overlap (Martin, 2011). It is possible that birds are able to "keep track" of where obstacles were and can account for their own motion over time in a feed-forward manner. Such an ability would enable birds successfully adjust the position of their wings even when the visual projection of the obstacle is very far from their region of high acuity and the quality of visual feedback is low. Like other birds, hummingbirds probably have mechanosensors at the base of their feathers (Saxod, 1996; for a review, see Altshuler et al., 2015) and one interesting alternative hypothesis is that hummingbirds may be able sense flow or pressure changes indicative of impending wing impacts in time to halt and reverse wing motion. Stopping wing motion mid-flap is also likely to require large control effort, and physical and mathematical models may

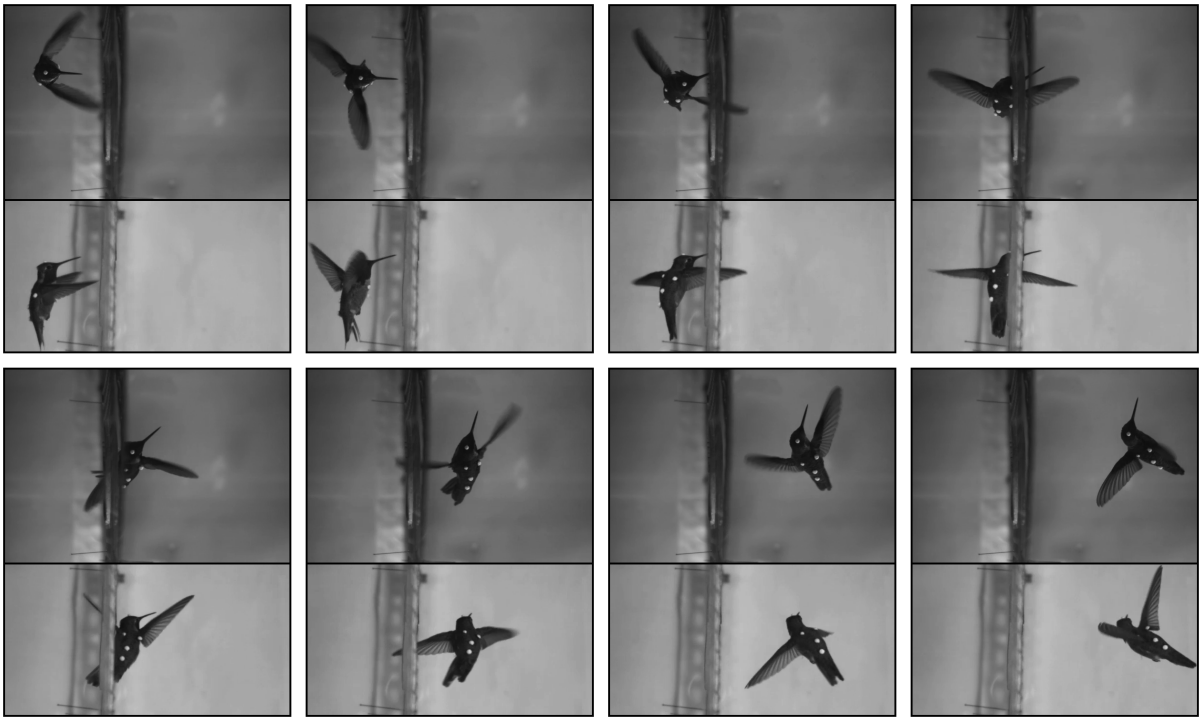

Figure 3.16: Image sequence showing a pivoting behavior, which was occasionally used to negotiate apertures while flying downstream. Time increases across the first row from left to right, then across the second row. Panels are 14 frames (28 ms) apart. Top and bottom portions of each panel show top-down and side views, respectively. In this trial, the bird pivoted around the left edge of the aperture.

provide rough estimates of how quickly flapping can be stopped and the power requirements to do so (Ma et al., 2013; Zhang, Cheng, and Deng, 2016).

One aspect of transits not addressed in this study is the potential issue of the body itself fitting through the aperture. Birds usually did not pitch or yaw their bodies away from the body elevation angle used during normal forward or backward flight (they did, however, roll during most asymmetric transits). The lack of changes in body elevation angle even during dynamic maneuvers suggests that body orientation imposed by forward and backward flight may be a relatively hard constraint. Body angle may be constrained by geometrically being able to fit through the 7 cm diameter aperture, as well as drag from the wind. The steep body angle associated with backward flight has only slightly higher parasite drag than the more horizontal body angle associated with forward flight (16.5% and 12.9% of body weight for backward and forward flight, respectively), according to tests on 3D printed models (Sapir and Dudley, 2012). On the other hand, the stroke plane is tilted much less into the wind during backward flight than it is for forward flight (0 degrees vs. 21 degrees), which is counter to what one would expect based on the drag measurements. Together these observations suggest that the actual direction of aerodynamic thrust produced by the bird

may be offset relative to the measured angle of the stroke plane. Further aerodynamic studies are needed to fully understand how the aerodynamic thrust produced by the bird relates to wing kinematics for dynamic maneuvers.

For example, flapping with one wing upstream and one wing downstream appeared to be effective during asymmetric transits because I did not observe any drastic changes in body orientation that would be expected if there was an imbalance between lift produced by the left and right wings. In the latter half of transit, the stroke plane angle relative to the horizontal was often about 20 degrees. In this configuration, the upstream wing may experience significant flow from the tip of the wing to the base of the wing. It would be interesting to investigate the effect of such reverse spanwise flow on the leading edge vortex, a structure known to be particularly important for developing lift in flapping flight (Warrick, Tobalske, and Powers, 2009; Ellington et al., 1996). In addition, the downstream wing almost always flapped through the wake generated by the bird's own body. Further study of how hummingbirds use and/or compensate for the interacting flows produced, and encountered by, the body and wings may provide insight for the control of robotic flyers designed to fly in windy environments.

In the wild, hummingbirds regularly forage, engage in agonistic interactions, and access nests within foliage during periods of high wind (Ortega-Jimenez et al., 2016). It is currently unknown, however, how frequently they negotiate openings less than one wingspan during such windy conditions. Regardless of whether the novel wing motions observed in this study were learned in the lab, they nonetheless demonstrate that hummingbirds can dynamically adjust wing kinematics in a way that deviates from simple linear combinations of previously demonstrated behaviors (Figure 3.1). Longitudinal shifts in the position of the stroke plane performed *via* bilateral–symmetric changes in mean anatomical wing sweep angle likely occur during other maneuvers, but have not yet been reported to my knowledge. The majority of the focus has been on more aerodynamically relevant changes in the stroke plane angle (e.g., Cheng et al., 2016a). The novel compensatory motions observed in this study, such as the ability to adjust the mean sweep angle of the wings during continuous flapping, suggest new principles for the design of flying devices. Hummingbirds make extensive use of anatomical wing sweep during maneuvering (Cheng et al., 2016a), and if implemented in flapping wing robots (e.g., Ma et al., 2013; Zhang, Cheng, and Deng, 2016), such an additional degree of freedom could improve their ability to negotiate simultaneous challenges in complex environments.

Bibliography

[1] Douglas L. Altshuler and Robert Dudley. "The ecological and evolutionary interface of hummingbird flight physiology". In: *Journal of Experimental Biology* 205.16 (2002), pp. 2325–2336. URL: http://jeb.biologists.org/content/205/16/2325.

[2] Douglas L. Altshuler, Elsa M. Quicazán-Rubio, Paolo S. Segre, and Kevin M. Middleton. "Wingbeat kinematics and motor control of yaw turns in Anna's hummingbirds (*Calypte anna*)". In: *Journal of Experimental Biology* 215.23 (2012), pp. 4070–4084. DOI: 10.1242/jeb.075044.

[3] Douglas L. Altshuler, Joseph W. Bahlman, Roslyn Dakin, Andrea H. Gaede, Benjamin Goller, David Lentink, Paolo S. Segre, and Dimitri A. Skandalis. "The biophysics of bird flight: functional relationships integrate aerodynamics, morphology, kinematics, muscles, and sensors". In: *Canadian Journal of Zoology* 93.12 (2015), pp. 961–975. DOI: 10.1139/cjz-2015-0103.

[4] Douglas Bates, Martin Mächler, Ben Bolker, and Steve Walker. "Fitting linear mixed-effects models using lme4". In: *Journal of Statistical Software* 67.1 (2015), pp. 1–48. DOI: 10.18637/jss.v067.i01.

[5] Yoav Benjamini and Daniel Yekutieli. "The control of the false discovery rate in multiple testing under dependency". In: *Annals of Statistics* 29.4 (2001), pp. 1165–1188.

[6] Melissa S. Bowlin and Martin Wikelski. "Pointed Wings, Low Wingloading and Calm Air Reduce Migratory Flight Costs in Songbirds". In: *PLoS ONE* 3.5 (May 2008), pp. 1–8. DOI: 10.1371/journal.pone.0002154.

[7] Angelo Canty and B. D. Ripley. *boot: Bootstrap R (S-Plus) functions*. R package version 1.3-17. 2015.

[8] Bo Cheng, Bret W. Tobalske, Donald R. Powers, Tyson L. Hedrick, Susan M. Wethington, George T. C. Chiu, and Xinyan Deng. "Flight mechanics and control of escape manoeuvres in hummingbirds I. Flight kinematics". In: *Journal of Experimental Biology* (2016). DOI: 10.1242/jeb.137539. URL: http://jeb.biologists.org/content/early/2016/09/02/jeb.137539.

[9] Bo Cheng, Bret W. Tobalske, Donald R. Powers, Tyson L. Hedrick, Yi Wang, Susan M. Wethington, George T.-C. Chiu, and Xinyan Deng. "Flight mechanics and control of escape manoeuvres in hummingbirds. II. Aerodynamic force production, flight control and performance limitations". In: *Journal of Experimental Biology* 219.22 (2016), pp. 3532–3543. DOI: 10.1242/jeb.137570. URL: http://jeb.biologists.org/content/219/22/3532.

[10] Stacey A. Combes and Robert Dudley. "Turbulence-driven instabilities limit insect flight performance". In: *Proceedings of the National Academy of Sciences* 106.22 (2009), pp. 9105–9108. DOI: 10.1073/pnas.0902186106.

[11] A. C. Davison and D. V. Hinkley. *Bootstrap Methods and Their Applications*. ISBN 0-521-57391-2. Cambridge, MA: Cambridge University Press, 1997.

[12] Jonathan P. Dyhr, Kristi A. Morgansen, Thomas L. Daniel, and Noah J. Cowan. "Flexible strategies for flight control: an active role for the abdomen". In: *Journal of Experimental Biology* 216.9 (2013), pp. 1523–1536. DOI: 10.1242/jeb.077644. URL: http://jeb.biologists.org/content/216/9/1523.

[13] Charles P Ellington, Coen van den Berg, Alexander P Willmott, and Adrian L R Thomas. "Leading-edge vortices in insect flight". In: *Nature* 384.6610 (1996), pp. 626–630.

[14] R. S. Fearing, K. H. Chiang, M. H. Dickinson, D. L. Pick, M. Sitti, and J. Yan. "Wing transmission for a micromechanical flying insect". In: *Proceedings 2000 ICRA. Millennium Conference. IEEE International Conference on Robotics and Automation. Symposia Proceedings (Cat. No.00CH37065)*. Vol. 2. 2000, 1509–1516 vol.2. DOI: 10.1109/ROBOT.2000.844811.

[15] Alex Fisher, Sridhar Ravi, Simon Watkins, Jon Watmuff, Chun Wang, Hao Liu, and Phred Petersen. "The gust-mitigating potential of flapping wings". In: *Bioinspiration & Biomimetics* 11.4 (2016), p. 046010. URL: http://stacks.iop.org/1748-3190/11/i=4/a=046010.

[16] Gordon A. Fox, Simoneta Negrete-Yankelevich, and Vinicio J. Sosa. *Ecological Statistics: Contemporary Theory and Application*. Oxford, UK: Oxford University Press, 2015, p. 314. ISBN: 9780199672547. DOI: 10.1093/acprof:oso/9780199672547.001.0001.

[17] Chris Fraley and Adrian E. Raftery. "Model-based clustering, discriminant analysis, and density estimation". In: *Journal of the American Statistical Association* 97.458 (2002), pp. 611–631.

[18] Chris Fraley, Adrian E. Rafferty, T. Brendan Murphy, and Luca Scrucca. *mclust Version 4 for R: Normal Mixture Modeling for Model-Based Clustering, Classification, and Density Estimation, 2012*.

[19] Sawyer Buckminster Fuller, Andrew D. Straw, Martin Y. Peek, Richard M. Murray, and Michael H. Dickinson. "Flying Drosophila stabilize their vision-based velocity controller by sensing wind with their antennae". In: *Proceedings of the National Academy of Sciences of the United States of America* 111.13 (2014), E1182–E1191.

[20] James A. Gillies, Adrian L. R. Thomas, and Graham K. Taylor. "Soaring and manoeuvring flight of a steppe eagle *Aquila nipalensis*". In: *Journal of Avian Biology* 42.5 (2011), pp. 377–386. DOI: 10.1111/j.1600-048X.2011.05105.x.

[21] Crawford H. Greenewalt. *Hummingbirds*. Doubleday, Garden City, NY, 1960, p. 116. ISBN: 0486264319.

[22] S. D. Healy and T. A. Hurly. "Rufous hummingbirds' (Selasphorus rufus) memory for flowers: Patterns or actual spatial locations?" In: *Journal of Experimental Psychology: Animal Behavior Processes* 24.4 (1998), pp. 396–404.

[23] Tyson L. Hedrick. "Software techniques for two-and three-dimensional kinematic measurements of biological and biomimetic systems". In: *Bioinspiration & Biomimetics* 3.3 (2008), p. 034001.

[24] Tyson L. Hedrick, Bo Cheng, and Xinyan Deng. "Wingbeat time and the scaling of passive rotational damping in flapping flight." In: *Science (New York, N.Y.)* 324.5924 (2009), pp. 252–255.

[25] Tyson L. Hedrick, Bret W. Tobalske, Ivo G. Ros, Douglas R. Warrick, and Andrew A. Biewener. "Morphological and kinematic basis of the hummingbird flight stroke: scaling of flight muscle transmission ratio". In: *Proceedings of the Royal Society of London B: Biological Sciences* 279.1735 (2012), pp. 1986–1992. DOI: 10.1098/rspb.2011.2238.

[26] Frederic M. Hoblit. *Gust Loads on Aircraft: Concepts and Applications*. Washington, D.C.: American Institute of Aeronautics and Astronautics, 1988. ISBN: 978-0-930403-45-4. DOI: 10.2514/4.861888.

[27] Andrew T. Hurly. "Spatial memory in rufous hummingbirds: memory for rewarded and non-rewarded sites". In: *Animal Behaviour* 51.1 (1996), pp. 177 –183. ISSN: 0003-3472. DOI: http://dx.doi.org/10.1006/anbe.1996.0015. URL: http://www.sciencedirect.com/science/article/pii/S0003347296900159.

[28] S. Karaman and E. Frazzoli. "High-speed flight in an ergodic forest". In: *2012 IEEE International Conference on Robotics and Automation (ICRA)*. 2012, pp. 2899–2906. DOI: 10.1109/ICRA.2012.6225235.

[29] Jun-seong Lee, Joong-kwan Kim, Jae-hung Han, and Charles P. Ellington. "Periodic Tail Motion Linked to Wing Motion Affects the Longitudinal Stability of Ornithopter Flight". In: *Journal of Bionic Engineering* 9.1 (2012), pp. 18–28.

[30] Gordon J. Leishman. *Principles of Helicopter Aerodynamics*. 2nd. Cambridge, MA: Cambridge University Press, 2006, pp. 258–260. ISBN: 9780521858601.

[31] Huai-Ti Lin, Ivo G. Ros, and Andrew A. Biewener. "Through the eyes of a bird: modelling visually guided obstacle flight". In: *Journal of The Royal Society Interface* 11.96 (2014). DOI: 10.1098/rsif.2014.0239.

[32] Kevin Y. Ma, Pakpong Chirarattananon, Sawyer B. Fuller, and Robert J. Wood. "Controlled flight of a biologically inspired, insect-scale robot". In: *Science* 340.6132 (2013), pp. 603–607. DOI: 10.1126/science.1231806.

[33] Graham R. Martin. "Visual fields and their functions in birds". In: *Journal of Ornithology* 148.2 (2007), pp. 547–562. DOI: 10.1007/s10336-007-0213-6.

[34] Graham R. Martin. "Understanding bird collisions with man-made objects: a sensory ecology approach". In: *Ibis* 153.2 (2011), pp. 239–254. DOI: 10.1111/j.1474-919X.2011.01117.x.

[35] Daniel Mellinger, Nathan Michael, and Vijay Kumar. "Trajectory generation and control for precise aggressive maneuvers with quadrotors". In: *The International Journal of Robotics Research* 31.5 (2012), pp. 664–674.

[36] Boris Moulin and Moti Karpel. "Gust Loads Alleviation Using Special Control Surfaces". In: *Journal of Aircraft* 44.1 (2007), pp. 17–25. DOI: 10.2514/1.19876.

[37] Victor M. Ortega-Jimenez, Nir Sapir, Marta Wolf, Evan A. Variano, and Robert Dudley. "Into turbulent air: size-dependent effects of von Kármán vortex streets on hummingbird flight kinematics and energetics". In: *Proceedings of the Royal Society of London B: Biological Sciences* 281.1783 (2014). DOI: 10.1098/rspb.2014.0180.

[38] Victor M. Ortega-Jimenez, Marc Badger, Hao Wang, and Robert Dudley. "Into rude air: hummingbird flight performance in variable aerial environments". In: *Philosophical Transactions of the Royal Society B-Biological Sciences* 371.1704 (2016).

[39] Victor Manuel Ortega-Jimenez, Jeremy S. M. Greeter, Rajat Mittal, and Tyson L. Hedrick. "Hawkmoth flight stability in turbulent vortex streets". In: *Journal of Experimental Biology* 216.24 (2013), pp. 4567–4579. DOI: 10.1242/jeb.089672.

[40] I. Penskiy, P. Samuel, J. S. Humbert, and S. Bergbreiter. "A bio-inspired active tail control actuator for nano air vehicles". In: *2012 IEEE International Conference on Robotics and Automation*. 2012, pp. 4635–4640. DOI: 10.1109/ICRA.2012.6225370.

[41] R Core Team. *R: A Language and Environment for Statistical Computing*. ISBN 3-900051-07-0. R Foundation for Statistical Computing. Vienna, Austria, 2016. URL: http://www.R-project.org.

[42] Sridhar Ravi, James D. Crall, Alex Fisher, and Stacey A. Combes. "Rolling with the flow: bumblebees flying in unsteady wakes". In: *Journal of Experimental Biology* 216.22 (2013), pp. 4299–4309. DOI: 10.1242/jeb.090845.

[43] Sridhar Ravi, James D. Crall, Lucas McNeilly, Susan F. Gagliardi, Andrew A. Biewener, and Stacey A. Combes. "Hummingbird flight stability and control in freestream turbulent winds". In: *Journal of Experimental Biology* 218.9 (2015), pp. 1444–1452. DOI: 10.1242/jeb.114553.

[44] Simon M. Reader, Julie Morand-Ferron, and Emma Flynn. "Animal and human innovation: novel problems and novel solutions". In: *Philosophical Transactions of the Royal Society B: Biological Sciences* 371.1690 (2016). DOI: 10.1098/rstb.2015.0182.

[45] Kate V. Reynolds, Adrian L. R. Thomas, and Graham K. Taylor. "Wing tucks are a response to atmospheric turbulence in the soaring flight of the steppe eagle *Aquila nipalensis*". In: *Journal of The Royal Society Interface* 11.101 (2014). DOI: 10.1098/rsif.2014.0645.

[46] Ivo G. Ros and Andrew A. Biewener. "Optic flow stabilizes flight in ruby-throated hummingbirds". In: *Journal of Experimental Biology* (2016). DOI: 10.1242/jeb.128488. URL: http://jeb.biologists.org/content/early/2016/06/08/jeb.128488.

[47] Ivo G. Ros, Marc A. Badger, Alyssa N. Pierson, Lori C. Bassman, and Andrew A. Biewener. "Pigeons produce aerodynamic torques through changes in wing trajectory during low speed aerial turns". In: *Journal of Experimental Biology* 218.3 (2015), pp. 480–490. DOI: 10.1242/jeb.104141.

[48] Nir Sapir and Robert Dudley. "Backward flight in hummingbirds employs unique kinematic adjustments and entails low metabolic cost". In: *Journal of Experimental Biology* 215.20 (2012), pp. 3603–3611. DOI: 10.1242/jeb.073114.

[49] Raymond Saxod. "Ontogeny of the cutaneous sensory organs". In: *Microscopy Research and Technique* 34.4 (1996), pp. 313–333. ISSN: 1097-0029.

[50] Ingo Schiffner, Hong D. Vo, Partha S. Bhagavatula, and Mandyam V. Srinivasan. "Minding the gap: in-flight body awareness in birds". In: *Frontiers in Zoology* 11.1 (2014), pp. 1–9. DOI: 10.1186/s12983-014-0064-y.

[51] Henrik Singmann, Ben Bolker, and Jake Westfall. *afex: Analysis of factorial experiments*. R package version 0.14-2. 2015. URL: http://CRAN.R-project.org/package=afex.

[52] F. Gary Stiles. "Behavioral, ecological and morphological correlates of foraging for arthropods by the hummingbirds of a tropical wet forest". In: *The Condor* 97.4 (1995), pp. 853–878.

[53] I. Suomi, T. Vihma, S.-E. Gryning, and C. Fortelius. "Wind-gust parametrizations at heights relevant for wind energy: a study based on mast observations". In: *Quarterly Journal of the Royal Meteorological Society* 139.674 (2013), pp. 1298–1310. DOI: 10.1002/qj.2039.

[54] The MathWorks, Inc. *MATLAB and Statistics Toolbox Release 2016a*. Version 9.0. Natick, MA, 2016. URL: https://www.mathworks.com/.

[55] J. T. Vance, I. Faruque, and J. S. Humbert. "Kinematic strategies for mitigating gust perturbations in insects". In: *Bioinspiration & Biomimetics* 8.1 (2013), p. 016004. URL: http://stacks.iop.org/1748-3190/8/i=1/a=016004.

[56] Douglas R. Warrick, Bret W. Tobalske, and Donald R. Powers. "Lift production in the hovering hummingbird". In: *Proceedings of the Royal Society of London B: Biological Sciences* 276.1674 (2009), pp. 3747–3752. DOI: 10.1098/rspb.2009.1003.

[57] C. David Williams and Andrew A. Biewener. "Pigeons trade efficiency for stability in response to level of challenge during confined flight". In: *Proceedings of the National Academy of Sciences* 112.11 (2015), pp. 3392–3396. DOI: 10.1073/pnas.1407298112.

[58] Larry L. Wolf and F. Reed Hainsworth. "Time and energy budgets of territorial hummingbirds". In: *Ecology* 52.6 (1971), pp. 980–988.

[59] Jian Zhang, Bo Cheng, and Xinyan Deng. "Instantaneous wing kinematics tracking and force control of a high-frequency flapping wing insect MAV". In: *Journal of Micro-Bio Robotics* 11.1 (2016), pp. 67–84. DOI: 10.1007/s12213-015-0085-4. URL: http://dx.doi.org/10.1007/s12213-015-0085-4.